


Advanced 
**Synthesis &
Catalysis**

Supporting Information

Supporting Information

Chemoenzymatic Synthesis of Glycosylated Macrolactam Analogues of the Macrolide Antibiotic YC-17

Pramod B. Shinde,^{a,‡} Hong-Se Oh,^b Hyemin Choi,^c Kris Rathwell,^a Yeon Hee Ban,^a Eun Ji Kim,^a Inho Yang,^a Dong Gun Lee,^c David H. Sherman,^d Han-Young Kang,^{b,*} and Yeo Joon Yoon^{a,*}

^a Department of Chemistry and Nano Science, Ewha Womans University, Seoul 120-750, Republic of Korea.

Fax: (+82)-2-3277-3419; Tel: (+82)-2-3277-4446; e-mail: joonyoon@ewha.ac.kr

^b Department of Chemistry, Chungbuk National University, Cheongju 361-763, Republic of Korea.

Fax: (+82)-43-267-2279 ; Tel: (+82)-43-261-2305; e-mail: hykang@chungbuk.ac.kr

^c School of Life Sciences, BK 21 Plus KNU Creative BioResearch Group, College of Natural Sciences, Kyungpook National University, Daehak-ro 80, Buk-gu, Daegu 702-701, Republic of Korea.

^d Department of Medicinal Chemistry, Life Science Institute, Department of Chemistry, and Department of Microbiology & Immunology, University of Michigan, Ann Arbor, Michigan 48109, United States.

[‡] Present address: Institute of Bioinformatics and Biotechnology (IBB), Savitribai Phule Pune University (Formerly University of Pune), Pune 411-007, India.

Table of Contents

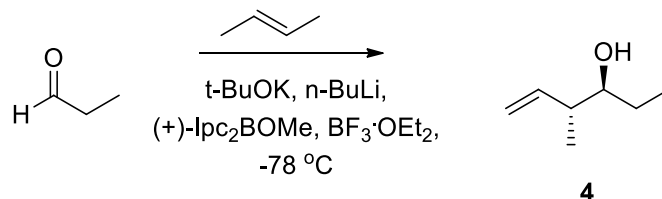
Synthesis of 1	S4
Construction of expression plasmids and <i>S. venezuelae</i> strains.....	S9
Cytotoxicity assay of 11 and 12	S9
Supporting references.....	S10
Table S1. Biosynthetic gene sets in the engineered strains of <i>S. venezuelae</i> and their products.	S11
Table S2. ¹³ C- and ¹ H-NMR data of isolated macrolactam glycosides.....	S12
Table S3. Comparison of the productivity of AZDM glycosides and their respective YC-17 analogues.....	S13
Table S4. <i>In vitro</i> antibacterial activities of macrolactam glycosides.....	S14
Table S5. <i>In vitro</i> antibacterial activities of lactams, counterpart lactones, and erythromycin	S15
Scheme S1. Retrosynthetic analysis of AZDM 1	S16
Figure S1. ¹ H NMR spectrum of 4 in CDCl ₃ at 400 MHz.....	S17
Figure S2. ¹³ C NMR spectrum of 4 in CDCl ₃ at 100 MHz.....	S18
Figure S3. ¹ H NMR spectrum of 5 in CDCl ₃ at 400 MHz.....	S19
Figure S4. ¹³ C NMR spectrum of 5 in CDCl ₃ at 100 MHz.....	S20
Figure S5. ¹ H NMR spectrum of 2 in CDCl ₃ at 400 MHz.....	S21
Figure S6. ¹³ C NMR spectrum of 2 in CDCl ₃ at 100 MHz.....	S22
Figure S7. ¹ H NMR spectrum of 6 in CDCl ₃ at 400 MHz.....	S23
Figure S8. ¹³ C NMR spectrum of 6 in CDCl ₃ at 100 MHz.....	S24
Figure S9. ¹ H NMR spectrum of 7 in CDCl ₃ at 400 MHz.....	S25
Figure S10. ¹³ C NMR spectrum of 7 in CDCl ₃ at 100 MHz.....	S26
Figure S11. ¹ H NMR spectrum of 8 in CDCl ₃ at 400 MHz.....	S27
Figure S12. ¹³ C NMR spectrum of 8 in CDCl ₃ at 100 MHz.....	S28
Figure S13. ¹ H NMR spectrum of 9 in CDCl ₃ at 400 MHz.....	S29
Figure S14. ¹³ C NMR spectrum of 9 in CDCl ₃ at 100 MHz.....	S30
Figure S15. ¹ H NMR spectrum of 10 in CDCl ₃ at 400 MHz.....	S31
Figure S16. ¹³ C NMR spectrum of 10 in CDCl ₃ at 100 MHz.....	S32
Figure S17. ESI-MS/MS spectrum of 1	S33
Figure S18. ¹ H NMR spectrum of 1 in CD ₃ OD at 500 MHz.....	S34
Figure S19. ¹³ C NMR spectrum of 1 in CD ₃ OD at 125 MHz.....	S35
Figure S20. COSY spectrum of 1 in CD ₃ OD at 500 MHz	S36
Figure S21. HSQC spectrum of 1 in CD ₃ OD at 500 MHz	S37
Figure S22. HMBC spectrum of 1 in CD ₃ OD at 500 MHz	S38
Figure S23. ESI-MS/MS spectrum of 11	S39
Figure S24. ESI-MS/MS spectrum of 12	S40
Figure S25. ESI-MS/MS spectrum of 13	S41
Figure S26. ESI-MS/MS spectrum of 14	S42
Figure S27. ESI-MS/MS spectrum of 15	S43

Figure S28. ESI-MS/MS spectrum of 16	S44
Figure S29. ESI-MS/MS spectrum of 17	S45
Figure S30. ESI-MS/MS spectrum of 18	S46
Figure S31. ¹ H NMR spectrum of 11 in CD ₃ OD at 500 MHz.....	S47
Figure S32. ¹³ C NMR spectrum of 11 in CD ₃ OD at 500 MHz.....	S48
Figure S33. COSY spectrum of 11 in CD ₃ OD at 500 MHz	S49
Figure S34. HSQC spectrum of 11 in CD ₃ OD at 500 MHz	S50
Figure S35. HMBC spectrum of 11 in CD ₃ OD at 500 MHz	S51
Figure S36. NOESY spectrum of 11 in CD ₃ OD at 500 MHz.....	S52
Figure S37. ¹ H NMR spectrum of 12 in CD ₃ OD at 900 MHz.....	S53
Figure S38. ¹³ C NMR spectrum of 12 in CD ₃ OD at 225 MHz.....	S54
Figure S39. COSY spectrum of 12 in CD ₃ OD at 900 MHz	S55
Figure S40. HSQC spectrum of 12 in CD ₃ OD at 900 MHz	S56
Figure S41. HMBC spectrum of 12 in CD ₃ OD at 900 MHz	S57
Figure S42. NOESY spectrum of 12 in CD ₃ OD at 900 MHz.....	S58
Figure S43. ¹ H NMR spectrum of 13 in CD ₃ OD at 500 MHz.....	S59
Figure S44. ¹³ C NMR spectrum of 13 in CD ₃ OD at 500 MHz.....	S60
Figure S45. COSY spectrum of 13 in CD ₃ OD at 500 MHz	S61
Figure S46. HSQC spectrum of 13 in CD ₃ OD at 500 MHz	S62
Figure S47. HMBC spectrum of 13 in CD ₃ OD at 500 MHz	S63
Figure S48. NOESY spectrum of 13 in CD ₃ OD at 500 MHz.....	S64
Figure S49. ¹ H NMR spectrum of 16 in CD ₃ OD at 500 MHz.....	S65
Figure S50. ¹³ C NMR spectrum of 16 in CD ₃ OD at 125 MHz.....	S66
Figure S51. COSY spectrum of 16 in CD ₃ OD at 500 MHz	S67
Figure S52. HSQC spectrum of 16 in CD ₃ OD at 500 MHz	S68
Figure S53. HMBC spectrum of 16 in CD ₃ OD at 500 MHz	S69
Figure S54. NOESY spectrum of 16 in CD ₃ OD at 500 MHz.....	S70
Figure S55. ¹ H NMR spectrum of 17 in CD ₃ OD at 500 MHz.....	S71
Figure S56. ¹³ C NMR spectrum of 17 in CD ₃ OD at 125 MHz.....	S72
Figure S57. COSY spectrum of 17 in CD ₃ OD at 500 MHz	S73
Figure S58. HSQC spectrum of 17 in CD ₃ OD at 500 MHz	S74
Figure S59. HMBC spectrum of 17 in CD ₃ OD at 500 MHz	S75
Figure S60. NOESY spectrum of 17 in CD ₃ OD at 500 MHz.....	S76
Figure S61. Key COSY, HMBC, and NOESY correlations in AZDM glycosides 11–13 , 16 , and 17	S77
Figure S62. HPLC–ESI-MS chromatogram of erythromycin esterase assay.....	S78
Figure S63. HPLC–ESI-MS chromatogram of simulated gastric fluid (SGF) assay.	S79
Figure S64. MS spectrum of L-rhamnosyl-10-deoxymethynolide.....	S80
Figure S65. HPLC–ESI-MS chromatogram of liver microsomal assay.....	S81

Supporting Experimental Procedures

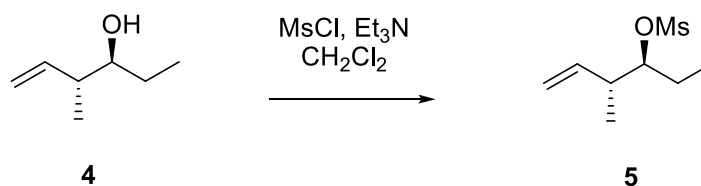
Synthesis of 1

i. (3*S*,4*R*)-4-Methyl-5-hexen-3-ol (**4**).^[1]



To a stirred mixture of potassium *tert*-butoxide (4.6 g, 41.5 mmol) in THF (15 mL) were added *trans*-2-butene (7.2 mL, 80 mmol) and *n*-butyllithium [26.0 mL (1.6 M in hexane), 41.5 mmol]. After the solution was stirred at -78 °C for 30 min, it was added to a solution of *B*-methoxydiisopinocampheylborane [50 mL (1.0 M in ether), 50 mmol] dropwise. The resultant solution was stirred at -78 °C for 30 min, and BF₃·OEt₂ (7.0 mL, 56.0 mmol) and propanal (4.3 mL, 58.5 mmol) was successively added dropwise at -78 °C. The solution was stirred at -78 °C for 3 h and then treated with 3 *N* NaOH (30 mL) and 30 % H₂O₂ (12 mL). The mixture was heated to reflux for 1 h before it was extracted with ether (3 × 40 mL). The organic phase was separated and washed with water (100 mL) and brine (100 mL). The organic layer was dried (MgSO₄) and concentrated. Purification by flash chromatography (hexane/EtOAc = 7:1) offered the alcohol **4** (2.8 g, 61%) as a colorless oil: [α]_D³⁰ +12.5 (*c* 0.88, CHCl₃); IR (film) ν_{max} 3363, 2963, 2932, 2875, 1640, 1460, 1109, 968 cm⁻¹; ¹H NMR (400 MHz, CDCl₃) δ 5.76 (ddd, *J* = 8.3, 11.3, 16.3 Hz, 1H), 5.10 (m, 2H), 3.33 (m, 1H), 2.22 (m, 1H), 1.60 (m, 1H), 1.40 (m, 1H), 1.03 (d, *J* = 6.8 Hz, 3H), 0.97 (t, *J* = 7.4 Hz, 3H); ¹³C NMR (100 MHz, CDCl₃) δ 140.4, 116.2, 76.0, 43.7, 27.0, 16.3, 10.0; HR-ESI-MS *m/z* 137.0936 [M + Na]⁺ (calcd for C₇H₁₄ONa, 137.0937).

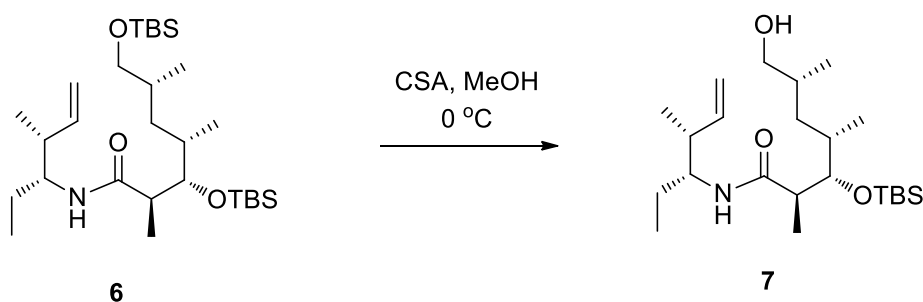
ii. (3*S*,4*R*)-3-Methanesulfonyloxy-4-methyl-5-hexen (**5**).



To a stirred solution of alcohol **4** (780 mg, 6.8 mmol) in CH₂Cl₂ (25 mL) were added triethylamine (3.3 mL, 23.9 mmol) and methanesulfonyl chloride (1.6 mL, 20.5 mmol) at 0 °C. The reaction mixture was stirred for 20 min at 0 °C before it was warmed to room temperature. After additional stirring for 2 h at room temperature, water (30 mL) was added, and the mixture was extracted with CH₂Cl₂ (3 × 30 mL). The organic layer was separated, dried (MgSO₄), and concentrated. Purification by flash chromatography (hexane/EtOAc = 7:1) offered the desired methanesulfonate ester **5** (1.16 g, 89%) as a colorless oil. [α]_D²⁹ -2.25 (*c* 1.59, CHCl₃); IR (film) ν_{max} 2971, 2879, 1641, 1463, 1418, 1341, 1175, 1048, 973 cm⁻¹; ¹H NMR (400 MHz, CDCl₃) δ 5.74 (m, 1H), 5.11 (m, 2H), 4.62 (ddd, *J* = 4.9, 6.2, 11.0 Hz, 1H), 3.02 (s, 3H), 2.60 (m, 1H), 1.71 (m, 2H),

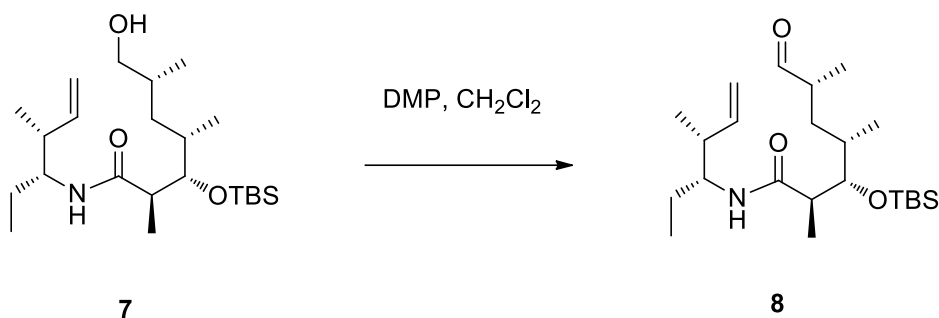
DIPEA (233 μ L, 1.35 mmol), HOBt (182 mg, 1.35 mmol), and EDC·HCl (259 mg, 1.35 mmol). The mixture was stirred for 15 min at 0 °C, and a solution of amine **2** (235 mg, 2.08 mmol) in CH₂Cl₂ (1 mL) was added. The mixture was stirred for 2 h at 0 °C before it was warmed to room temperature. After additional stirring for 16 hr at room temperature, saturated NH₄Cl (10 mL) was added to the solution, and the mixture was extracted with CH₂Cl₂ (3 \times 10 mL). The organic layer was separated, dried (MgSO₄), and concentrated. Purification by flash chromatography (hexane/EtOAc = 7:1) offered the desired amide **6** (445 mg, 81%) as a colorless oil: $[\alpha]_D^{25} +4.6$ (*c* 1.41, CHCl₃); IR (film) ν_{\max} 3306, 2958, 2858, 1639, 1540, 1464, 1383, 1256, 1074, 913 cm⁻¹; ¹H NMR (400 MHz, CDCl₃) δ 5.73 (ddd, *J* = 7.9, 9.8, 17.7 Hz, 1H), 5.49 (bd, *J* = 9.4 Hz, 1H), 5.01 (m, 2H), 3.81 (m, 1H), 3.49 (dd, *J* = 4.8, 9.7 Hz, 1H), 3.24 (dd, *J* = 7.2, 9.7 Hz, 1H), 2.40 (m, 1H), 2.31 (m, 1H), 1.77~1.57 (m, 4H), 1.47 (m, 1H), 1.21 (m, 1H), 1.15 (d, *J* = 7.1 Hz, 3H), 1.02 (d, *J* = 6.9 Hz, 3H), 0.89 (m, 27H), 0.05 (m, 12H); ¹³C NMR (100 MHz, CDCl₃) δ 174.9, 140.6, 115.2, 77.6, 67.9, 54.0, 44.8, 42.0, 36.5, 36.2, 33.8, 26.0, 25.9, 24.4, 18.4, 18.3(\times 2), 16.9, 16.3, 15.7, 10.7, -4.1, -5.4; HR-ESI-MS *m/z* 550.4087 [M + Na]⁺ (calcd for C₂₉H₆₁NO₃Si₂Na, 550.4082).

- v. (2*R*,3*S*,4*S*,6*R*)-3-(*tert*-Butyldimethylsilyloxy)-7-hydroxy-2,4,6-trimethyl-*N*-((3*R*,4*R*)-4-methylhex-5-en-3-yl)heptanamide (**7**).



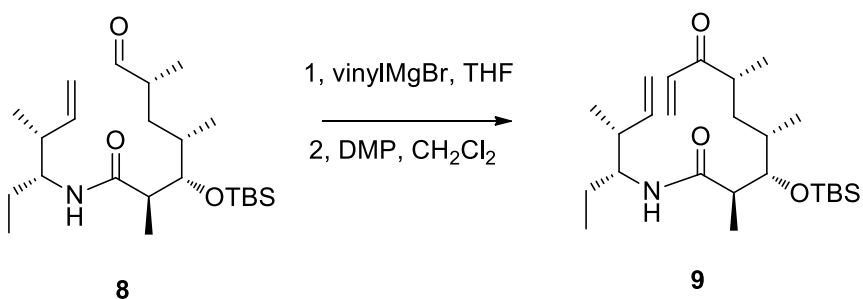
Amide **6** (445 mg, 0.84 mmol) was dissolved in methanol (10 mL) at 0 °C. To this solution was added DL-10-camphorsulfonic acid (58 mg, 0.25 mmol). The resulting solution was stirred at 0 °C for 1 h. The reaction was terminated by the addition of Et₃N (200 μ L, 1.43 mmol). After the solution was concentrated, purification by flash chromatography (hexane/EtOAc = 4:1) gave the desired primary alcohol **7** (297 mg, 86 %) as a colorless oil: $[\alpha]_D^{31} +6.8$ (*c* 1.05, CHCl₃); IR (film) ν_{\max} 3298, 2960, 2931, 1643, 1546, 1461, 1380, 1254, 1069, 911 cm⁻¹; ¹H NMR (400 MHz, CDCl₃) δ 5.72 (m, 1H), 5.58 (bd, *J* = 9.3 Hz, 1H), 5.01 (m, 2H), 3.77 (m, 2H), 3.54 (dd, *J* = 4.3, 10.9 Hz, 1H), 3.33 (dd, *J* = 5.4, 10.8 Hz, 1H), 2.76 (bs, 1H), 2.43 (m, 1H), 2.32 (m, 1H), 1.81 (m, 1H), 1.63 (m, 3H), 1.24 (m, 1H), 1.16 (d, *J* = 7.0 Hz, 3H), 1.03 (d, *J* = 6.9 Hz, 3H), 0.93 (m, 15H), 0.86 (t, *J* = 7.4 Hz, 3H), 0.08 (s, 6H); ¹³C NMR (100 MHz, CDCl₃) δ 175.4, 140.5, 115.5, 77.7, 66.6, 54.3, 45.3, 41.8, 35.2, 34.8, 32.8, 26.0, 24.2, 18.3, 17.7, 16.6, 16.1, 10.5, -4.0, -4.2; HR-ESI-MS *m/z* 436.3219 [M + Na]⁺ (calcd for C₂₃H₄₇NO₃SiNa, 436.3217).

- vi. (2*R*,3*S*,4*S*,6*R*)-3-((*tert*-butyldimethylsilyl)oxy)-2,4,6-trimethyl-*N*-((3*R*,4*R*)-4-methylhex-5-en-3-yl)-7-oxoheptanamide (**8**).



To a solution of alcohol **7** (297 mg, 0.72 mmol) in CH₂Cl₂ (20 mL) was added Dess-Martin periodinane (DMP) (611 mg, 1.44 mmol). The resultant solution was stirred for 2 h at room temperature before saturated NaHCO₃ (10 mL) and Na₂SO₄ (5 mL) were added. The mixture was extracted with CH₂Cl₂ (3 × 15 mL), and the organic layer was separated, dried (MgSO₄), and concentrated. Purification by flash chromatography (hexane/EtOAc = 5:1) offered the desired aldehyde **8** (246 mg, 83 %) as a colorless liquid: $[\alpha]_D^{29} +29.4$ (*c* 1.70, CHCl₃); IR (film) ν_{max} 3313, 2931, 1726, 1641, 1537, 1461, 1254, 1066, 836 cm⁻¹; ¹H NMR (400 MHz, CDCl₃) δ 9.59 (d, *J* = 1.9 Hz, 1H), 5.71 (m, 1H), 5.64 (bd, *J* = 9.4 Hz, 1H), 5.01 (m, 2H), 3.80 (m, 2H), 2.46 (m, 2H), 2.31 (m, 1H), 1.93 (ddd, *J* = 3.5, 9.5, 13.8 Hz, 1H), 1.59 (m, 3H), 1.25 (m, 1H), 1.16 (d, *J* = 7.1 Hz, 3H), 1.11 (d, *J* = 7.2 Hz, 3H), 0.99 (d, *J* = 6.9 Hz, 3H), 0.93 (m, d, *J* = 6.9 Hz, 3H), 0.88 (m, 12H), 0.08 (s, 3H), 0.07 (s, 3H); ¹³C NMR (100 MHz, CDCl₃) δ 205.4, 174.9, 140.8, 115.0, 54.2, 45.4, 44.3, 41.8, 36.2, 32.8, 26.1, 24.5, 18.3, 17.2, 16.2, 16.0, 14.9, 10.7, -3.9, -4.0; HR-ESI-MS *m/z* 434.3062 [M + Na]⁺ calcd for C₂₃H₄₅NO₃SiNa, 434.3061).

- vii. (2*R*,3*S*,4*S*,6*R*)-3-((*tert*-butyldimethylsilyl)oxy)-2,4,6-trimethyl-*N*-((3*R*,4*R*)-4-methylhex-5-en-3-yl)-7-oxonon-8-enamide (**9**).

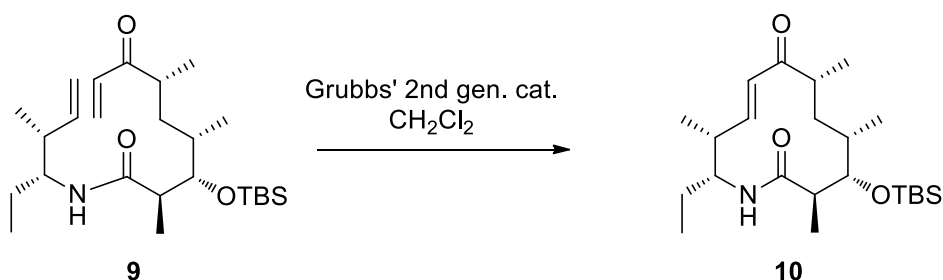


To a stirred solution of aldehyde **8** (246 mg, 0.60 mmol) in THF (10 mL) was added vinylmagnesium bromide (1 M in THF) (1.20 mL, 1.20 mmol) at 0 °C. After 1 h, the solution was diluted by adding Et₂O (10 mL), and then a saturated aqueous NH₄Cl solution (10 mL) was added. The organic layers were separated, and the aqueous layer was extracted with ether (3 × 10 mL). The organic solutions were combined, dried (MgSO₄), and concentrated. Purification of the residue by flash chromatography (hexane/EtOAc = 5:1) afforded the desired vinyl alcohol (201 mg, 76 %) as a

colorless oil.

The vinyl alcohol (201 mg, 0.46 mmol) was dissolved in CH₂Cl₂ (10 mL), Dess-Martin periodinane (DMP) (390 mg, 0.92 mmol) was added, and the resultant solution was stirred for 2 h at room temperature. After the reaction was complete, aqueous saturated NaHCO₃ (10 mL) and Na₂SO₄ (5 mL) were added. The mixture was extracted with CH₂Cl₂ (3 × 10 mL). The organic layer was separated, dried (MgSO₄), and concentrated. Purification by flash chromatography (hexane/EtOAc = 5:1) offered the desired vinyl ketone **9** (145 mg, 72 %) as a colorless liquid: [α]_D²⁸ +32.4 (*c* 0.53, CHCl₃); IR (film) ν_{max} 3302, 2928, 2358, 1726, 1645, 1532, 1461, 1379, 1254, 1064, 910 cm⁻¹; ¹H NMR (400 MHz, CDCl₃) δ 6.44 (dd, *J* = 10.4, 17.5 Hz, 1H), 6.28 (dd, *J* = 1.4, 17.5 Hz, 1H), 5.80 (m, 2H), 5.67 (ddd, *J* = 8.0, 10.3, 17.2 Hz, 1H), 4.98 (m, 2H), 3.74 (m, 2H), 2.93 (m, 1H), 2.61 (m, 1H), 2.21 (m, 1H), 2.02 (m, 1H), 1.27 (m, 2H), 1.15 (m, 6H), 0.91 (m, 18H), 0.08 (s, 3H), 0.07 (s, 3H); ¹³C NMR (100 MHz, CDCl₃) δ 204.7, 175.4, 141.1, 135.6, 128.3, 114.7, 77.6, 54.4, 45.7, 42.1, 41.2, 36.2, 34.1, 26.2, 24.8, 18.9, 18.4, 17.8, 16.6, 16.0, 10.6, -3.7, -3.8; HR-ESI-MS *m/z* 460.3219 [M + Na]⁺ (calcd for C₂₅H₄₇NO₃SiNa, 460.3217).

viii. (*E*)-(3*R*,4*S*,5*S*,7*R*,11*R*,12*R*)-4-((*tert*-butyldimethylsilyl)oxy)-12-ethyl-3,5,7,11-tetramethylazacyclododec-9-ene-2,8-dione (**10**).



Vinyl ketone **9** (145 mg, 0.33 mmol) was dissolved in CH₂Cl₂ (20 mL) at room temperature. Grubbs' catalyst (second generation) (56 mg, 20 mol%) was added, producing a light brown solution which was stirred for 19 h at room temperature. The mixture was then concentrated, and purification of this residue by flash chromatography (hexane/EtOAc = 4:1) afforded the product **10** (83 mg, 61 %) as a white solid: mp : 184-186 °C; [α]_D²⁹ +35.9 (*c* 0.69, CHCl₃); IR (film) ν_{max} 3300, 2928, 1735, 1691, 1632, 1544, 1462, 1379, 1255, 1092, 1050, 1023, 979 cm⁻¹; ¹H NMR (400 MHz, CDCl₃) δ 6.73 (dd, *J* = 5.3, 15.9 Hz, 1H), 6.32 (dd, *J* = 1.3, 15.9 Hz, 1H), 5.23 (bd, *J* = 10.3 Hz, 1H), 4.09 (m, 1H), 3.64 (d, *J* = 8.8 Hz, 1H), 2.73 (m, 1H), 2.52 (m, 1H), 2.30 (m, 1H), 1.48 (m, 3H), 1.36 (m, 2H), 1.21 (d, *J* = 6.9 Hz, 6H), 1.00 (d, *J* = 7.0 Hz, 3H), 0.95 (m, 3H), 0.92 (m, 3H), 0.90 (s, 9H), 0.08 (s, 3H), 0.07 (s, 3H); ¹³C NMR (100 MHz, CDCl₃) δ 205.1, 174.8, 147.3, 125.6, 79.9, 77.2, 50.5, 46.8, 44.7, 37.7, 34.5, 33.8, 29.7, 26.6, 26.3, 18.5, 17.8, 11.0, 9.6, -3.2, -3.5; HR-ESI-MS *m/z* 432.2903 [M + Na]⁺ (calcd for C₂₃H₄₃NO₃SiNa, 432.2904).

ix. (3*R*,4*S*,5*S*,7*R*,9*E*,11*R*,12*R*)-12-ethyl-4-hydroxy-3,5,7,11-tetramethylazacyclododec-9-ene-2,8-dione [aza-10-deoxymethynolide, AZDM, **1**].

fetal bovine serum (10%), penicillin (100 U·mL⁻¹) and streptomycin (100 µg·mL⁻¹). And the microplates were kept in incubator for 24 h (37 °C, 5% CO₂). Before treatment, all the medium were exchanged with the fresh supplemented medium. The tested compounds dissolved in DMSO were treated at concentration of 100, 50, 25, 12.5, 6.25, 3.13 and 1.56 µmol in triplicate. The microplates were kept in incubator for 24 h (37 °C, 5% CO₂). 20 µL of the MTT solution in DPBS (5 mg·mL⁻¹) were added into each well of the microplate and the microplate were kept in incubator for 4 h (37 °C, 5% CO₂). All the medium were exchanged with 100 µL DMSO and the optical density were recorded at 570 nm. Erythromycin was treated as a positive control (IC₅₀ = 65.5 µmol).

Supporting References

- [1] a) H. C. Brown, K. S. Bhat, *J. Am. Chem. Soc.* **1986**, *108*, 5919–5923; b) K. Fujita, M. Schlosser, *Helv. Chim. Acta.* **1982**, *65*, 1258–1263; c) Y. Kobayashi, Y. Kitano, F. Sato, *J. Chem. Soc., Chem. Commun.* **1984**, *20*, 1329–1330.
- [2] R. Xuan, H.-S. Oh, Y. Lee, H.-Y. Kang, *J. Org. Chem.* **2008**, *73*, 1456–1461.
- [3] a) P. B. Shinde, A. R. Han, J. Cho, S. R. Lee, Y. H. Ban, Y. J. Yoo, E. J. Kim, E. Kim, M.-C. Song, J. W. Park, D. G. Lee, Y. J. Yoon, *J. Biotechnol.* **2013**, *168*, 142–148; b) A. R. Han, P. B. Shinde, J. W. Park, J. Cho, S. R. Lee, Y. H. Ban, Y. J. Yoo, E. J. Kim, E. Kim, S. R. Park, B. G. Kim, D. G. Lee, Y. J. Yoon, *Appl. Microbiol. Biot.* **2012**, *93*, 1147–1156.
- [4] W. S. Jung, A. R. Han, J. S. Hong, S. R. Park, C. Y. Choi, J. W. Park, Y. J. Yoon, *Appl. Microbiol. Biot.* **2007**, *76*, 1373–1381.
- [5] W.-H. Jiao, T.-T. Xu, H.-B. Yu, G.-D. Chen, X.-J. Huang, F. Yang, Y.-S. Li, B.-N. Han, X.-Y. Liu, H.-W. Lin, *J. Nat. Prod.* **2014**, *77*, 346–350.

Table S1. Biosynthetic gene sets in the engineered strains of *S. venezuelae* and their products.

Plasmid	Combination of genes	Products
pLRHAM2	<i>desVIII-desVII-desIII-desIV-oleL-oleU</i>	11, 12
pDQNV	<i>desVIII-desVII-desIII-desIV</i>	12
pDDSS	<i>desVIII-desVII-desIII-desIV-desI-desII-desV-desVI</i>	12, 13, 14, 15, 16
pLOLV2	<i>desVIII-desVII-desIII-desIV-oleV-oleW-oleL-oleU</i>	12, 17, 18

Table S2. ¹³C- and ¹H-NMR data of isolated macrolactam glycosides in CD₃OD at 125 MHz and 500 MHz, respectively.

No.	11		12^a		13		16		17	
	δ_C	δ_H (m, <i>J</i> in Hz)	δ_C	δ_H (m, <i>J</i> in Hz)	δ_C	δ_H (m, <i>J</i> in Hz)	δ_C	δ_H (m, <i>J</i> in Hz)	δ_C	δ_H (m, <i>J</i> in Hz)
1	177.4		177.8		177.8		177.7		177.6	
2	46.1	2.69 (dq, 10.0, 7.0)	46.1	2.76 (dq, 9.9, 6.3)	46.2	2.76 (dq, 9.5, 6.5)	46.1	2.76 (m, 9.5, 6.5)	45.9	2.68 (dq, 10.0, 7.0)
3	91.2	3.48 (d, 9.5)	87.7	3.54 (d, 9.9)	87.5	3.54 (m, 8.5) ^b	88.4	3.59 (d, 10.0)	88.5	3.53 (d, 10.0)
4	34.3	1.33 (m)	34.2	1.32 (overlapped)	34.3	1.29 (m) ^b	34.3	1.30 (m)	34.2	1.25 (overlapped)
5	35.3	1.71 (t, 13.0)	35.5	1.71 (br t, 12.6)	35.5	1.72 (t, 12.5)	35.4	1.76 (t, 14.0)	35.2	1.66 (t, 13.5)
		1.41 (td, 13.0, 3.0)		1.41 (td, 12.6, 3.6)		1.42 (td, 12.5, 3.0)		1.45 (m)		1.40 (m, 13.5, 4.0)
6	46.4	2.48 (m)	46.4	2.47 (m)	46.4	2.47 (m)	46.5	2.48 (m)	46.4	2.48 (m)
7	207.6		207.9		208.0		207.9		207.4	
8	126.5	6.44 (d, 16.0)	126.6	6.44 (d, 15.3)	126.6	6.44 (d, 15.5)	126.6	6.44 (d, 15.5)	126.6	6.44 (d, 16.0)
9	149.7	6.72 (dd, 15.5, 5.5)	149.5	6.72 (dd, 16.2, 6.3)	149.5	6.72 (dd, 15.5, 5.5)	149.6	6.72 (dd, 16, 5.5)	149.5	6.72 (dd, 16.0, 6.0)
10	39.6	2.73 (m)	39.7	2.73 (m)	39.7	2.73 (m)	39.7	2.73 (m)	39.6	2.71 (m)
11	51.9	3.97 (m)	51.9	3.97 (ddd, 9.0, 5.3,	51.9	3.97 (m)	51.9	3.97 (m) ^b	51.9	3.96 (m)
12	27.2	1.52 (m)	27.2	1.52 (m)	27.2	1.52 (m)	27.2	1.52 (m)	27.2	1.52 (m)
13	11.5	0.93 (t, 7.5)	11.5	0.93 (t, 7.2)	11.5	0.93 (t, 7.0)	11.5	0.93 (t, 7.0)	11.5	0.93 (t, 7.0)
14	17.7 ^b	1.24 (overlapped) ^b	17.5	1.34 (d, 7.2)	17.6 ^b	1.34 (d, 7.0)	17.4	1.33 (d)	17.6 ^b	1.22 (d, 6.5)
15	17.9	1.00 (d, 6.5)	17.9 ^b	0.97 (d, 7.2)	17.9	0.97 (d, 7.0)	18.0	1.04 (d, 7.0)	17.7 ^b	0.98 (d, 6.0)
16	17.7 ^b	1.23 (overlapped) ^b	17.7	1.20 (d, 7.2)	17.7 ^b	1.20 (d, 6.5)	17.7	1.23 (d, 6.5)	17.7 ^b	1.21 (d, 7.0)
17	10.0	1.07 (d, 6.5)	10.0	1.07 (d, 6.3)	10.0	1.07 (d, 6.5)	10.0	1.07 (d, 7.5)	10.0	1.07 (d, 7.0)
1'	105.1	4.67 (br s)	105.1	4.27 (d, 8.1)	105.4	4.20 (d, 7.5)	106.4	4.39 (d, 8.0)	102.7	4.47 (dd, 9.5, 1.5)
2'	72.5 ^b	3.92 (br s)	76.0	3.16 (dd, 8.1, 9.0)	77.5	3.05 (t, 8.5)	79.6	3.96 (m) ^b	40.7	2.17 (ddd, 12.0, 5.5, 1.5)
										1.43 (m)
3'	72.4 ^b	3.59 (dd, 9.5, 3.0)	78.1	3.28 (t, 9.0)	72.5	3.54 (m, 8.5) ^b	206.9		72.3	3.48 (ddd, 12.0, 9.0, 5.5)
4'	73.7	3.40 (t, 9.5)	77.2	2.97 (t, 9.0)	42.2	1.90 (dd, 12.5, 5)	48.3	2.44 (d, 6.0)	78.5	2.87 (t, 9.0)
						1.27 (m)				
5'	70.4	3.71 (dq, 9.5, 7.0)	72.9	3.23 (dq, 9.0, 6.0)	68.8	3.54 (m, 8.5) ^b	68.9	3.70 (m, 12.5, 6.5)	73.1	3.17 (m, 9.2, 6.3)
6'	17.6 ^b	1.24 (overlapped) ^b	18.0 ^b	1.24 (d, 6.3)	21.2	1.19 (d, 6.5)	21.5	1.32 (d)	18.2	1.25 (d, 6.0)

^a ¹H- and ¹³C-NMR spectra were measured at 900 MHz and 225 MHz, respectively.^b Similar values from the same column may be interchanged.

Table S3. Comparison of the productivity of AZDM glycosides and their respective YC-17 analogues.

Sugar	macrolactam glycosides (mg L ⁻¹)	YC-17 analogues ^a (mg L ⁻¹)
L-rhamnosyl	0.58	0.50
D-quinovosyl	0.16	3.40
D-desosaminyll	trace	1.10
3- <i>O</i> -demethyl-D-chalcosyl	0.50	not detected
D-olivosal	0.26	0.10
L-olivosal	trace	0.30
3-keto-4,6-dideoxy-D-glucosyl	0.75	not detected
<i>N</i> -dedimethyl- <i>N</i> -acetyl-D-desosaminyll	trace	not detected
L-digitoxosal	not detected	not detected
D-boivinosyl	not detected	0.02

^aPreviously reported.^[3a]

Table S4. *In vitro* antibacterial activities of macrolactam glycosides.

No.	MIC (μM) ^a			
	<i>E. faecium</i> ATCC19434	<i>E. faecium</i> P00558	<i>S. aureus</i> ATCC25923	<i>S. aureus</i> P00740
11	7.5	30.0	15.0	30.0
12	7.5	30.0	15.0	15.0
13	30.0	120.0	60.0	120.0
16	30.0	120.0	60.0	120.0
17	30.0	>120.0	60.0	60.0
Erythromycin	30.0	>120.0	60.0	120.0

^a*E. faecium* ATCC 19434 and *S. aureus* ATCC 25923 are erythromycin-susceptible pathogens and *E. faecium* P00558 and *S. aureus* P00740 are clinically isolated erythromycin-resistant pathogens.

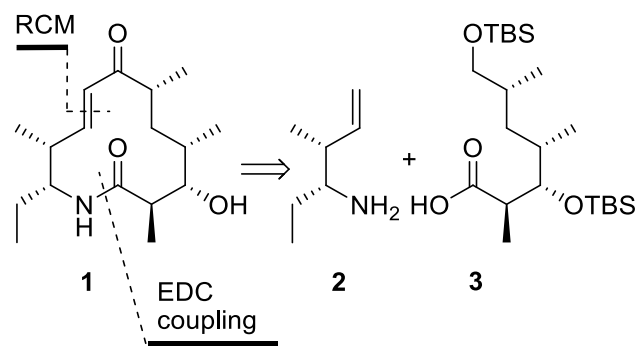
Table S5. *In vitro* antibacterial activities of lactams, counterpart lactones, and erythromycin.

Sugar	MIC (μM) ^a							
	macrolactam glycosides				macrolactone glycosides ^b			
	<i>E. faecium</i> ATCC19434	<i>E. faecium</i> P00558	<i>S. aureus</i> ATCC25923	<i>S. aureus</i> P00740	<i>E. faecium</i> ATCC19434	<i>E. faecium</i> P00558	<i>S. aureus</i> ATCC25923	<i>S. aureus</i> P00740
L- rhamnosyl	7.5	30.0	15.0	30.0	11.3	5.6	5.6	5.6
D-quinovosyl	7.5	30.0	15.0	15.0	11.3	11.3	22.6	22.6
D-olivoyl	30.0	>120.0	60.0	60.0	23.2	46.5	46.5	23.2
Erythromycin	–	–	–	–	30.0	>120.0	60.0	120.0

^a*E. faecium* ATCC 19434 and *S. aureus* ATCC 25923 are erythromycin-susceptible pathogens and *E. faecium* P00558 and *S. aureus* P00740 are clinically isolated erythromycin-resistant pathogens.

^bPreviously reported.^[3a]

Scheme S1. Retrosynthetic analysis of AZDM **1**



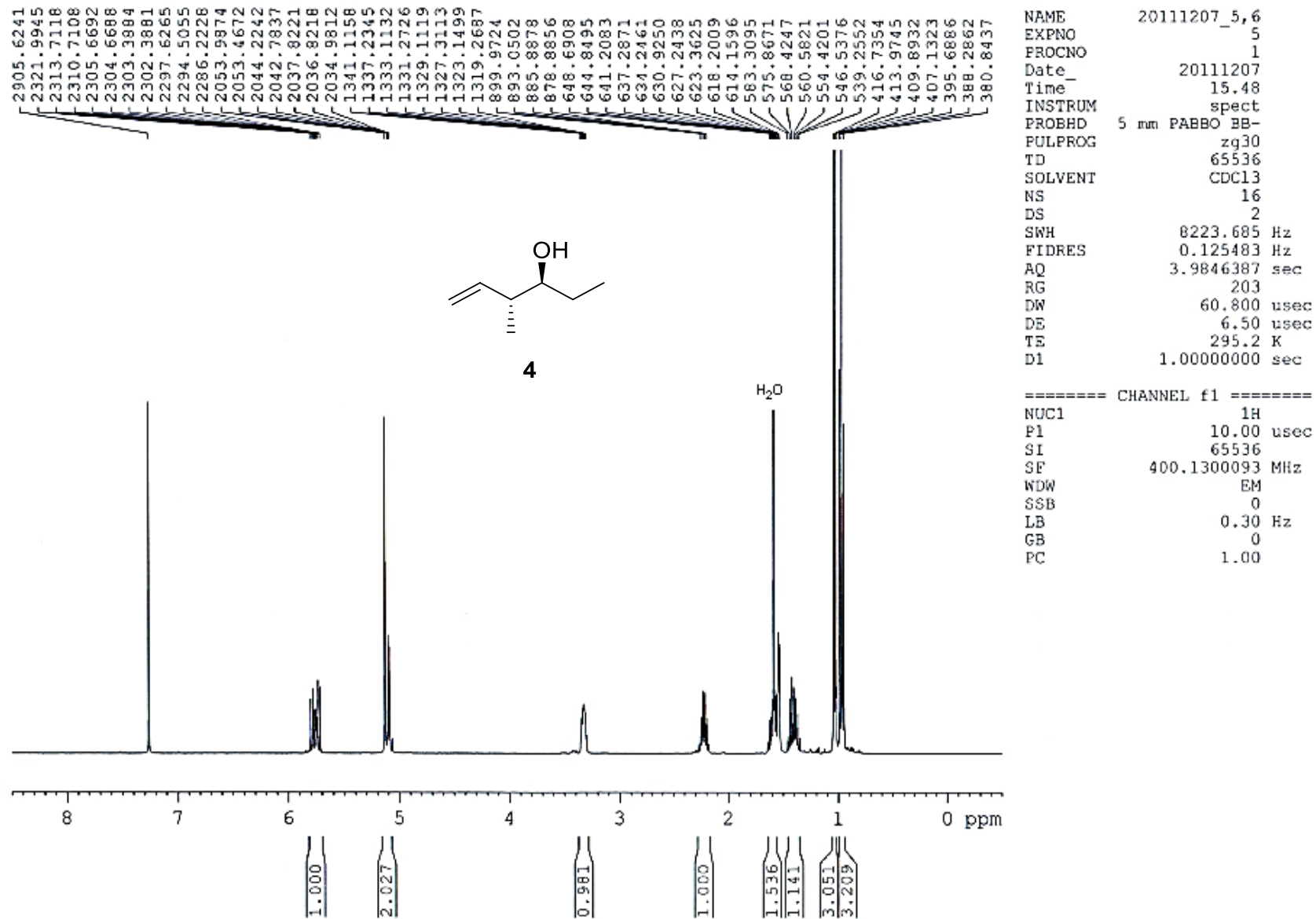


Figure S1. ¹H NMR spectrum of **4** in CDCl₃ at 400 MHz.

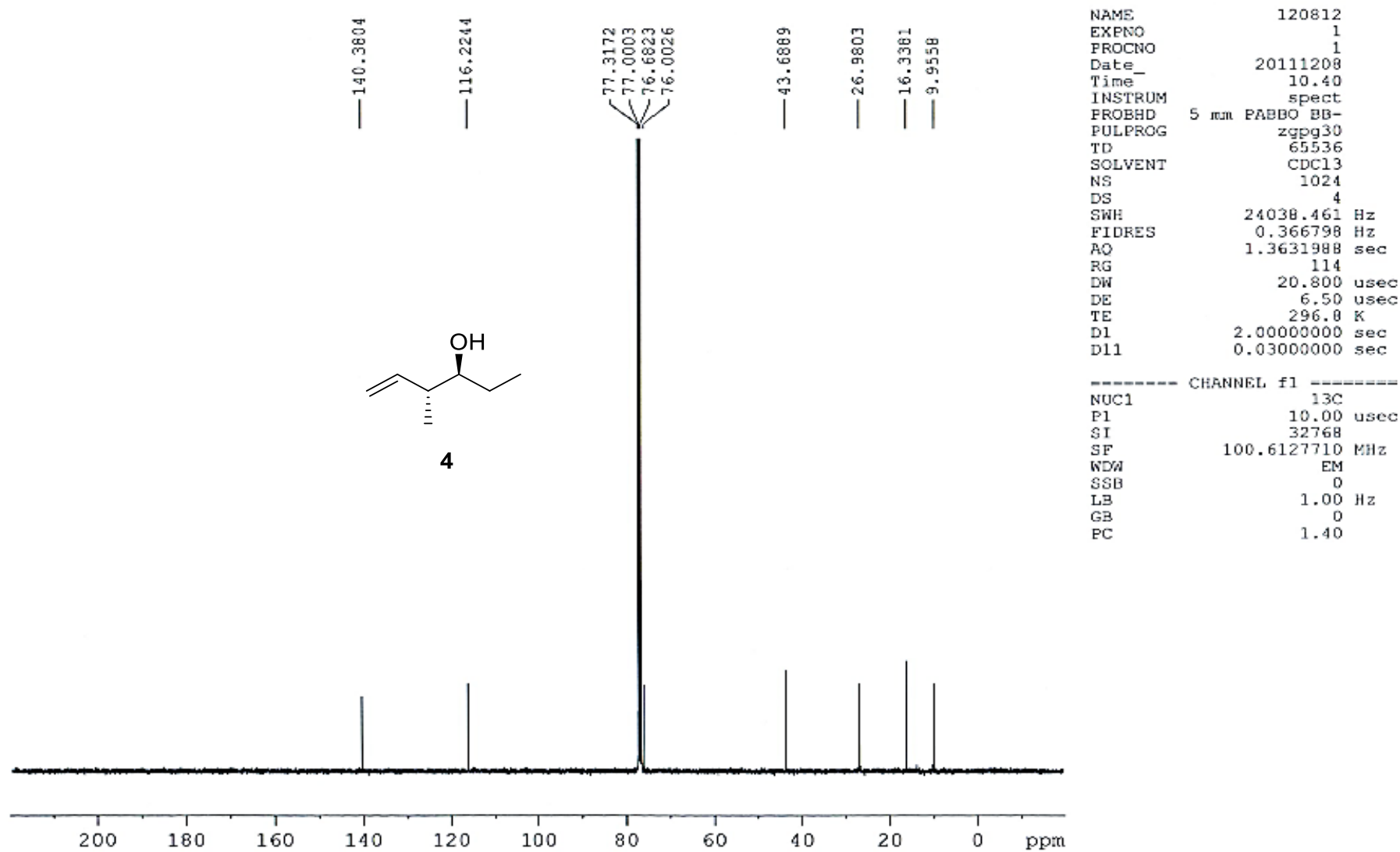


Figure S2. ¹³C NMR spectrum of **4** in CDCl₃ at 100 MHz.

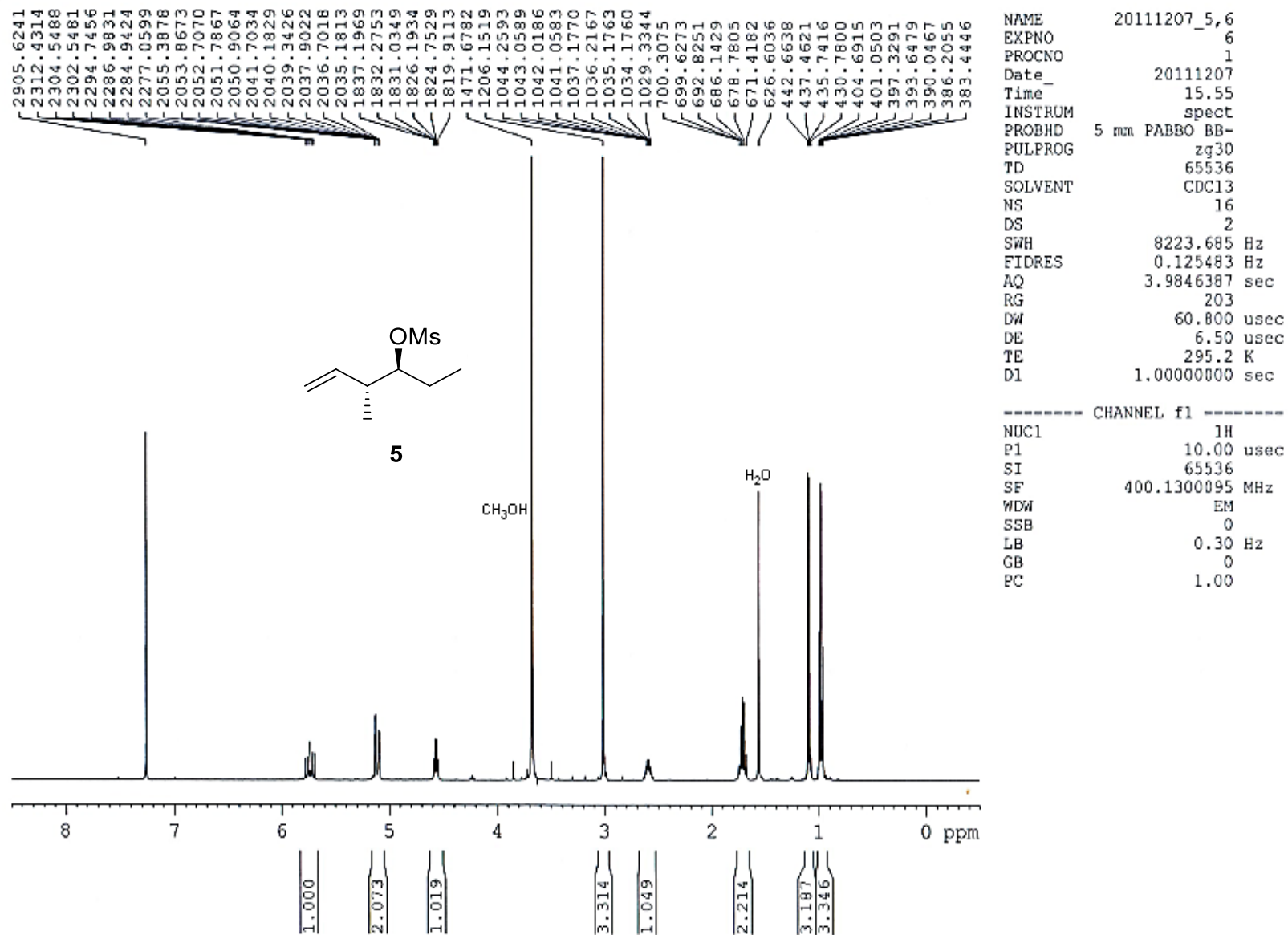


Figure S3. ^1H NMR spectrum of **5** in CDCl_3 at 400 MHz.

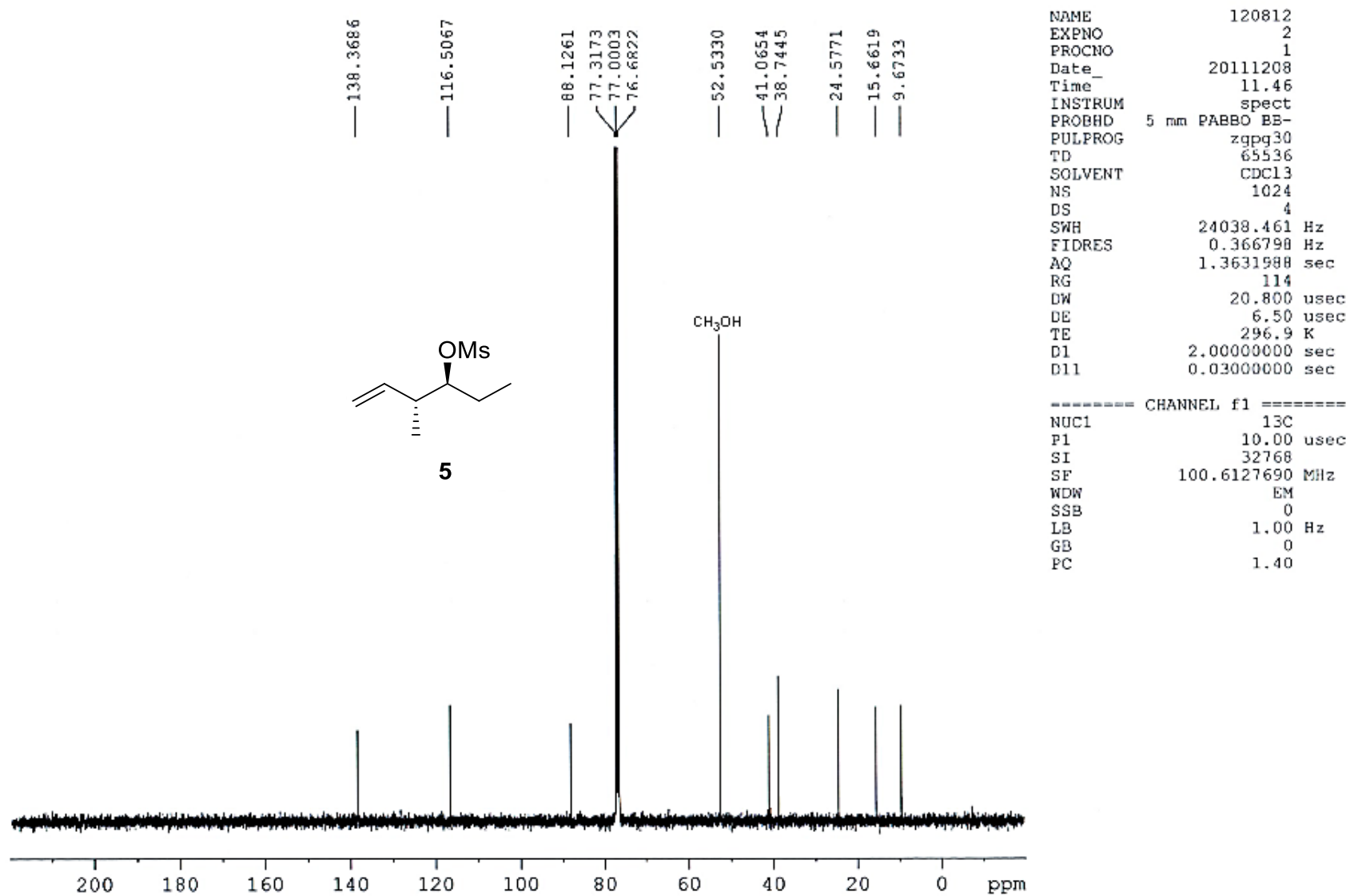


Figure S4. ¹³C NMR spectrum of **5** in CDCl₃ at 100 MHz.

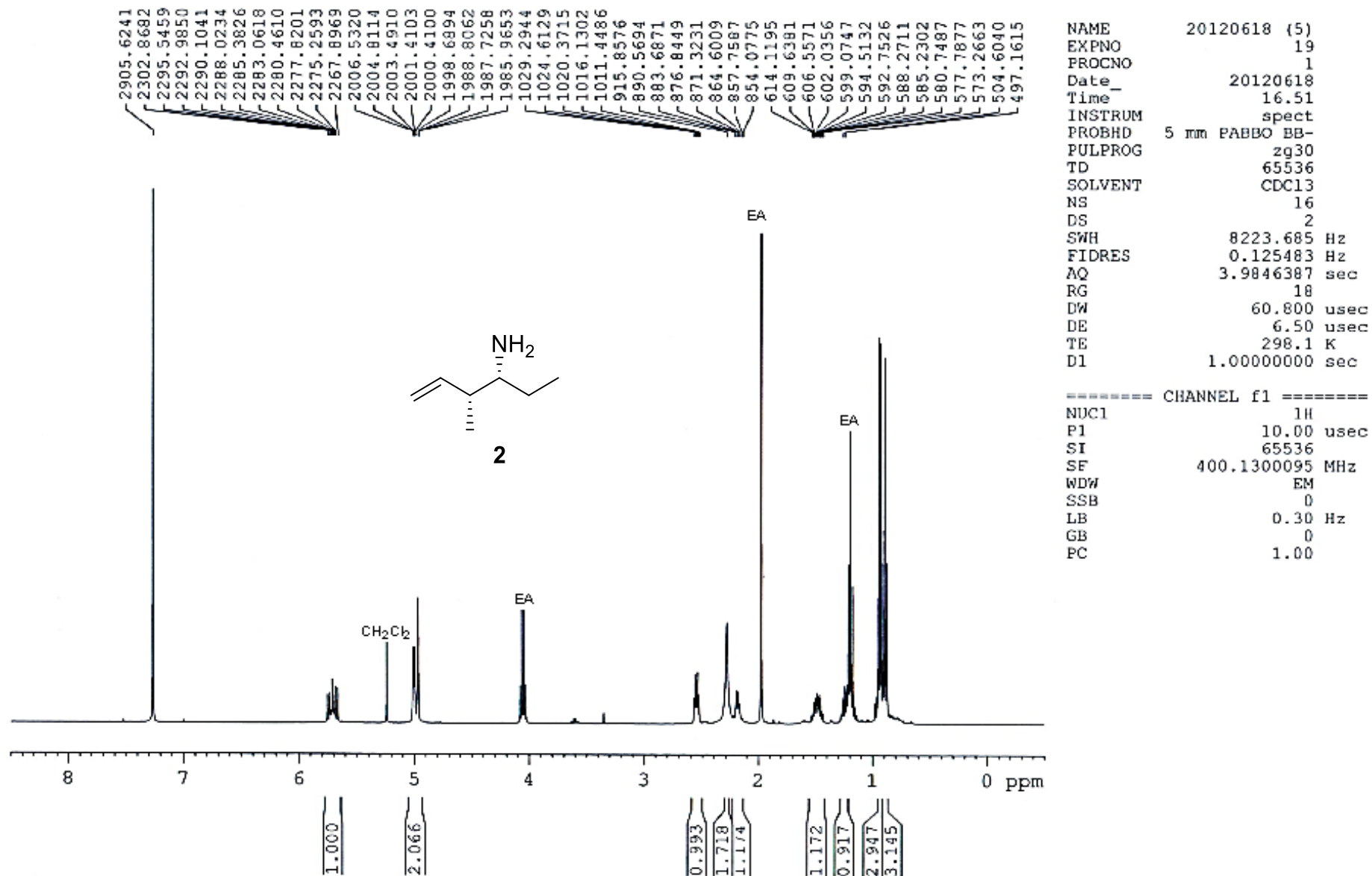


Figure S5. ¹H NMR spectrum of **2** in CDCl₃ at 400 MHz.

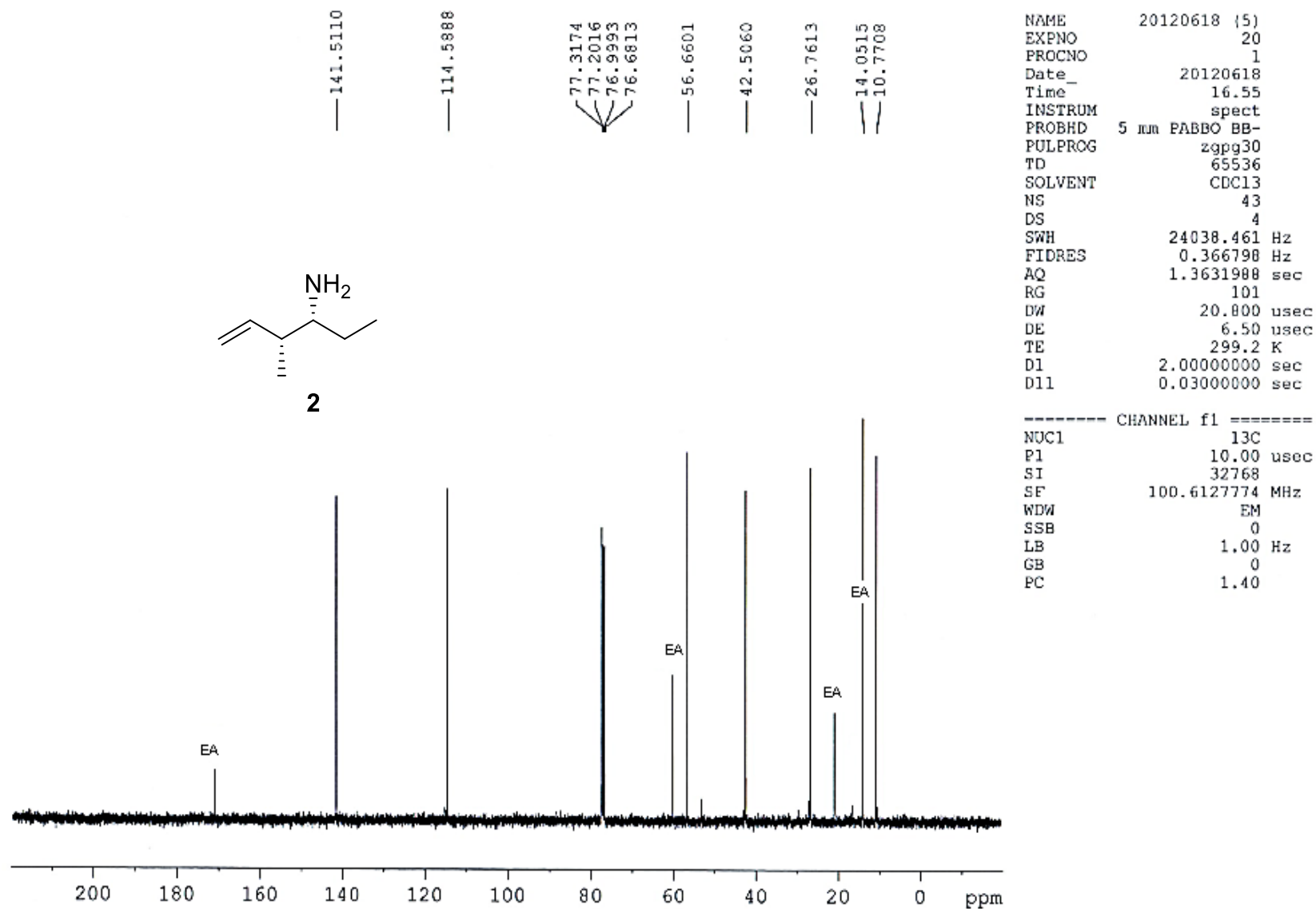


Figure S6. ^{13}C NMR spectrum of **2** in CDCl_3 at 100 MHz.

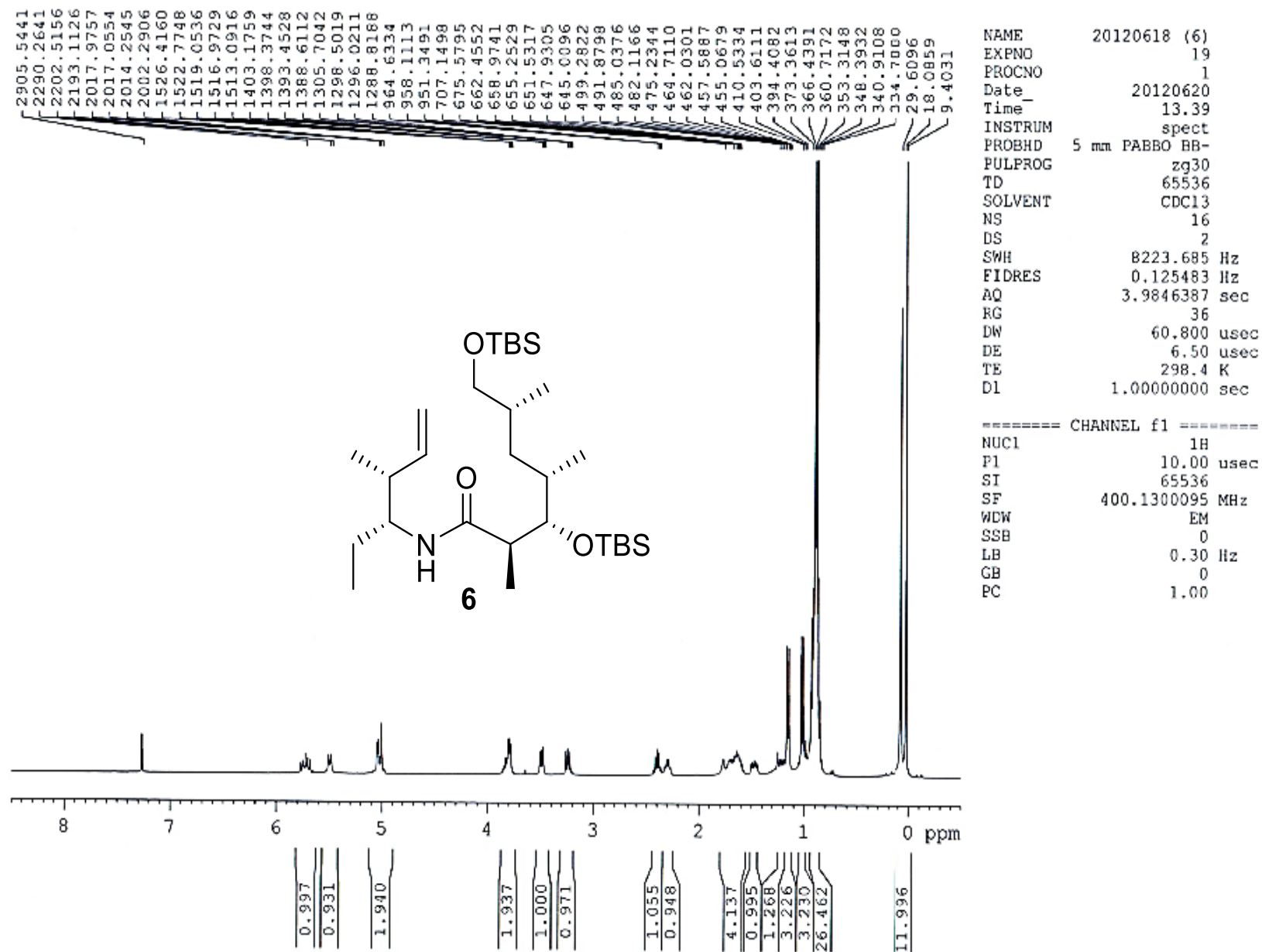


Figure S7. ¹H NMR spectrum of **6** in CDCl₃ at 400 MHz.

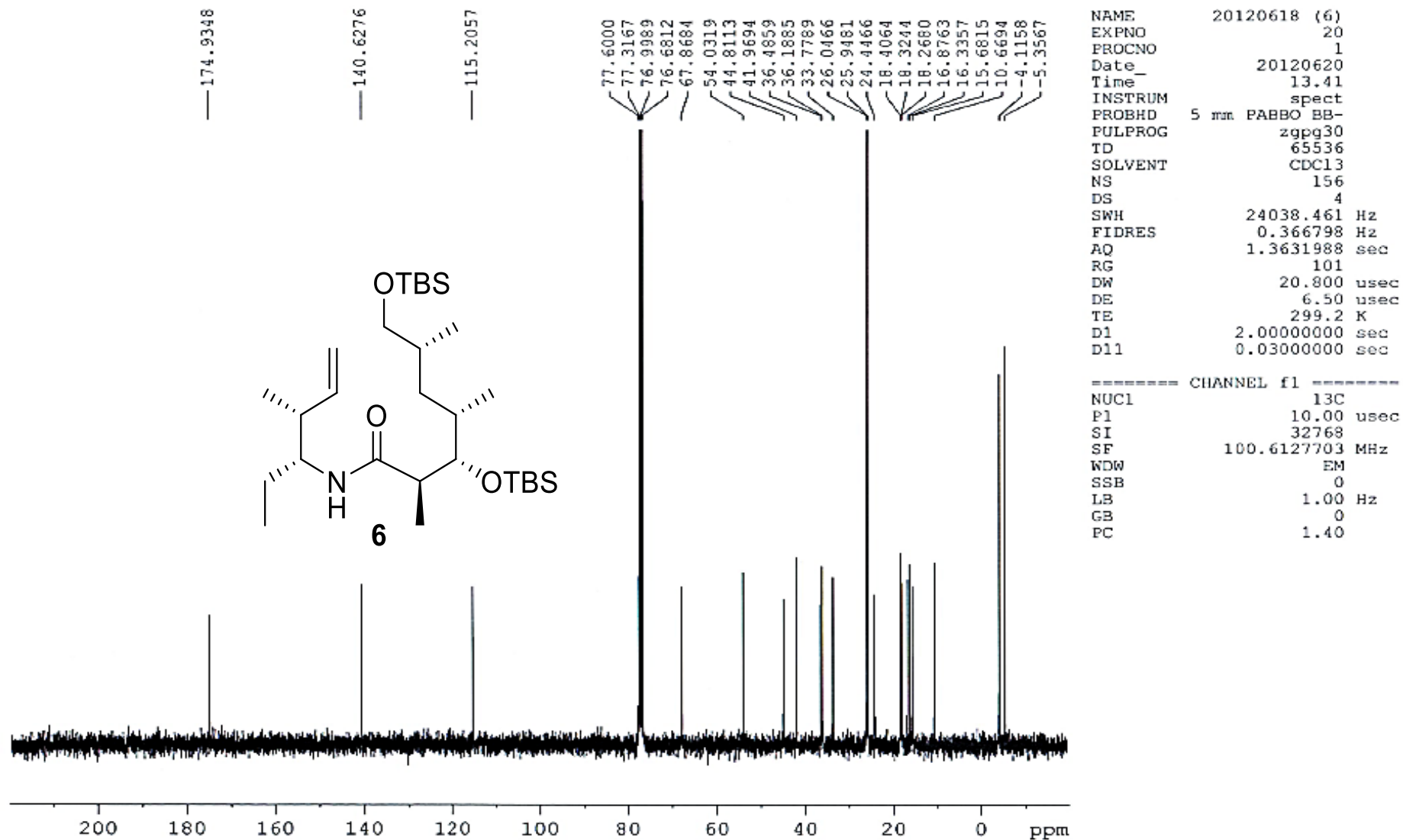


Figure S8. ¹³C NMR spectrum of **6** in CDCl₃ at 100 MHz.

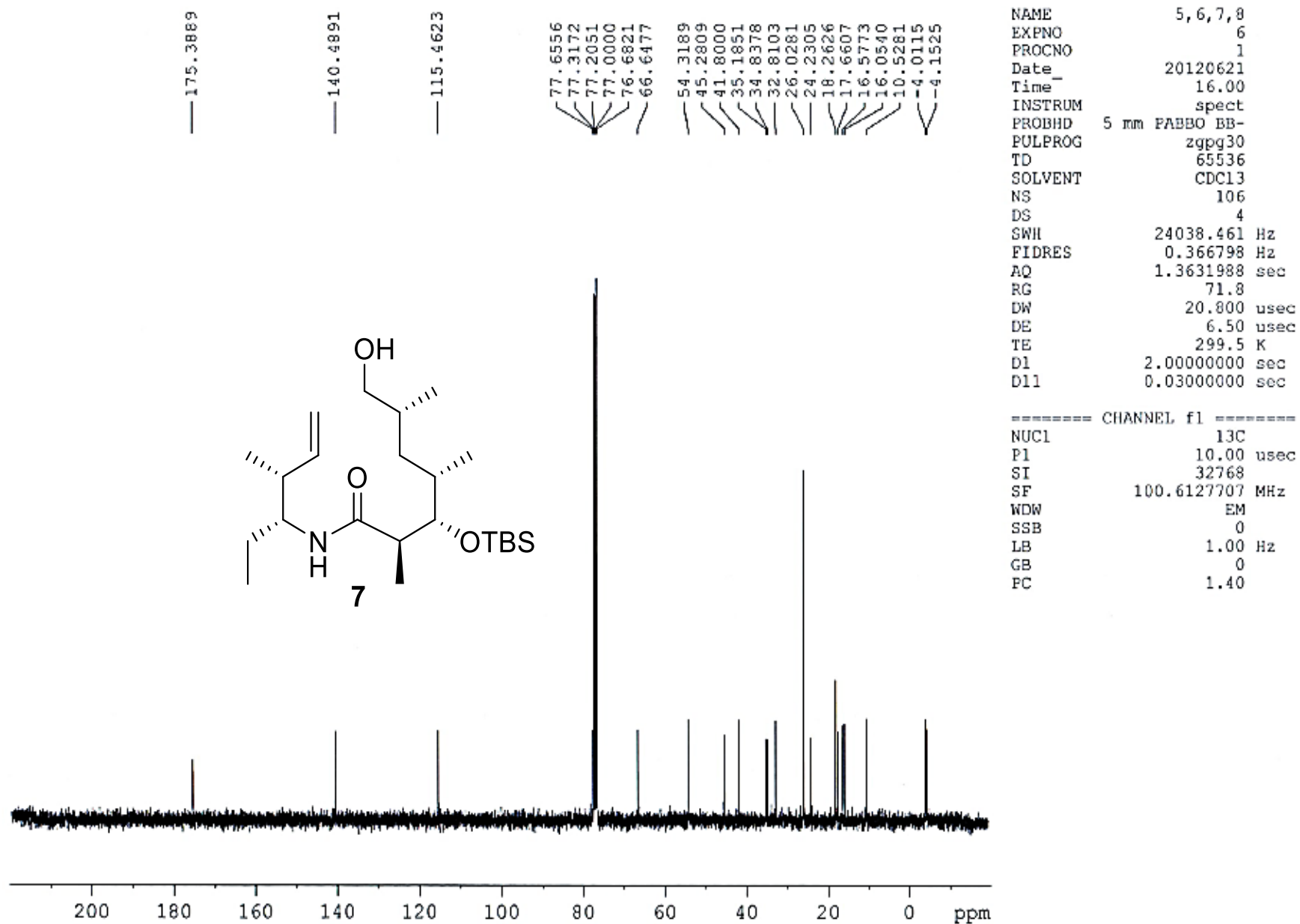
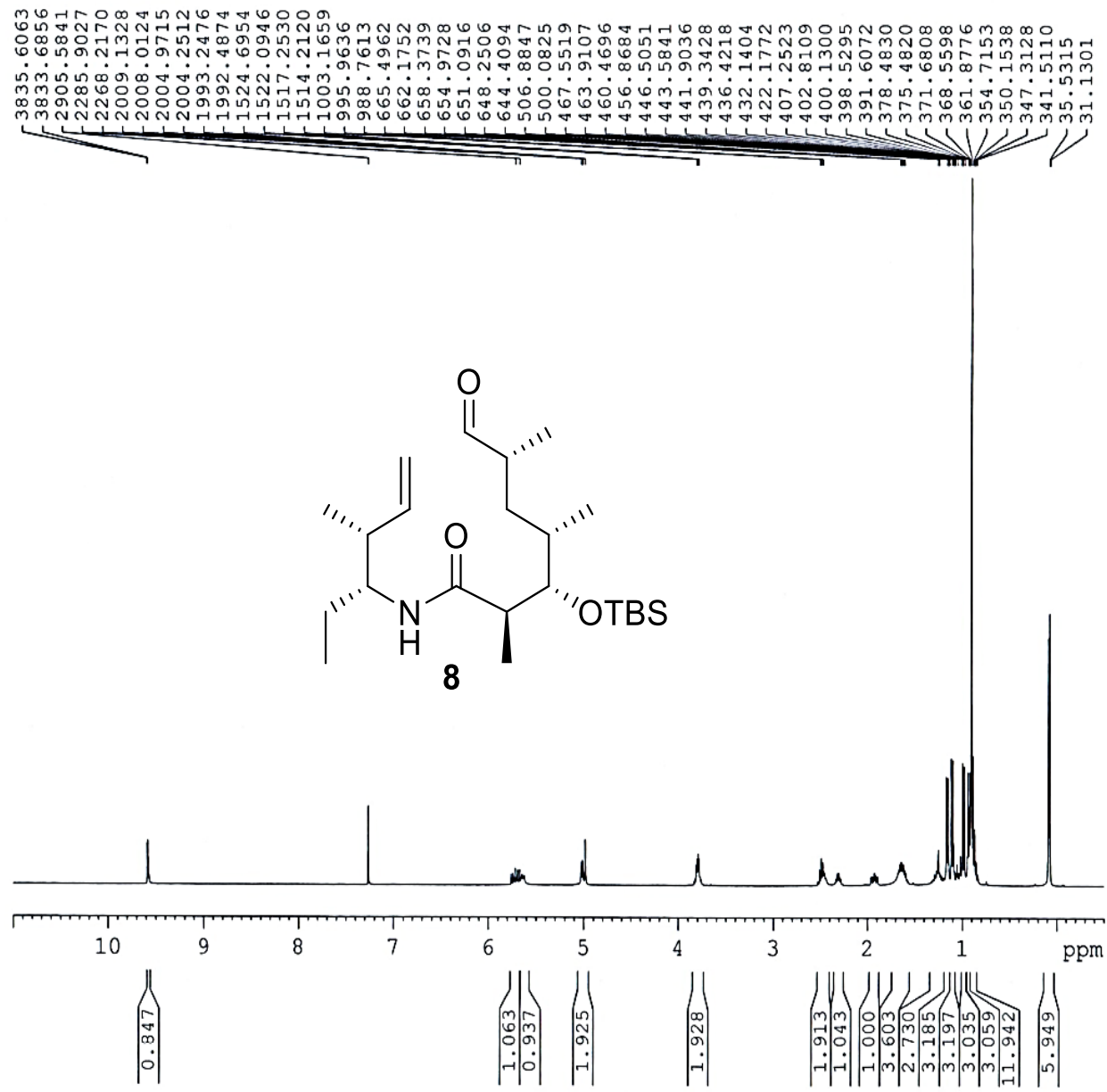


Figure S10. ¹³C NMR spectrum of **7** in CDCl₃ at 100 MHz.



```

NAME          20120720
EXPNO         1
PROCNO        1
Date_         20120720
Time          12.06
INSTRUM       spect
PROBHD        5 mm PABBO BB-
PULPROG       zg30
TD            65536
SOLVENT       CDC13
NS            16
DS            2
SWH           8223.685 Hz
FIDRES        0.125483 Hz
AQ            3.9846387 sec
RG            101
DW            60.800 usec
DE            6.50 usec
TE            299.0 K
D1            1.00000000 sec

```

```

===== CHANNEL f1 =====
NUC1          1H
P1            10.00 usec
SI            65536
SF            400.1300095 MHz
WDW           EM
SSB           0
LB            0.30 Hz
GB            0
PC            1.00

```

Figure S11. ¹H NMR spectrum of **8** in CDCl₃ at 400 MHz.

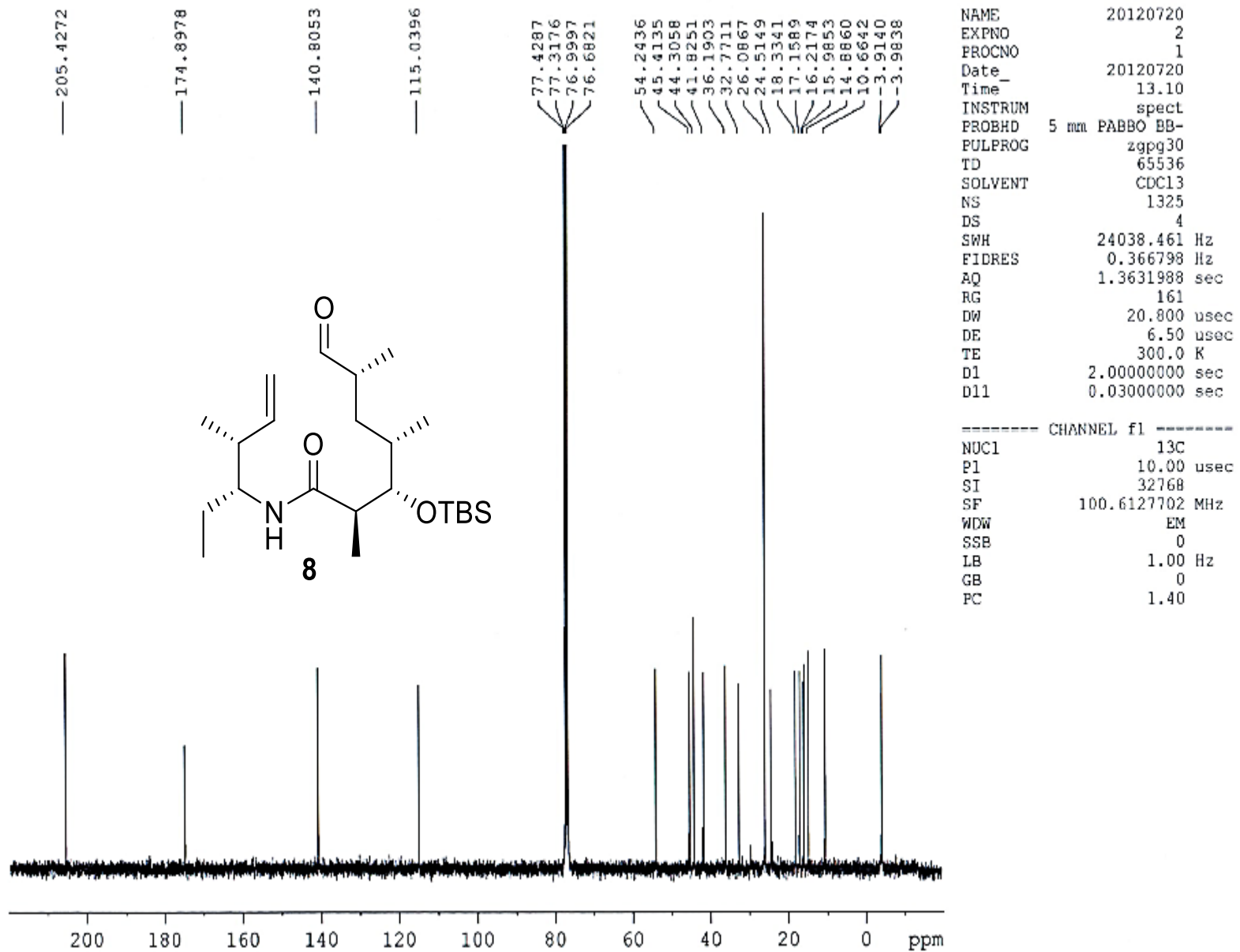


Figure S12. ¹³C NMR spectrum of **8** in CDCl₃ at 100 MHz.

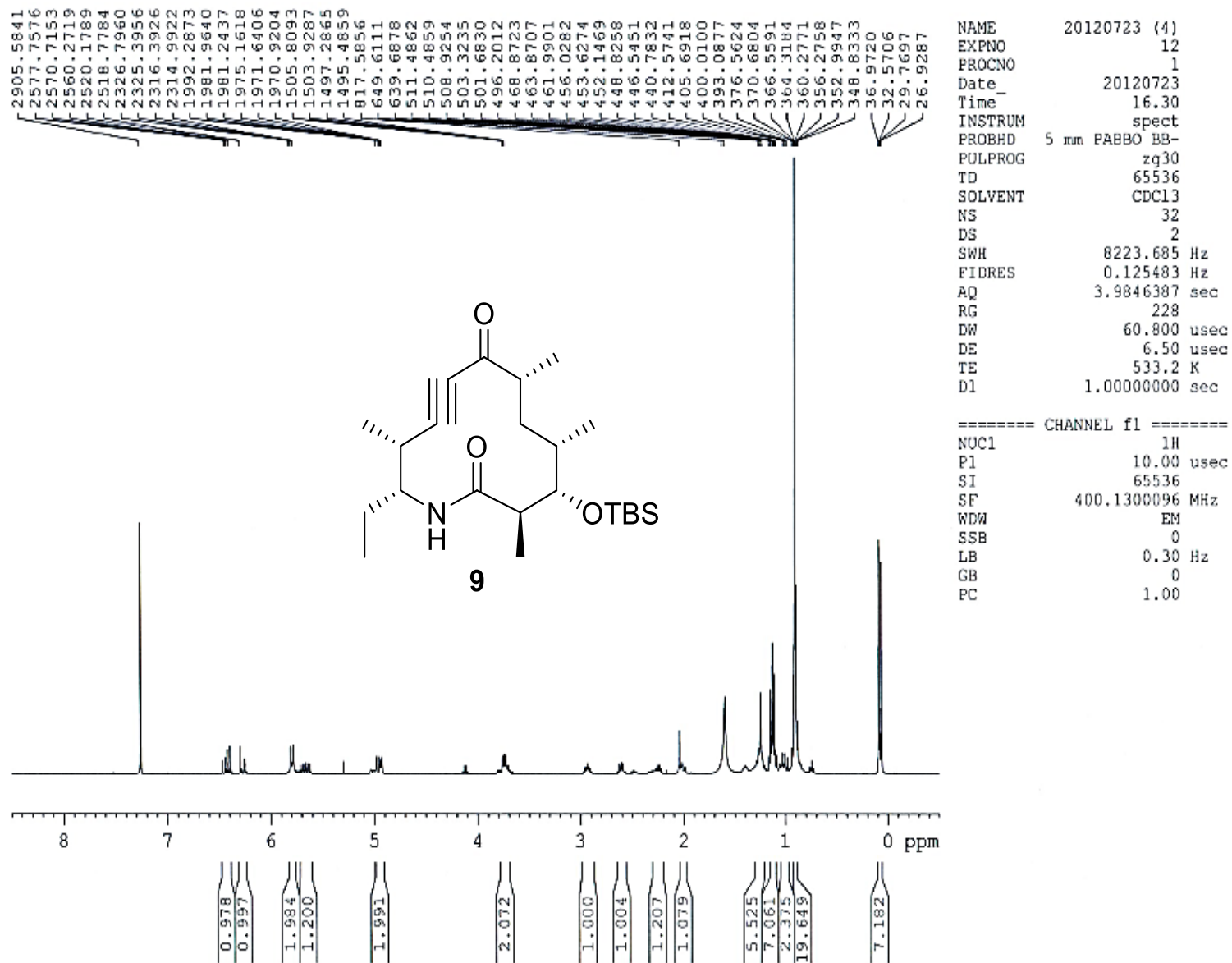


Figure S13. ^1H NMR spectrum of **9** in CDCl_3 at 400 MHz.

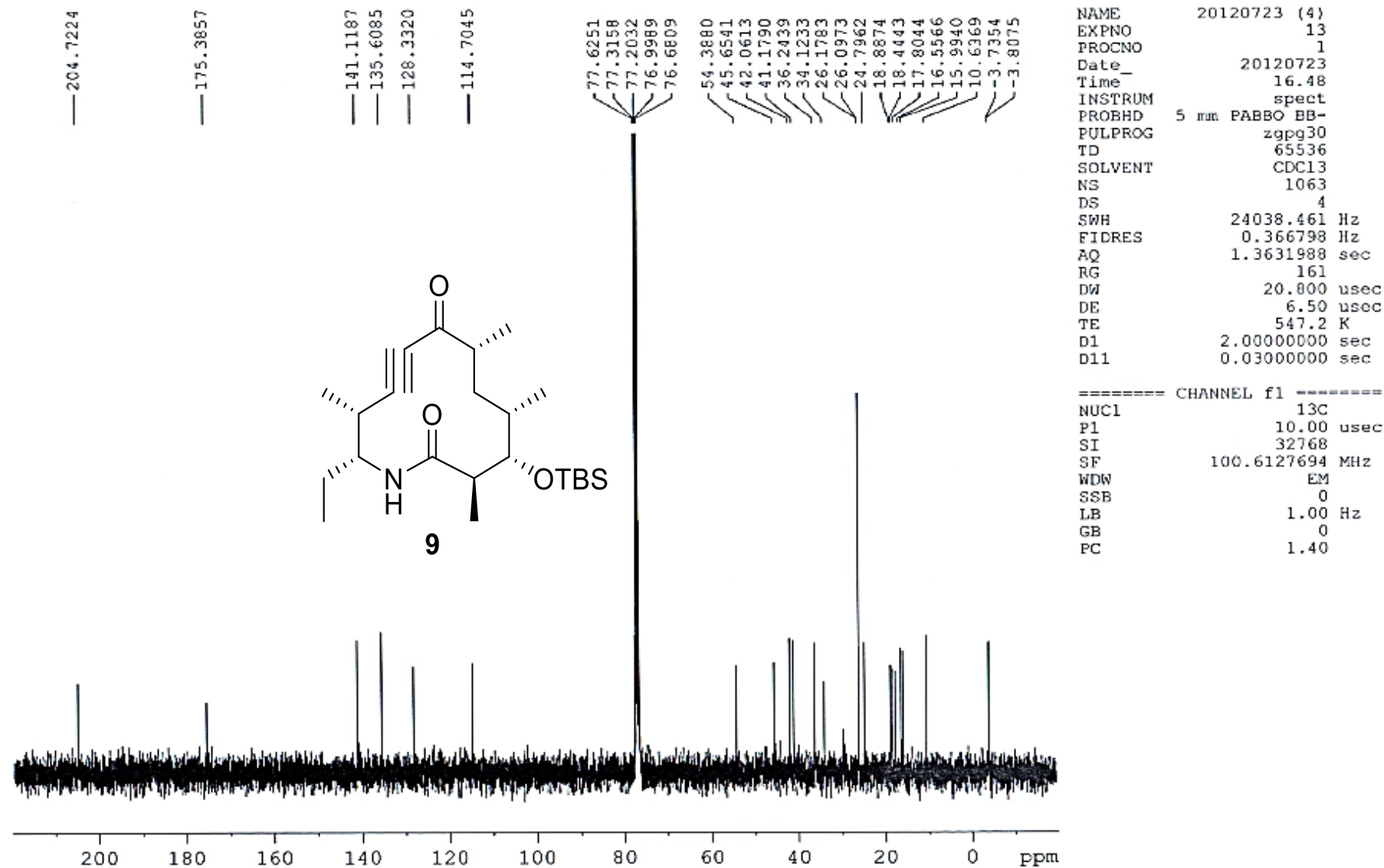


Figure S14. ¹³C NMR spectrum of **9** in CDCl₃ at 100 MHz.

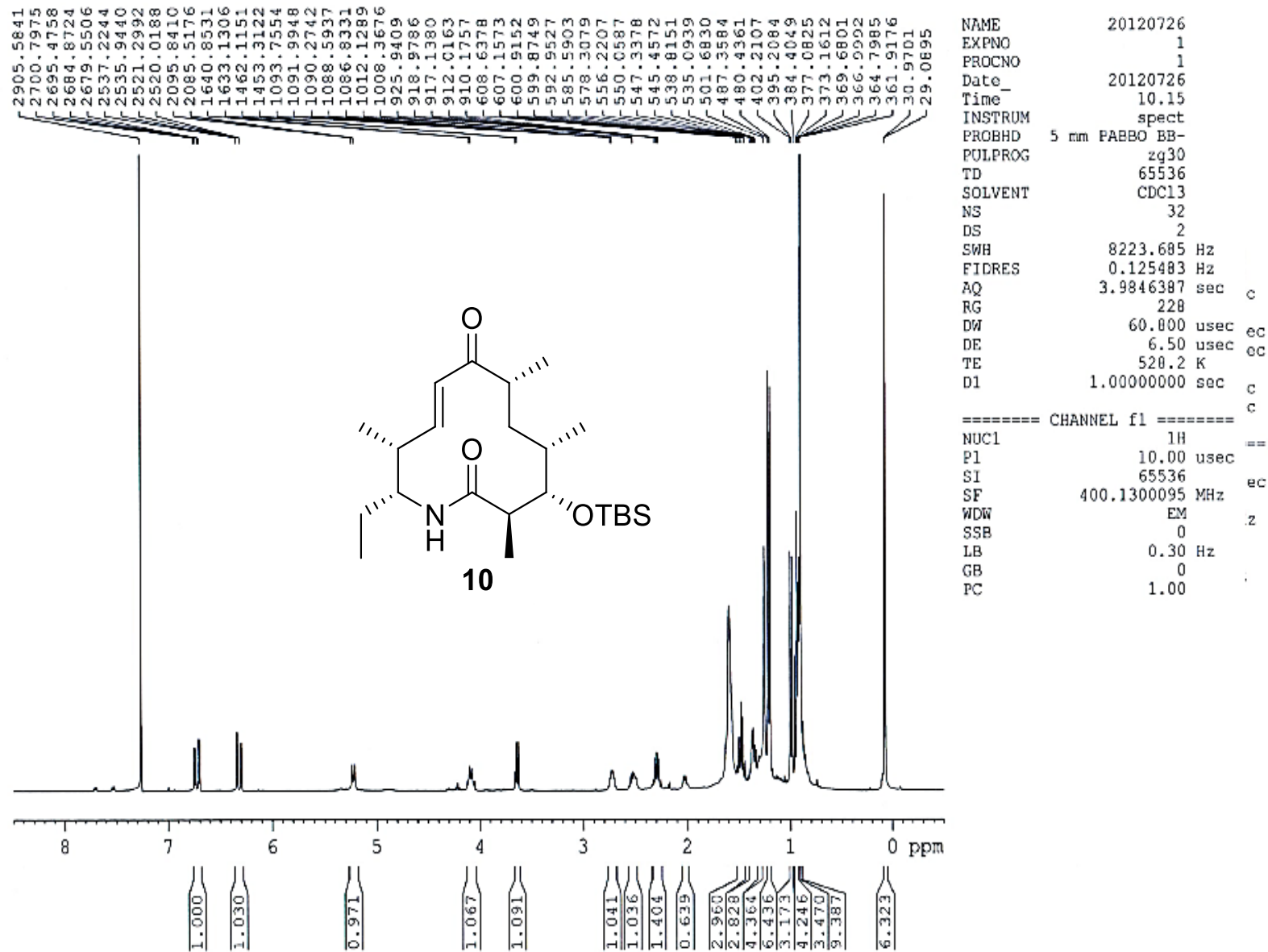


Figure S15. ^1H NMR spectrum of **10** in CDCl_3 at 400 MHz.

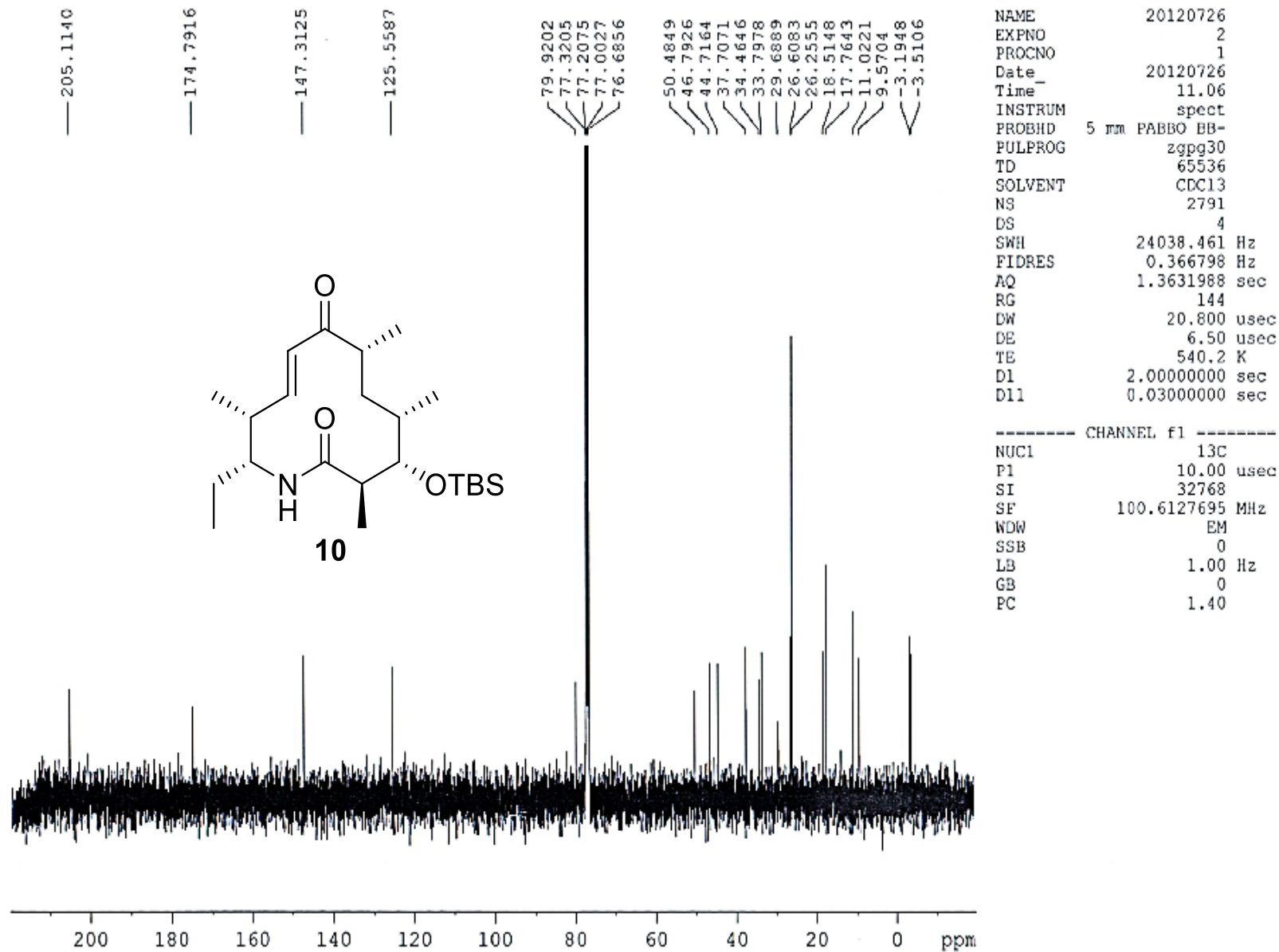


Figure S16. ¹³C NMR spectrum of **10** in CDCl₃ at 100 MHz.

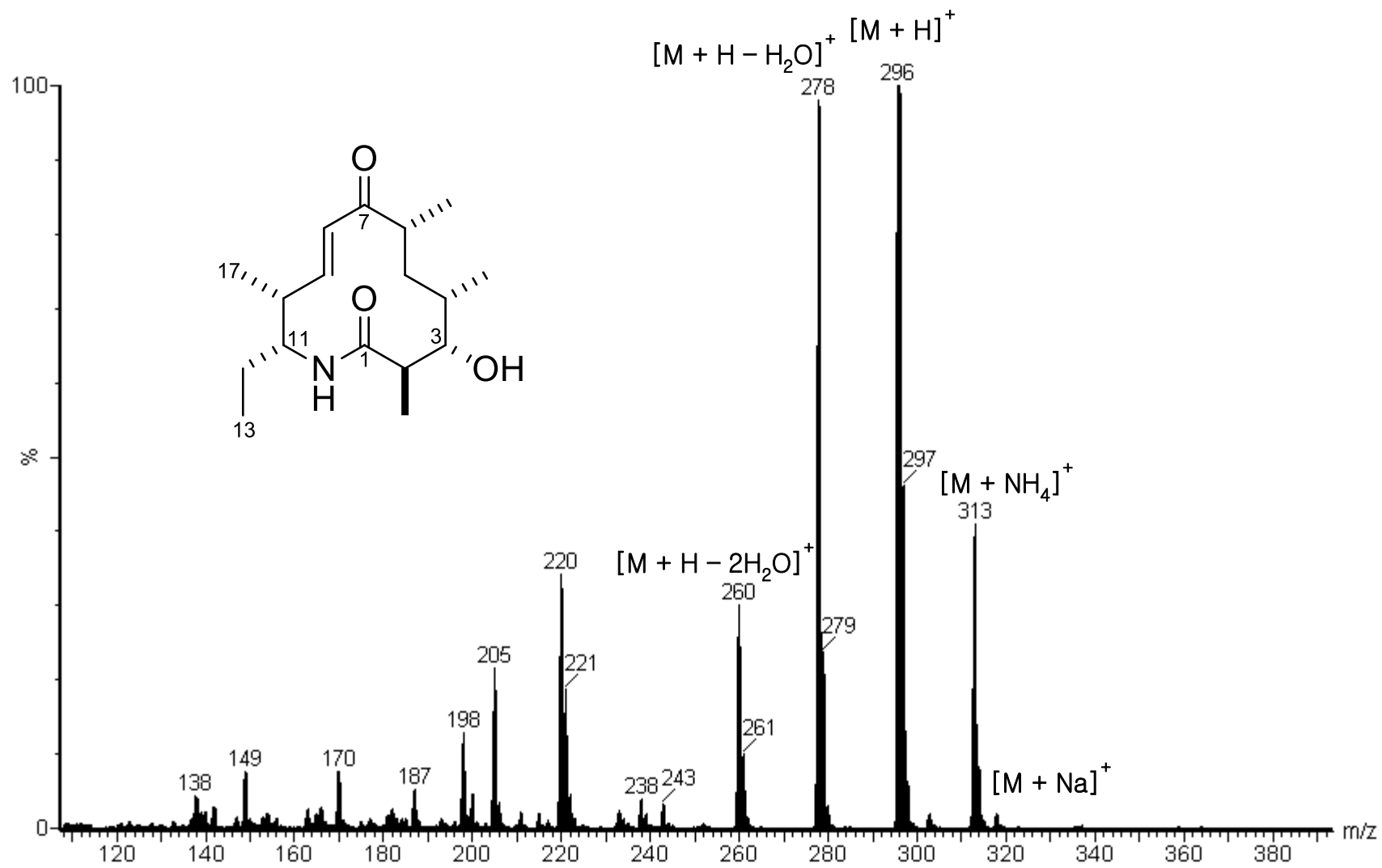


Figure S17. ESI-MS/MS spectrum of **1**.

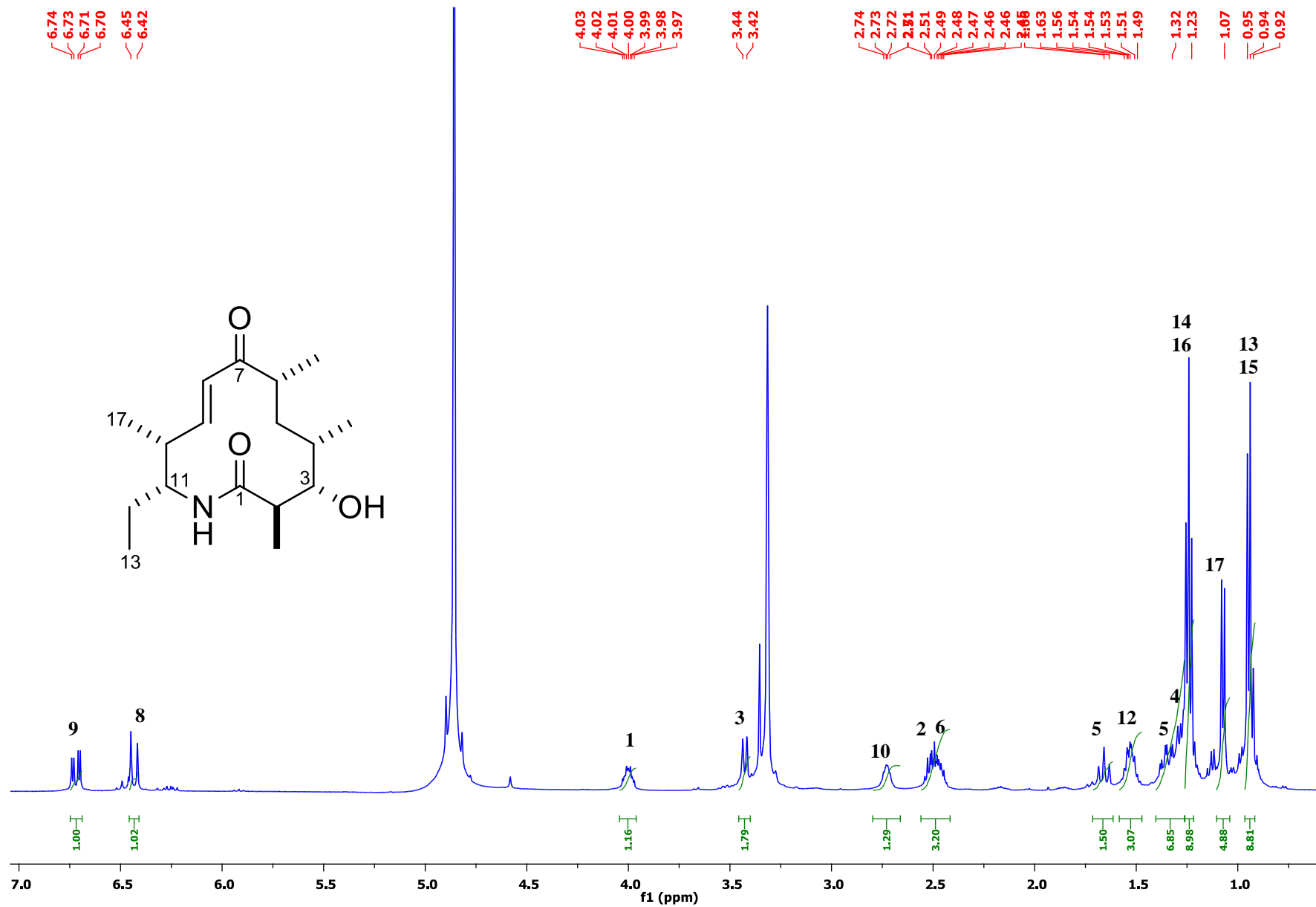


Figure S18. ¹H NMR spectrum of **1** in CD₃OD at 500 MHz.

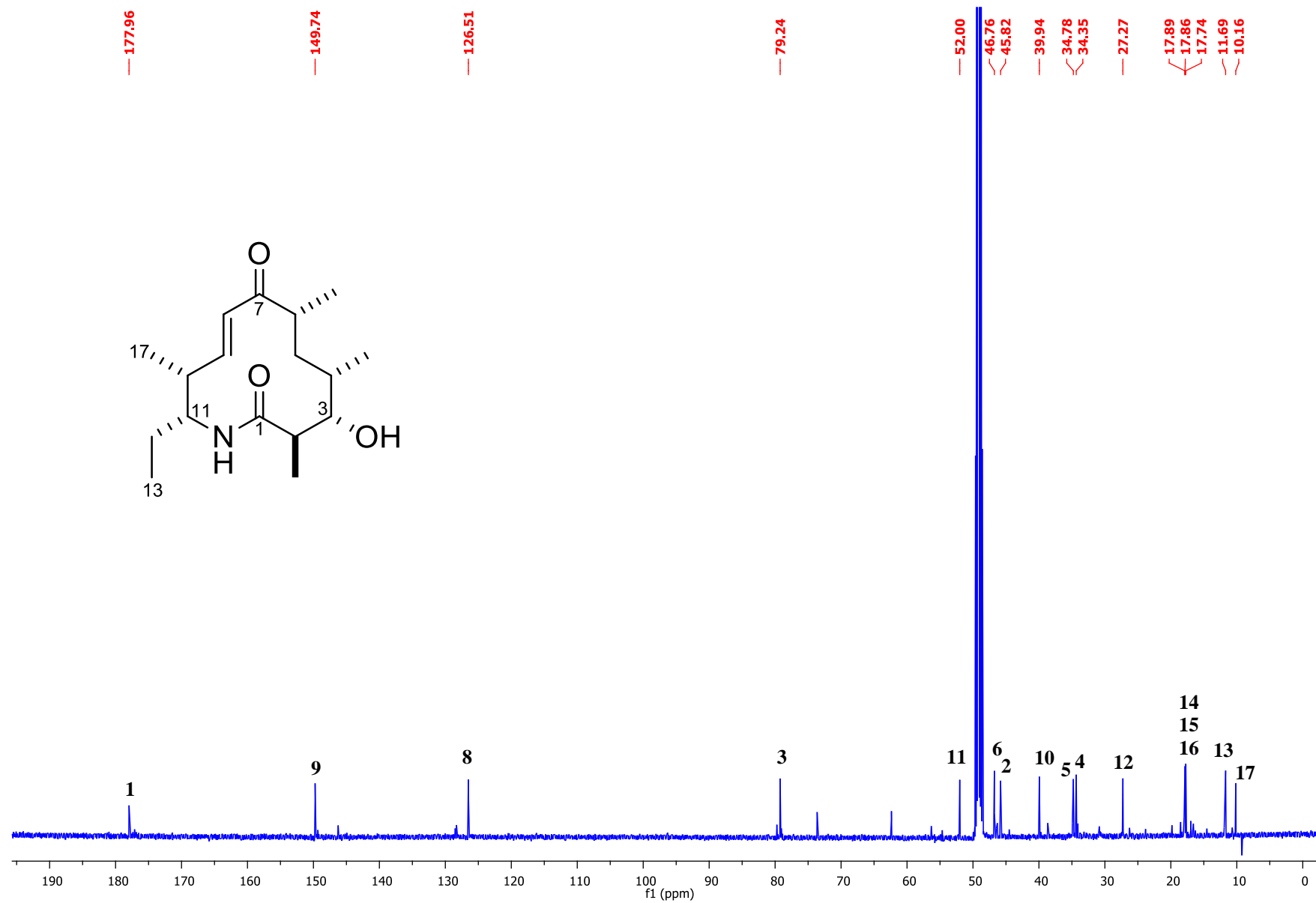


Figure S19. ^{13}C NMR spectrum of **1** in CD_3OD at 125 MHz.

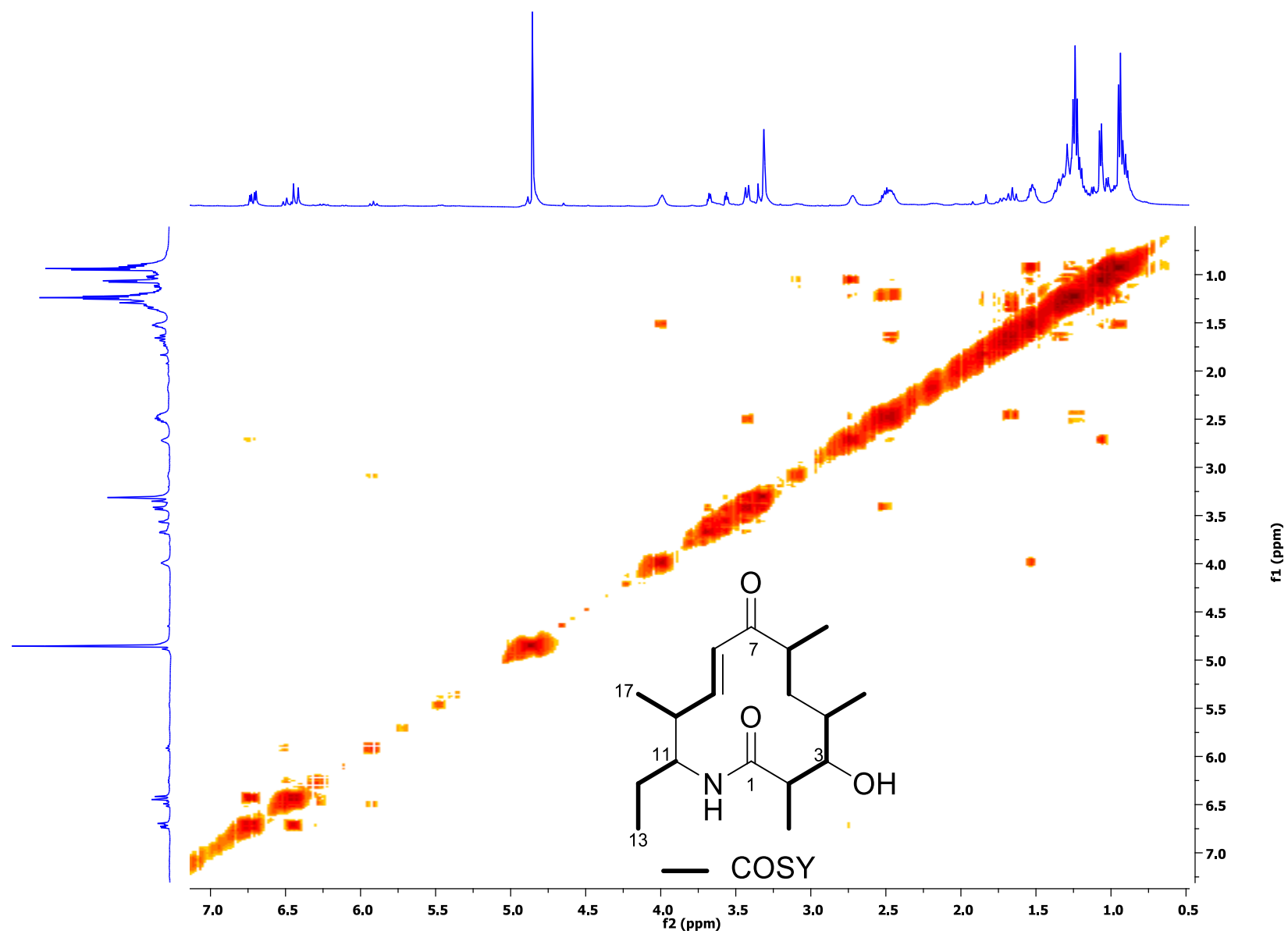


Figure S20. COSY spectrum of **1** in CD₃OD at 500 MHz.

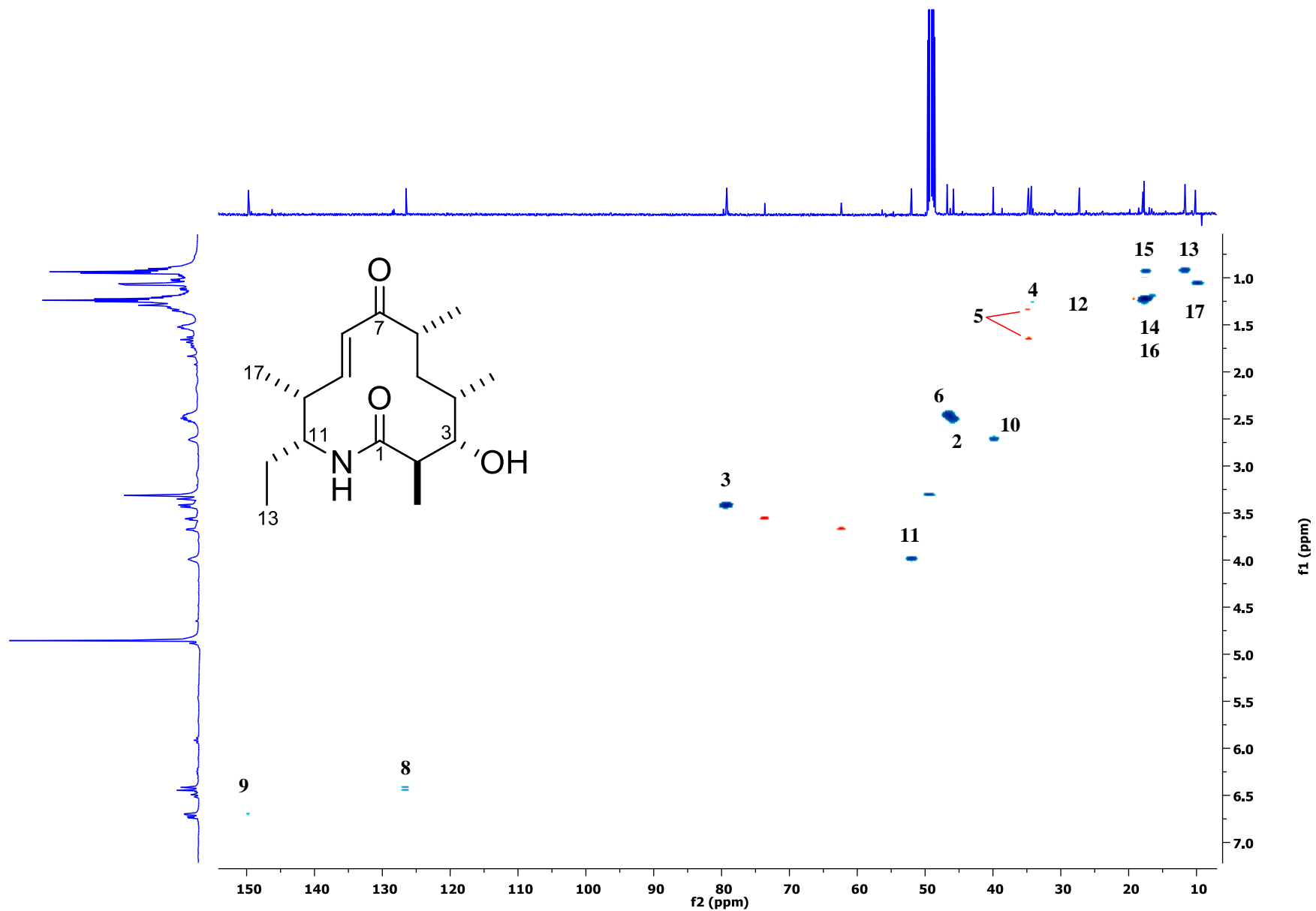


Figure S21. HSQC spectrum of **1** in CD₃OD at 500 MHz.

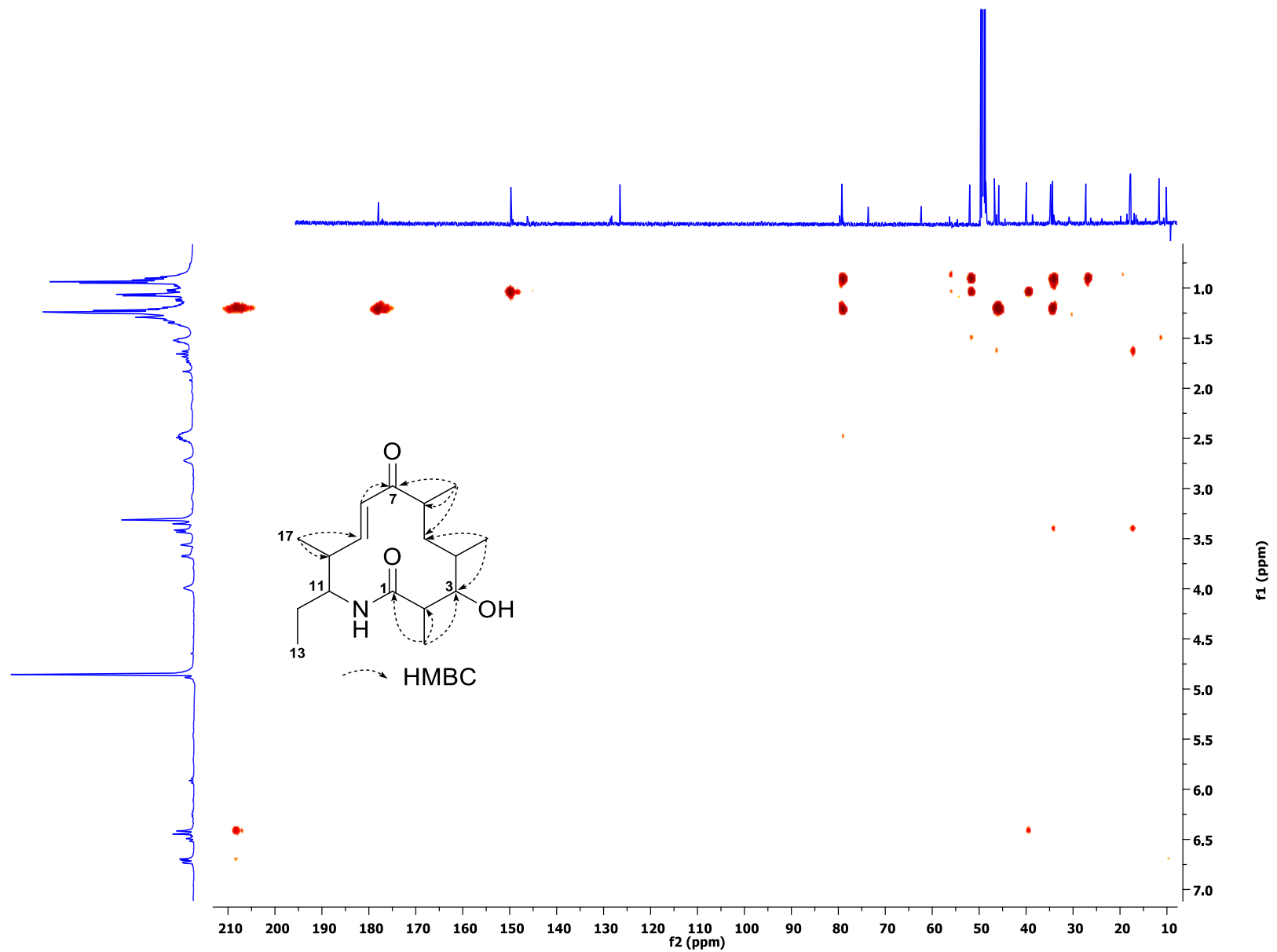


Figure S22. HMBC spectrum of **1** in CD₃OD at 500 MHz.

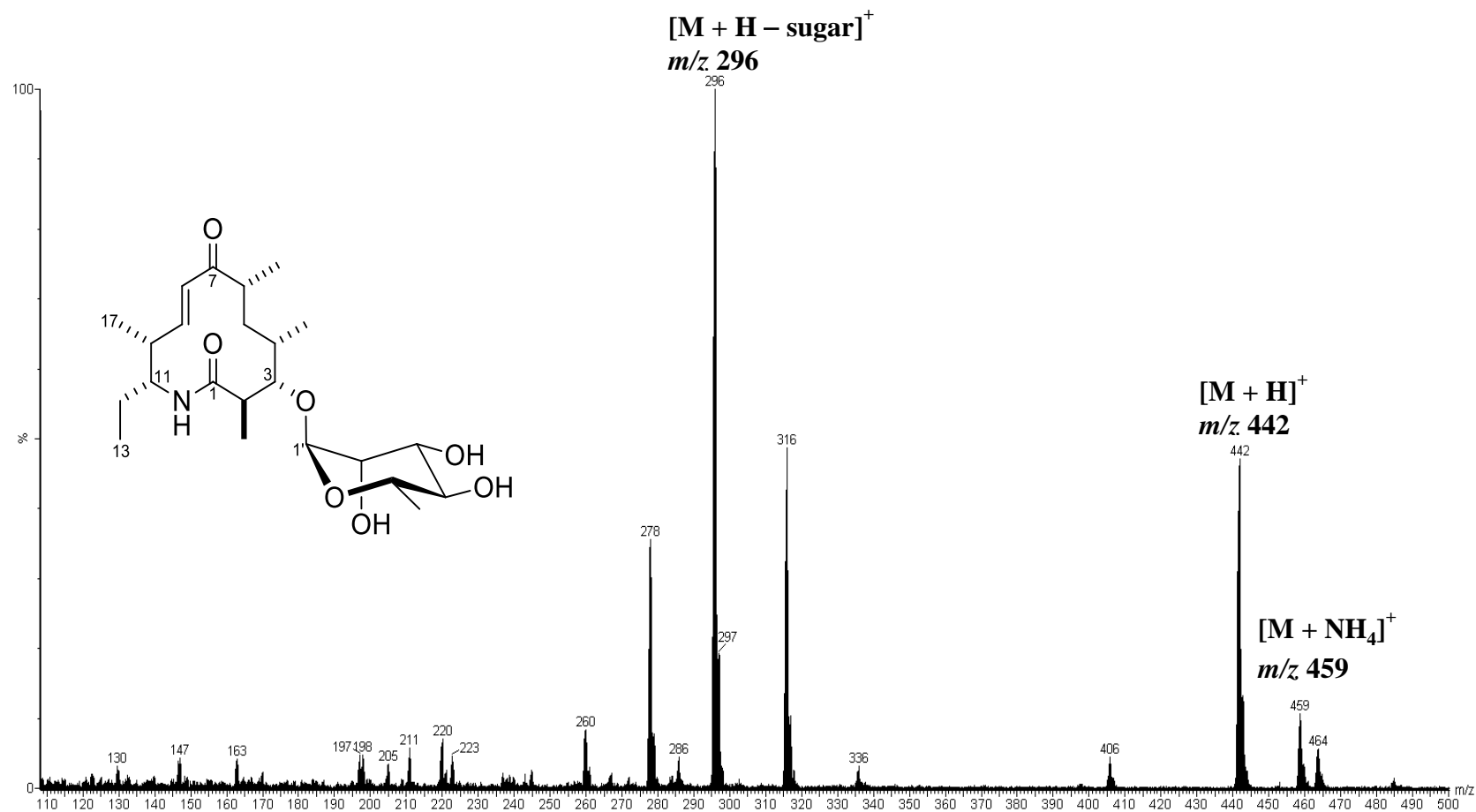


Figure S23. ESI-MS/MS spectrum of **11**.

Compound **11** displayed ammonium adduct ion at m/z 459 in the MS spectrum. MS/MS analysis showed the characteristic fragmentation pattern with the parent ion at m/z 442 and daughter ion at m/z 296.

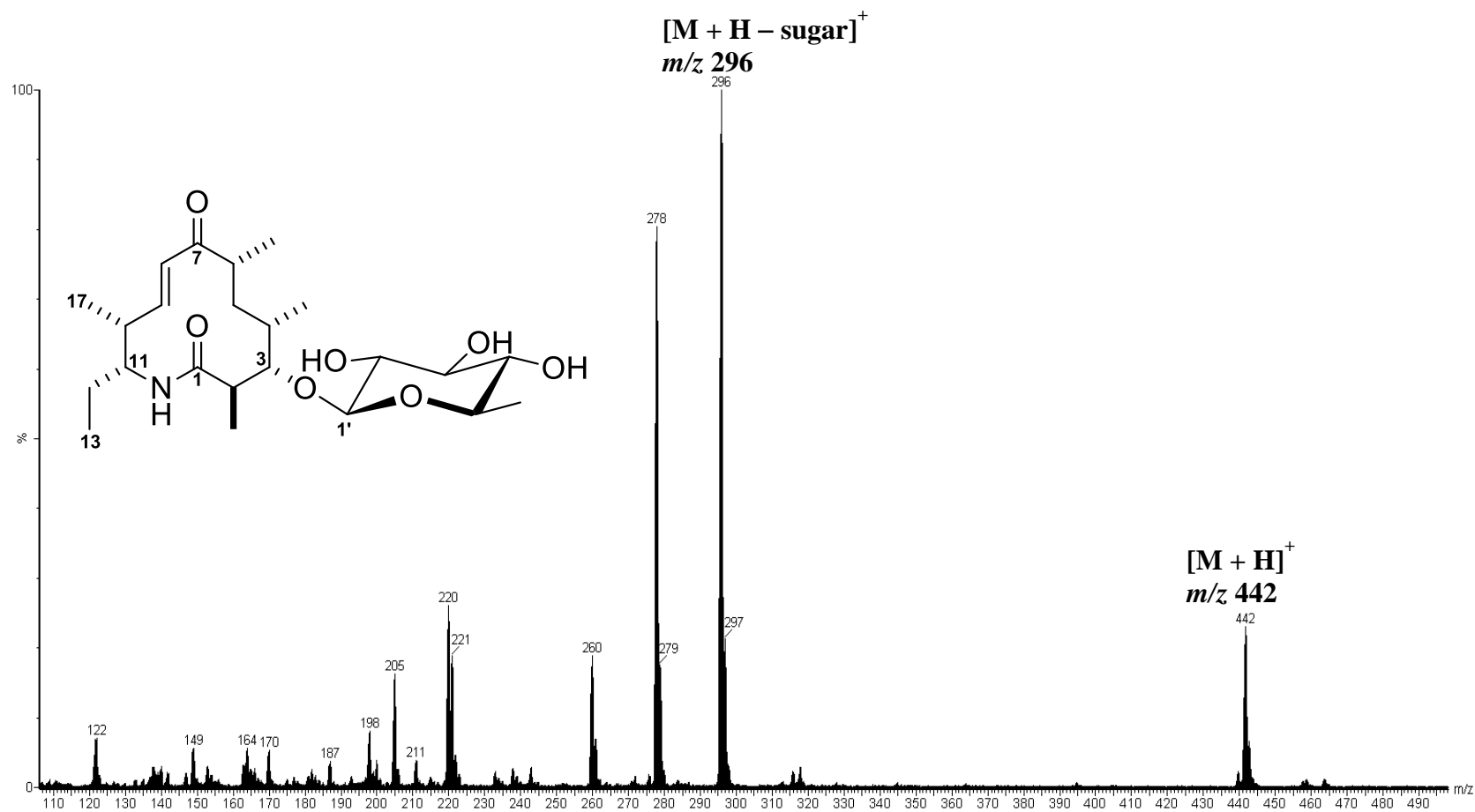


Figure S24. ESI-MS/MS spectrum of **12**.

Compound **12** revealed proton adduct ion at m/z 442 in the MS spectrum. MS/MS analysis displayed the characteristic fragmentation pattern with the daughter ion at m/z 296.

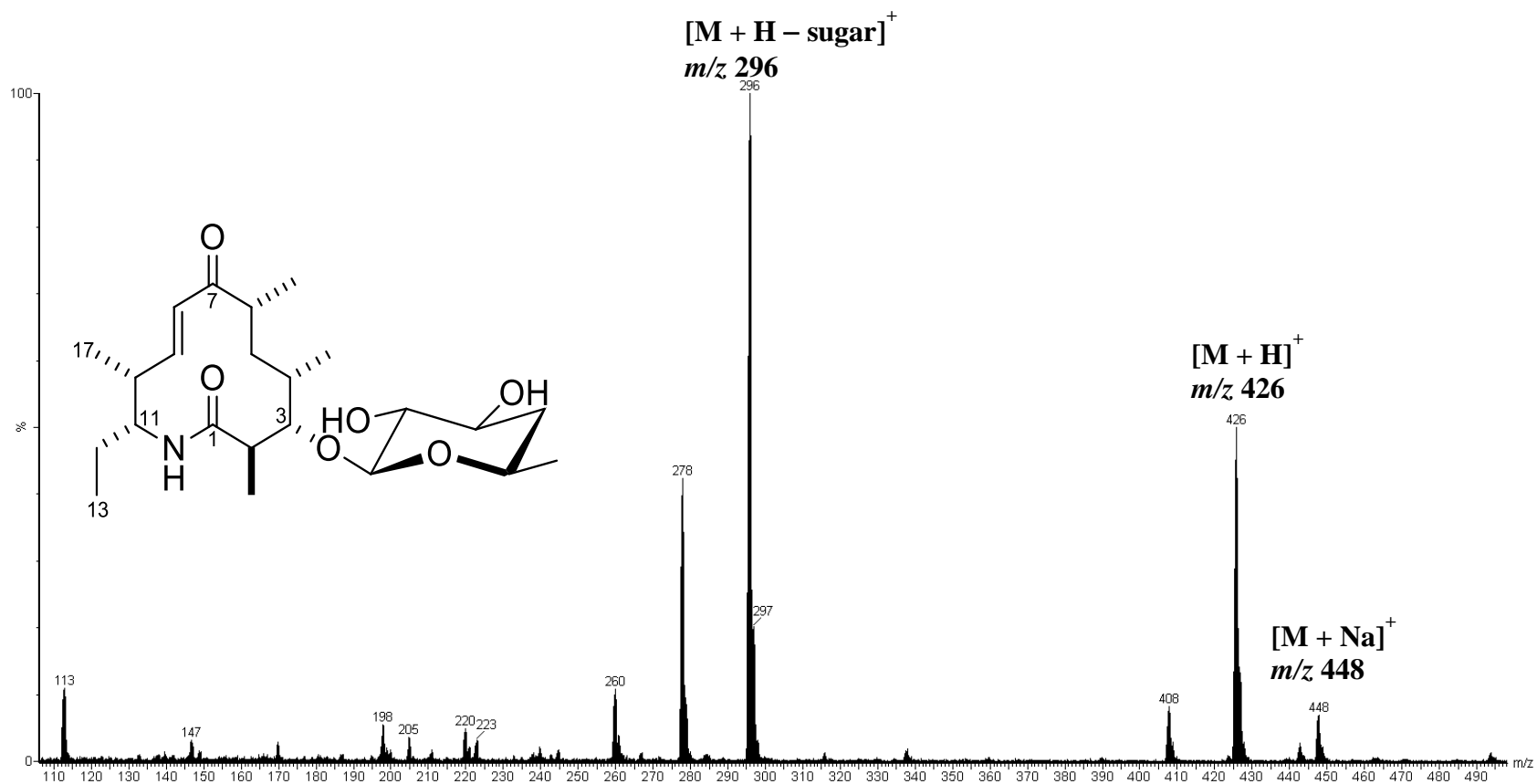


Figure S25. ESI-MS/MS spectrum of **13**.

Compound **13** showed sodium adduct ion at m/z 448 in the MS spectrum. MS/MS analysis exhibited the characteristic fragmentation pattern with the parent ion at m/z 426 and daughter ion at m/z 296.

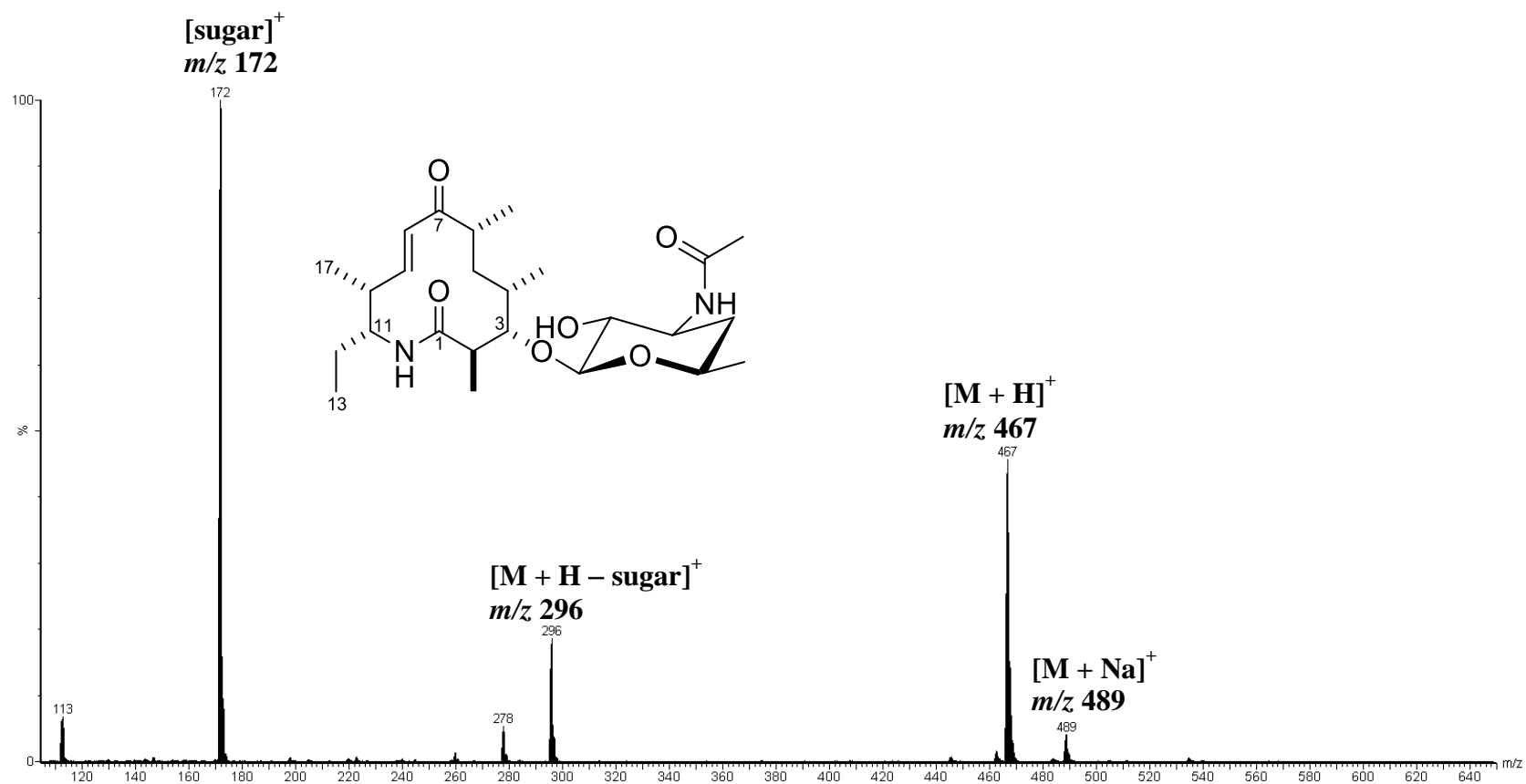


Figure S26. ESI-MS/MS spectrum of **14**.

Compound **14** exhibited sodium adduct ion at m/z 489 in the MS spectrum. MS/MS analysis displayed the characteristic fragmentation pattern with the parent ion at m/z 467 and daughter ions at m/z 296 and m/z 172.

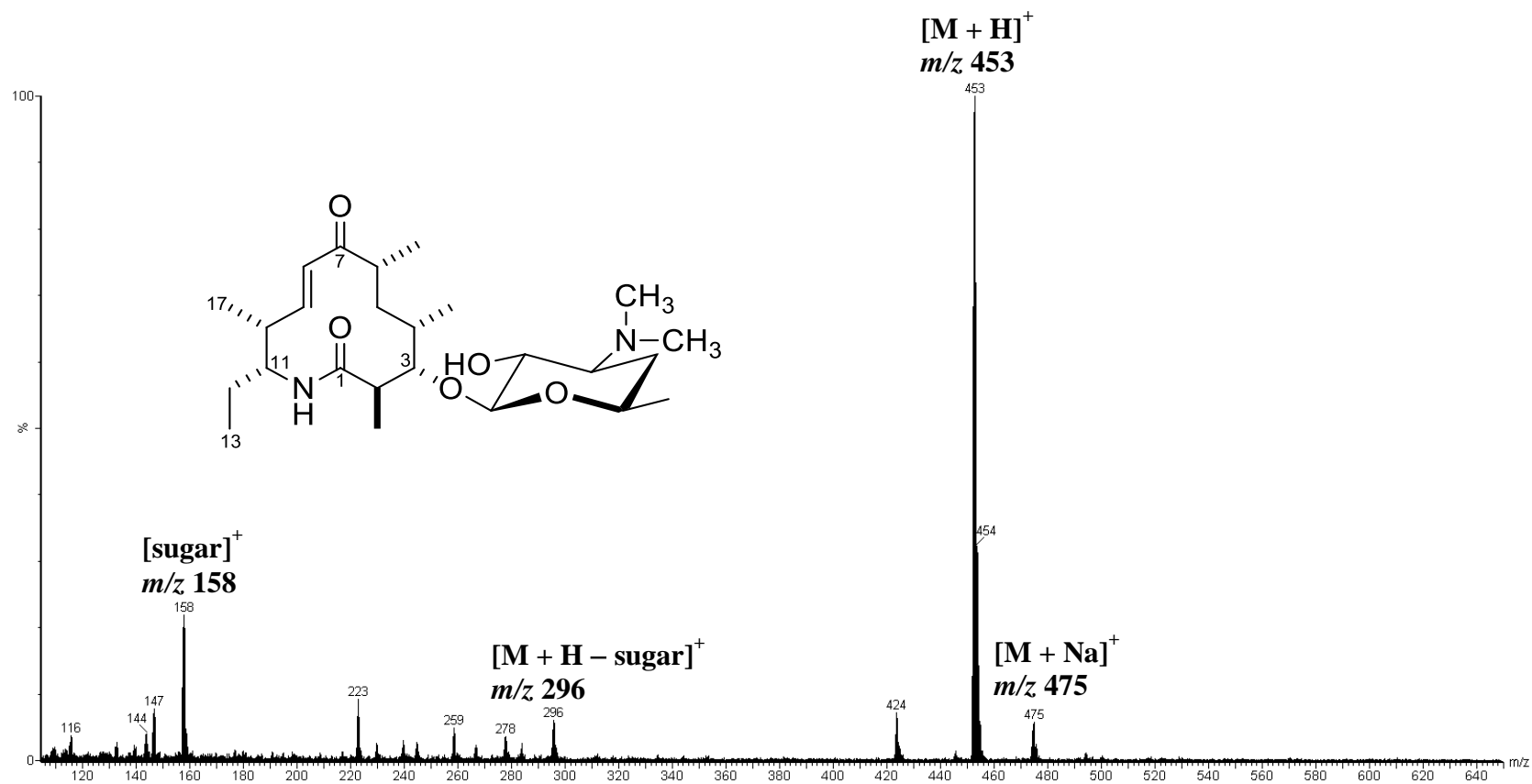


Figure S27. ESI-MS/MS spectrum of **15**.

Compound **15** revealed sodium adduct ion at m/z 475 in the MS spectrum. MS/MS analysis exhibited the characteristic fragmentation pattern with parent ion at m/z 453 and daughter ions at m/z 296 and m/z 158.

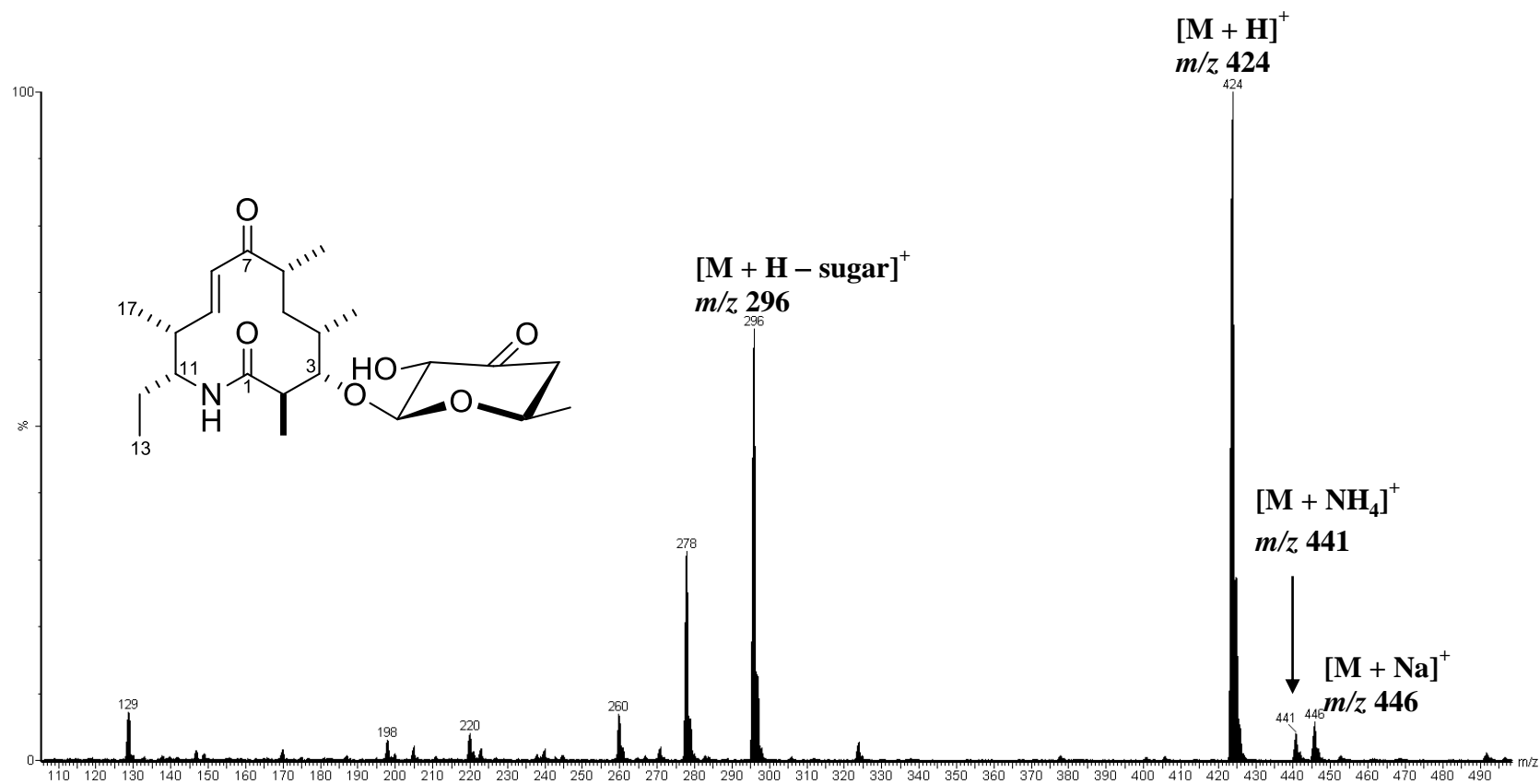


Figure S28. ESI-MS/MS spectrum of **16**.

Compound **16** showed ammonium adduct ion at m/z 441 in the MS spectrum. MS/MS analysis displayed the characteristic fragmentation pattern with parent ion at m/z 424 and daughter ion at m/z 296.

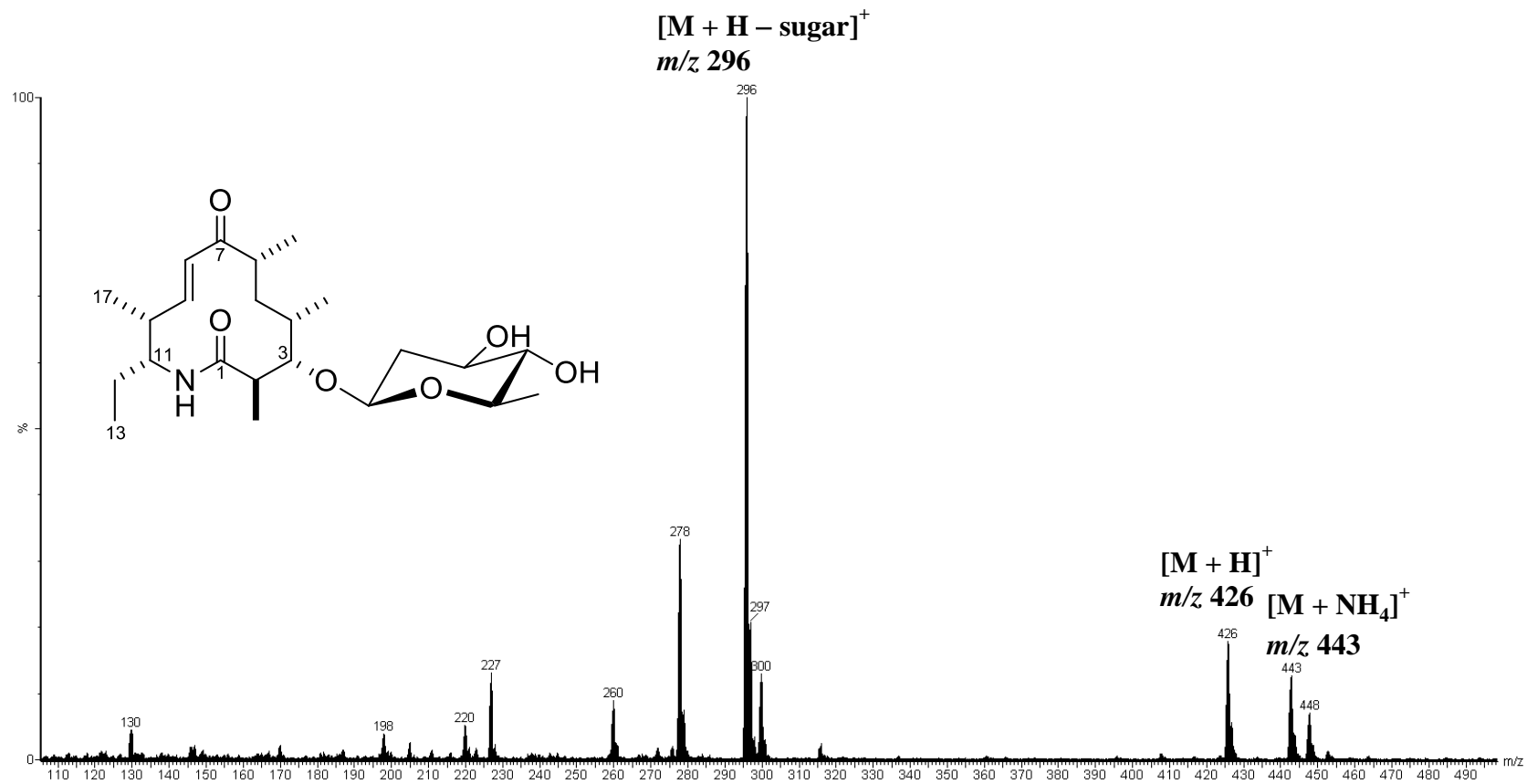


Figure S29. ESI-MS/MS spectrum of **17**.

Compound **17** exhibited ammonium adduct ion at m/z 443 in the MS spectrum. MS/MS analysis displayed the characteristic fragmentation pattern with parent ion at m/z 426 and daughter ion at m/z 296.

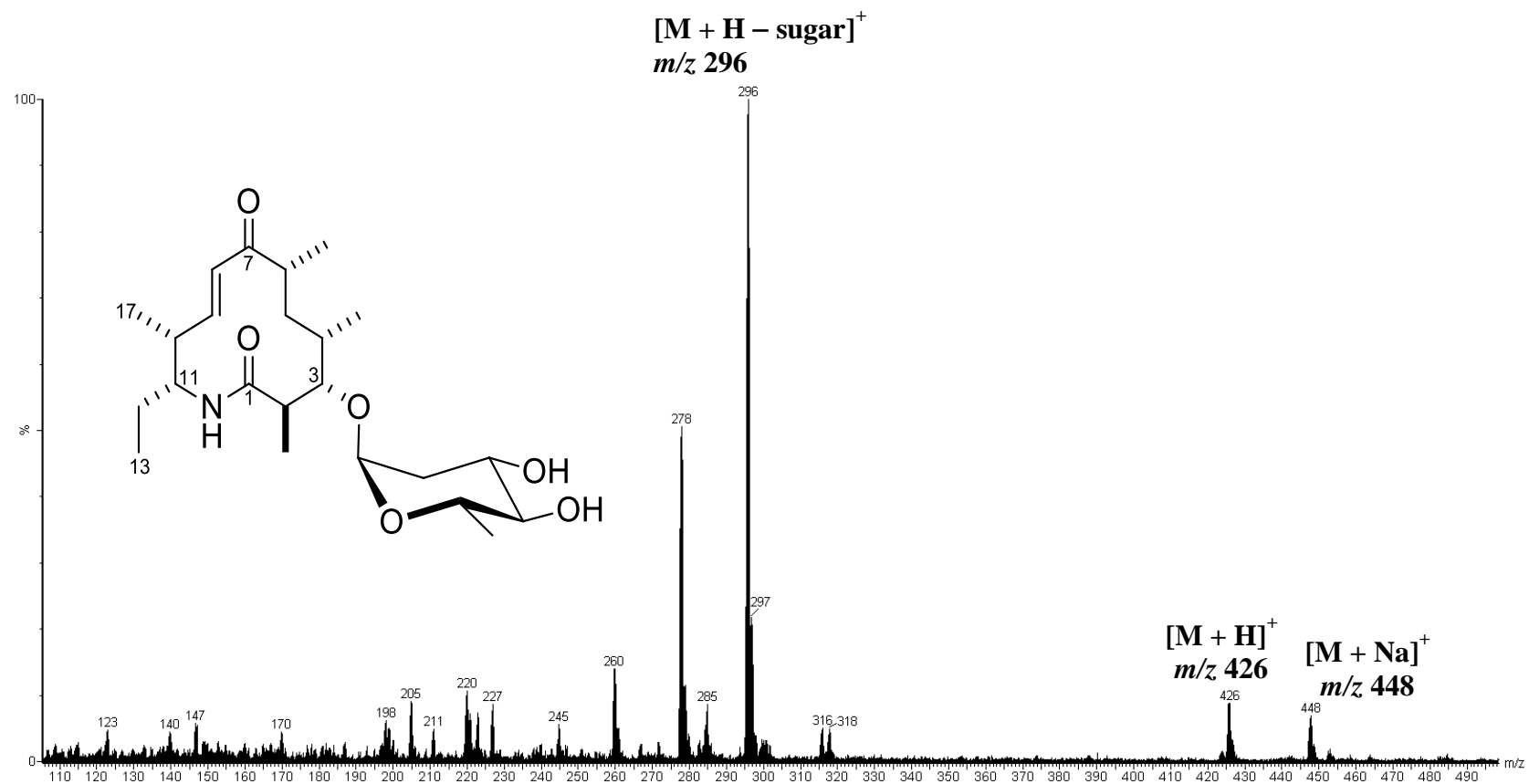


Figure S30. ESI-MS/MS spectrum of **18**.

Compound **18** showed sodium adduct ion at m/z 448 in the MS spectrum. MS/MS analysis exhibited the characteristic fragmentation pattern with parent ion at m/z 426 and daughter ion at m/z 296.

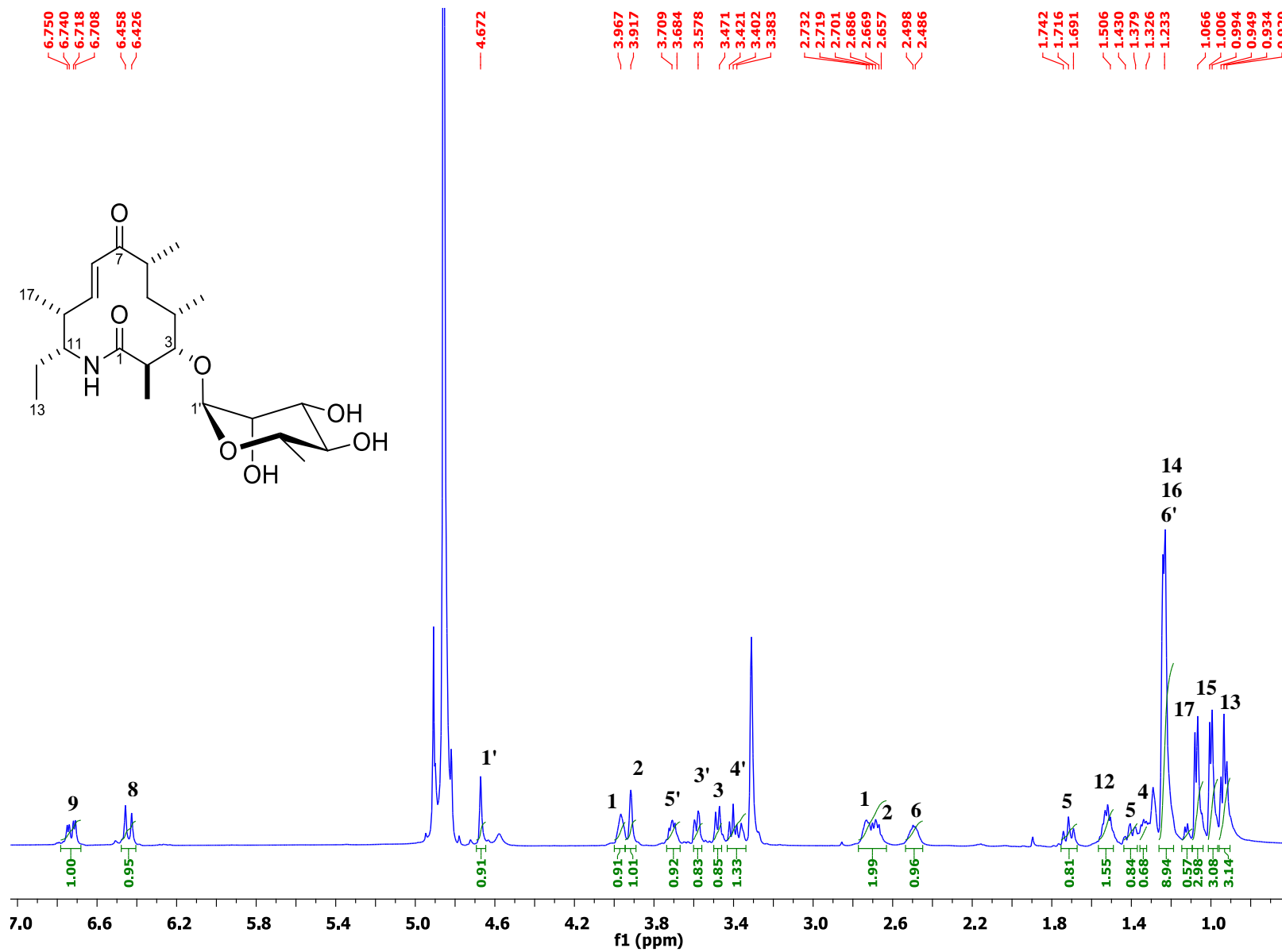


Figure S31. ^1H NMR spectrum of **11** in CD_3OD at 500 MHz.

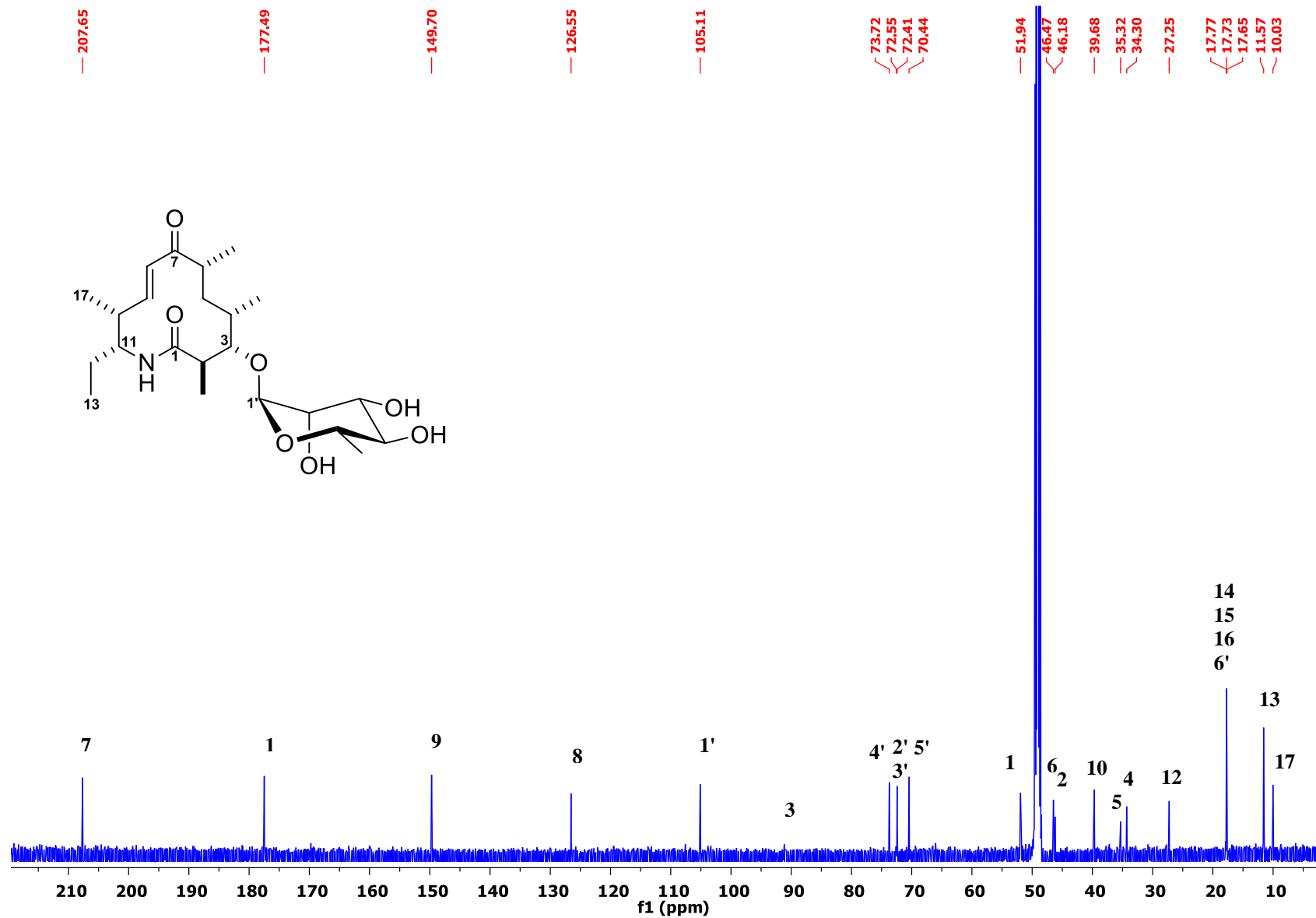


Figure S32. ¹³C NMR spectrum of 11 in CD₃OD at 500 MHz.

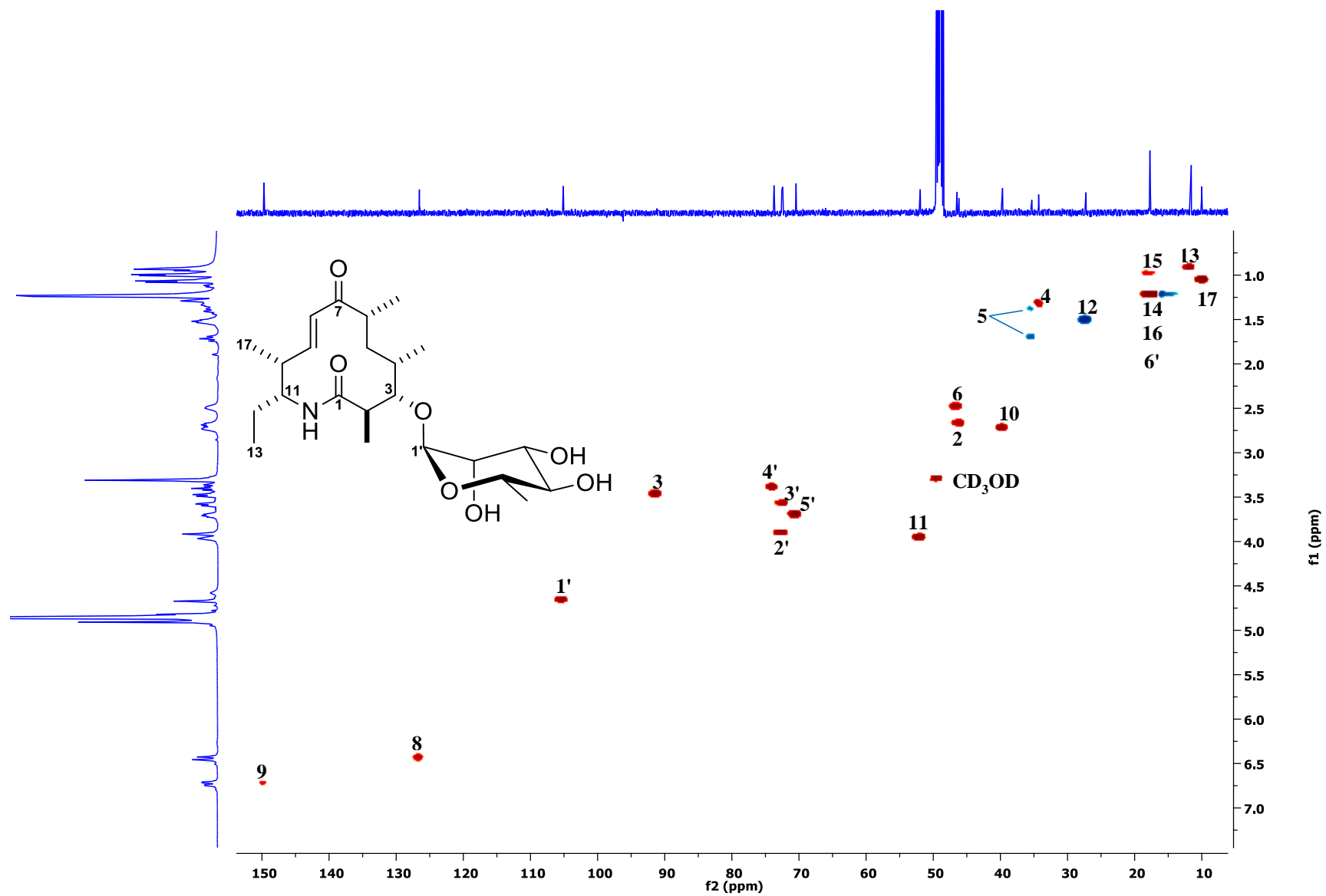


Figure S34. HSQC spectrum of **11** in CD₃OD at 500 MHz.

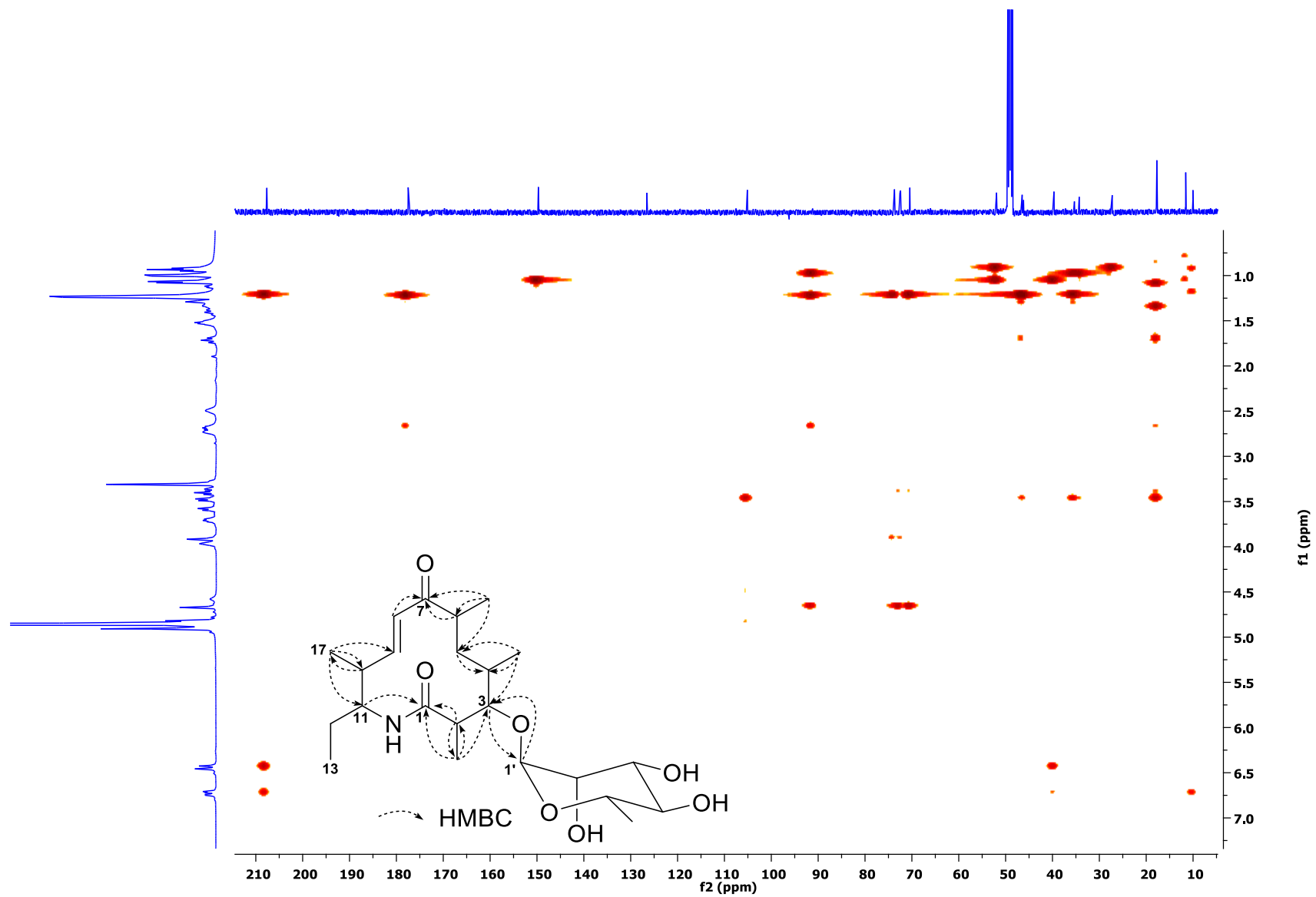


Figure S35. HMBC spectrum of **11** in CD₃OD at 500 MHz.

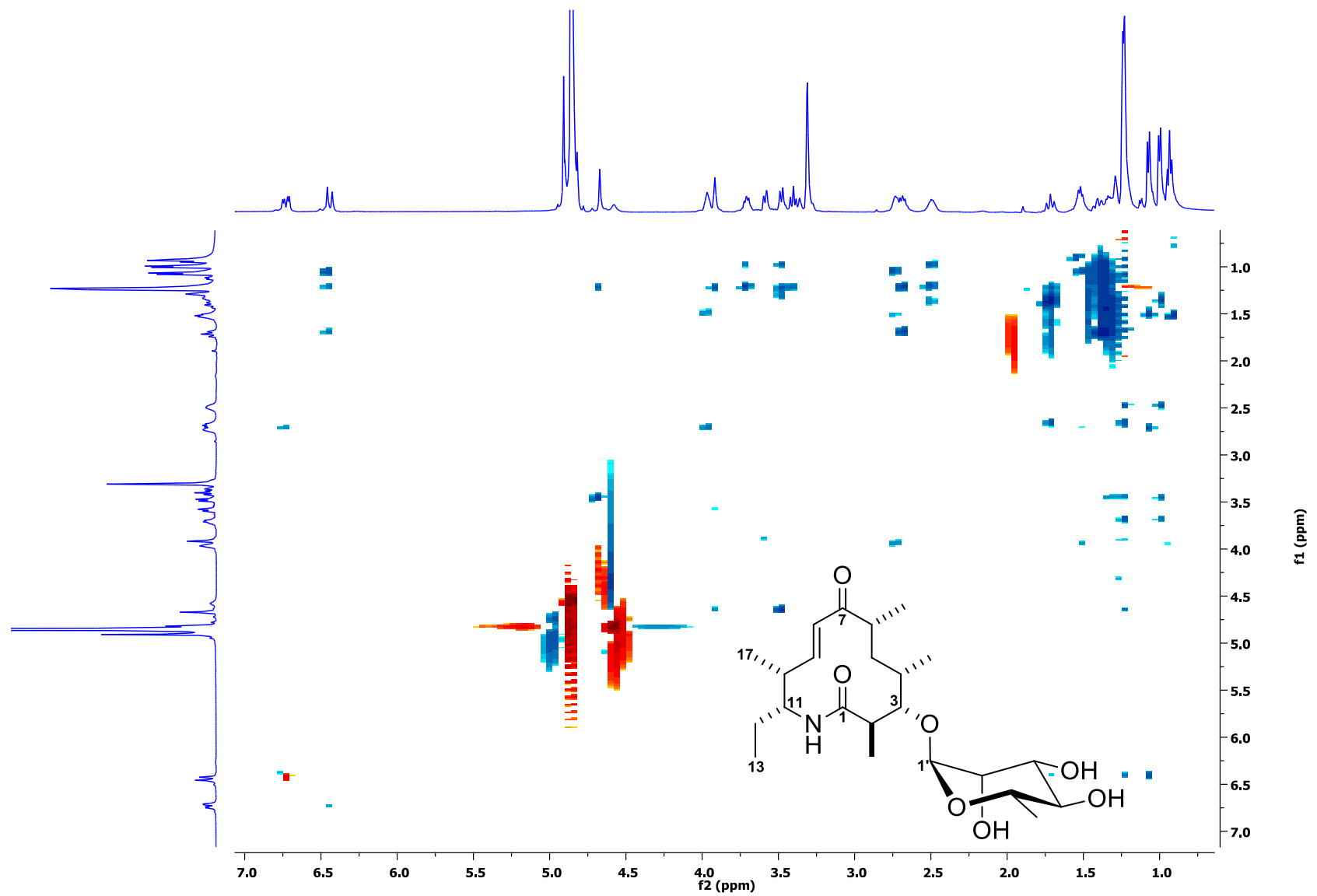


Figure S36. NOESY spectrum of **11** in CD₃OD at 500 MHz.

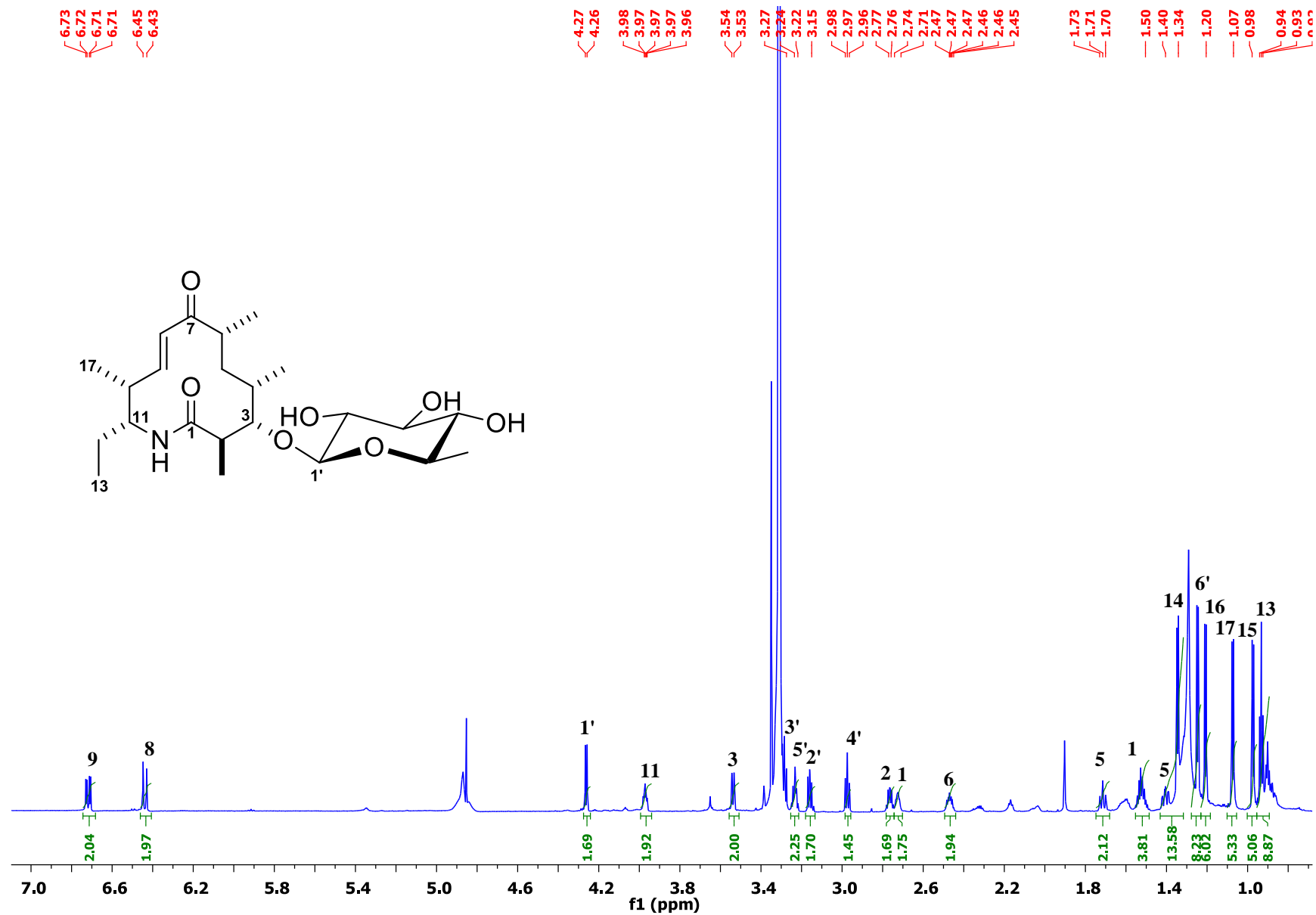


Figure S37. ¹H NMR spectrum of **12** in CD₃OD at 900 MHz.

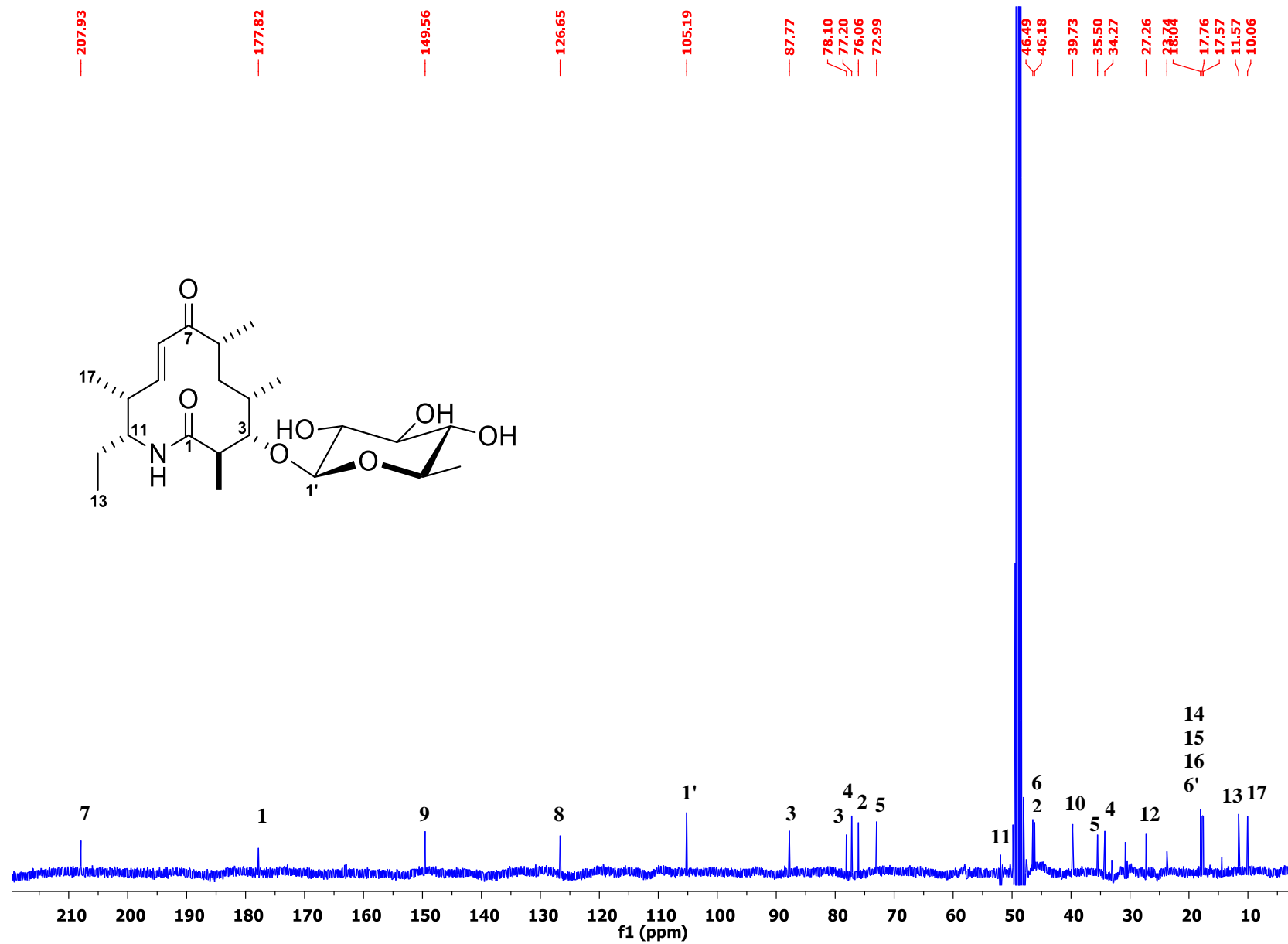


Figure S38. ^{13}C NMR spectrum of **12** in CD_3OD at 225 MHz.

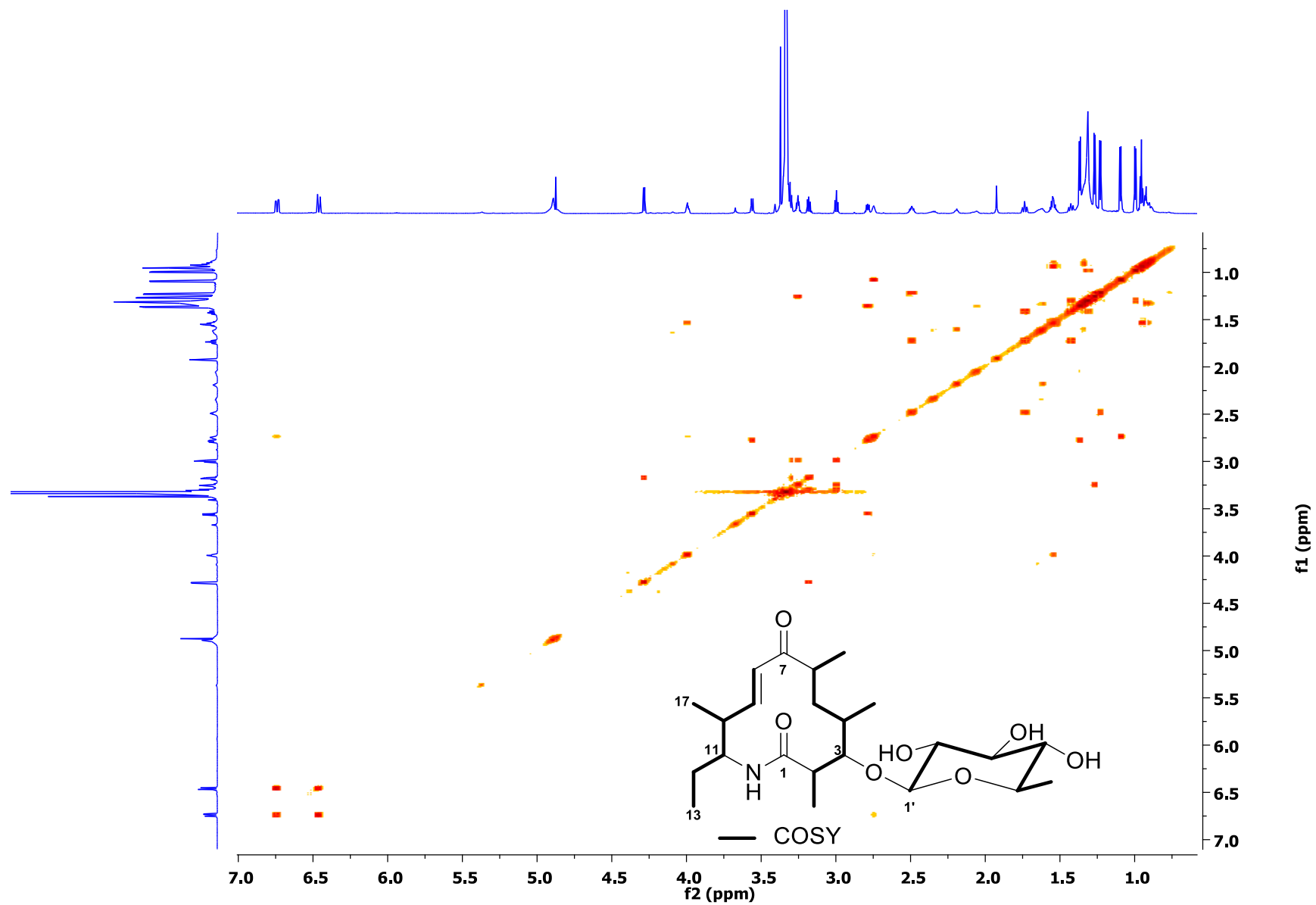


Figure S39. COSY spectrum of **12** in CD₃OD at 900 MHz.

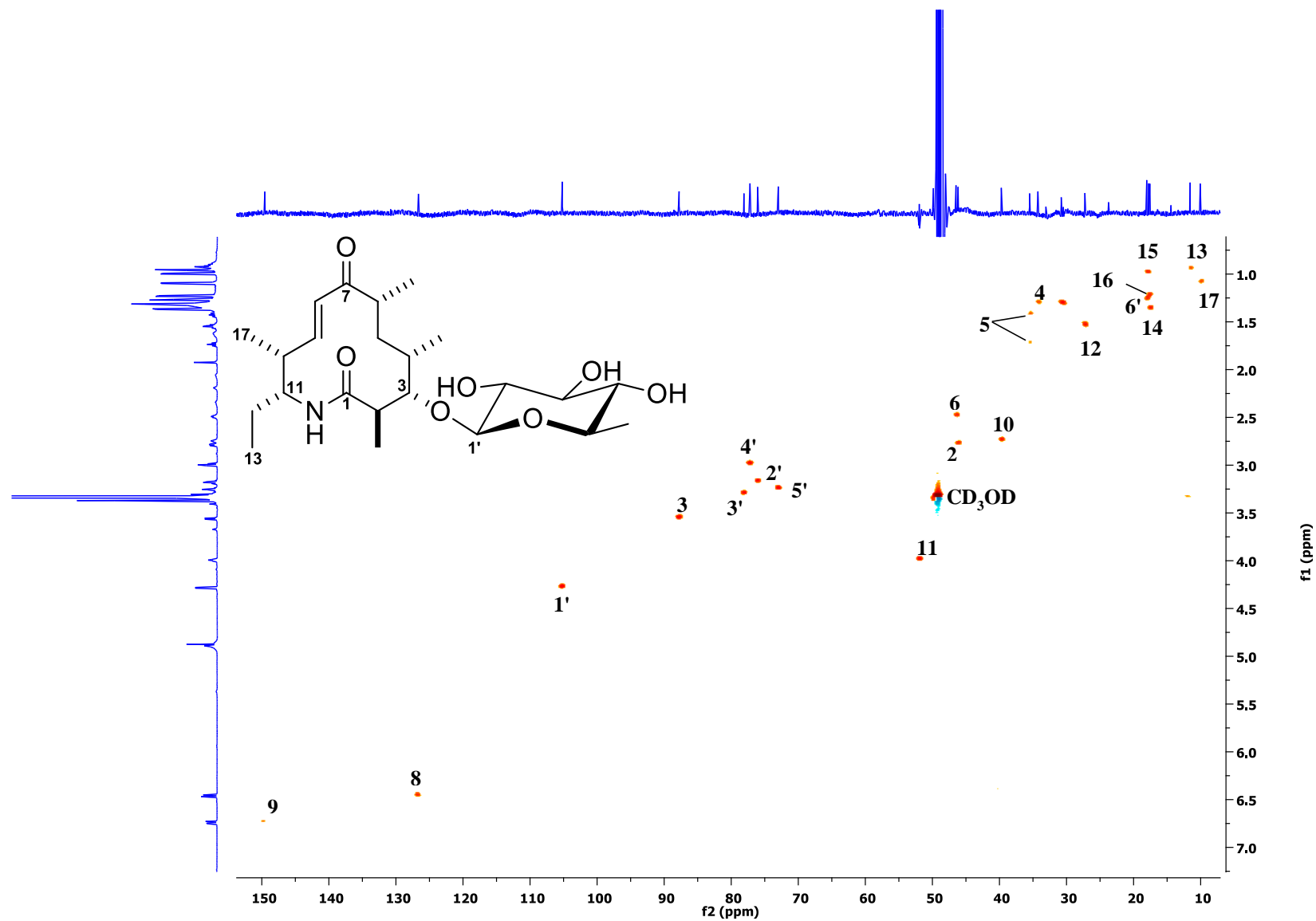


Figure S40. HSQC spectrum of **12** in CD₃OD at 900 MHz.

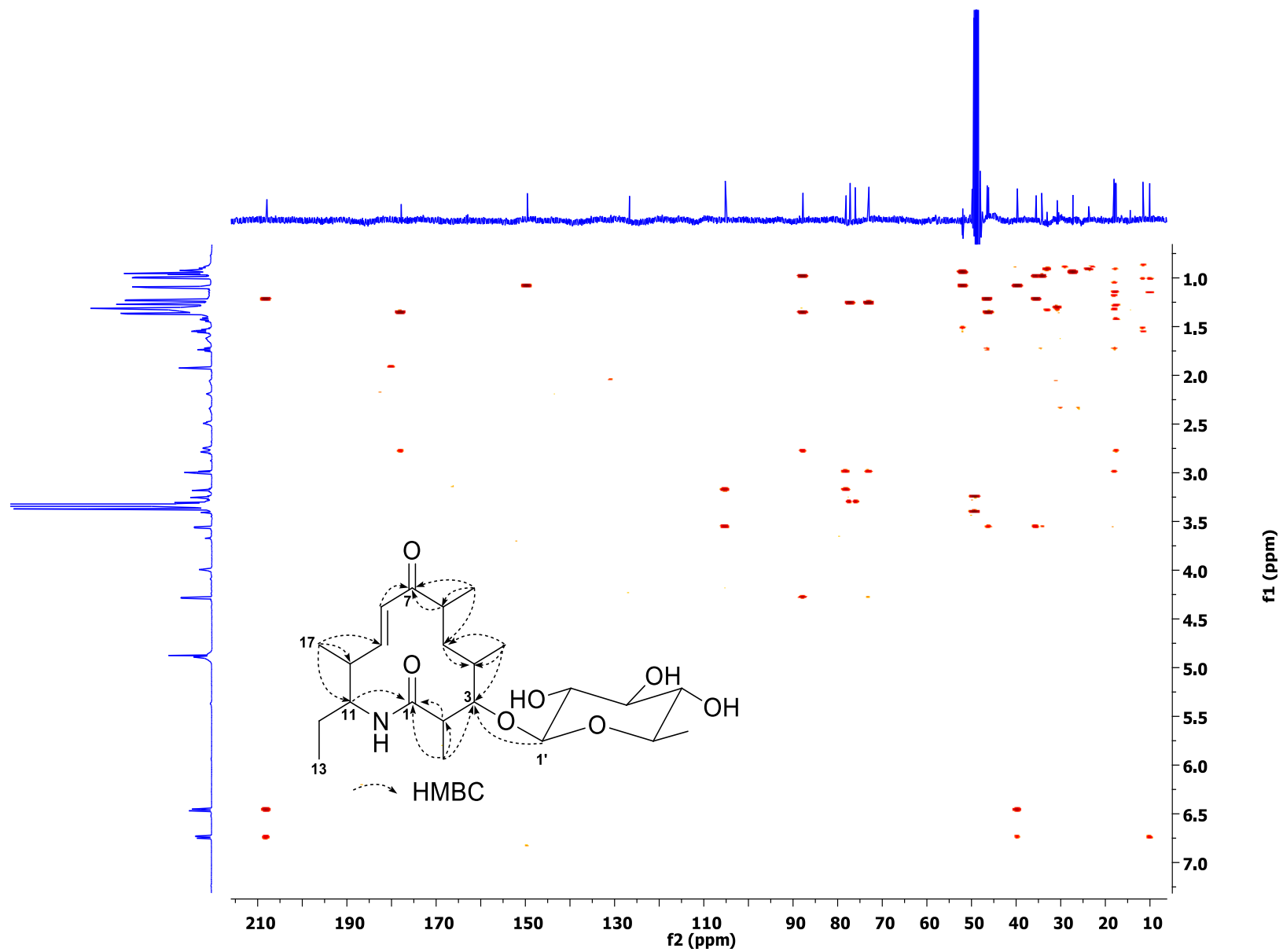
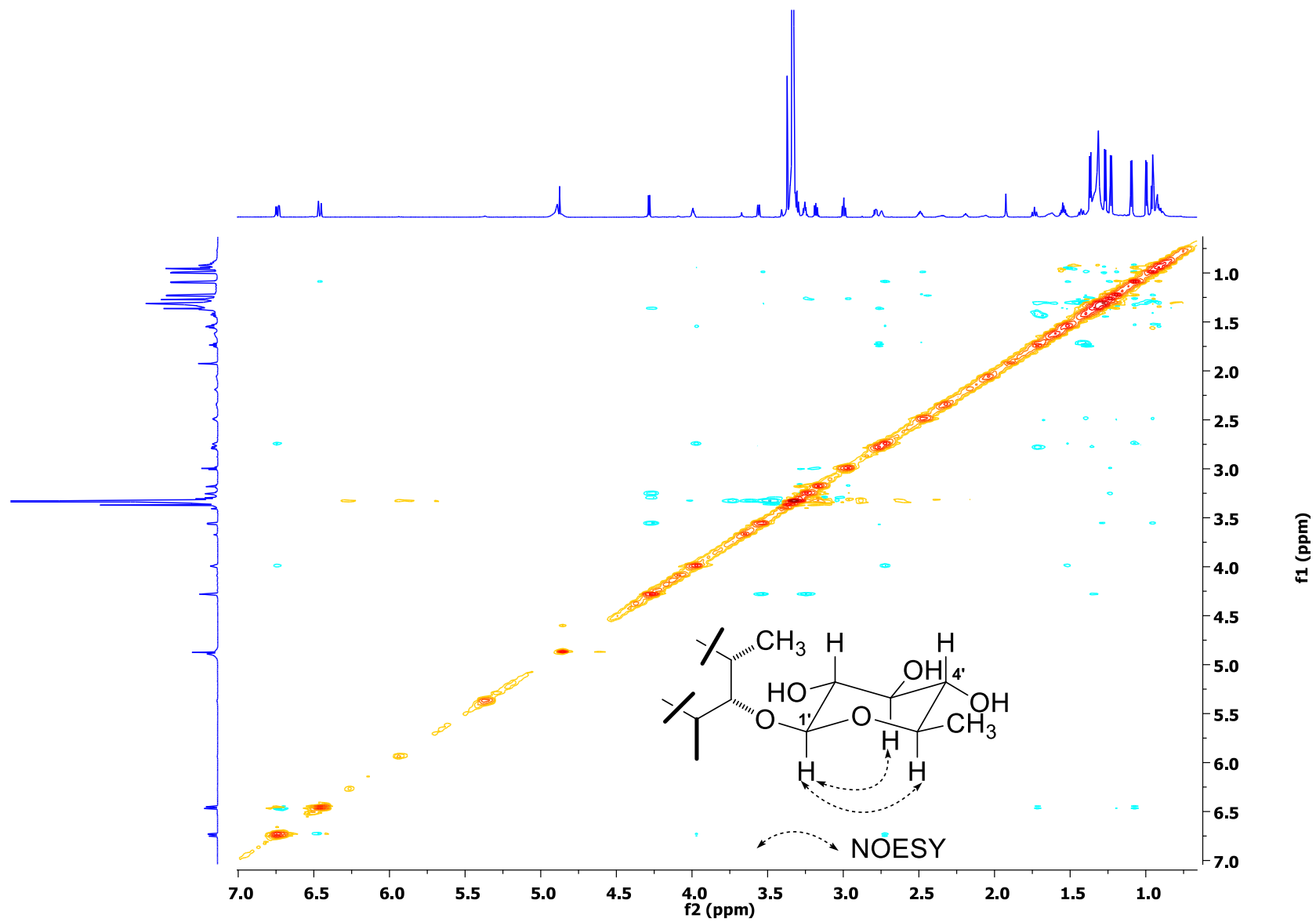


Figure S41. HMBC spectrum of **12** in CD₃OD at 900 MHz.



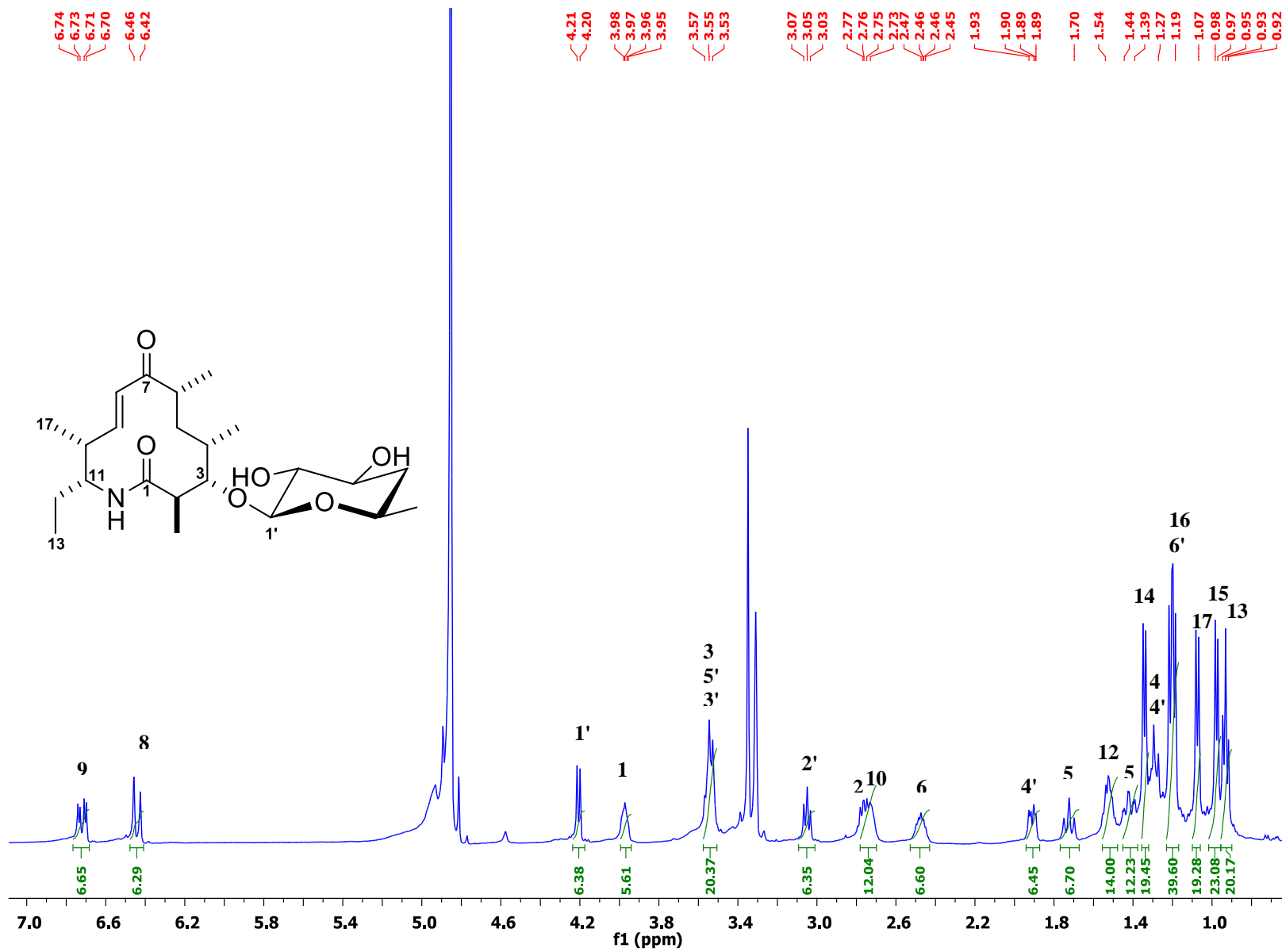


Figure S43. ¹H NMR spectrum of **13** in CD₃OD at 500 MHz.

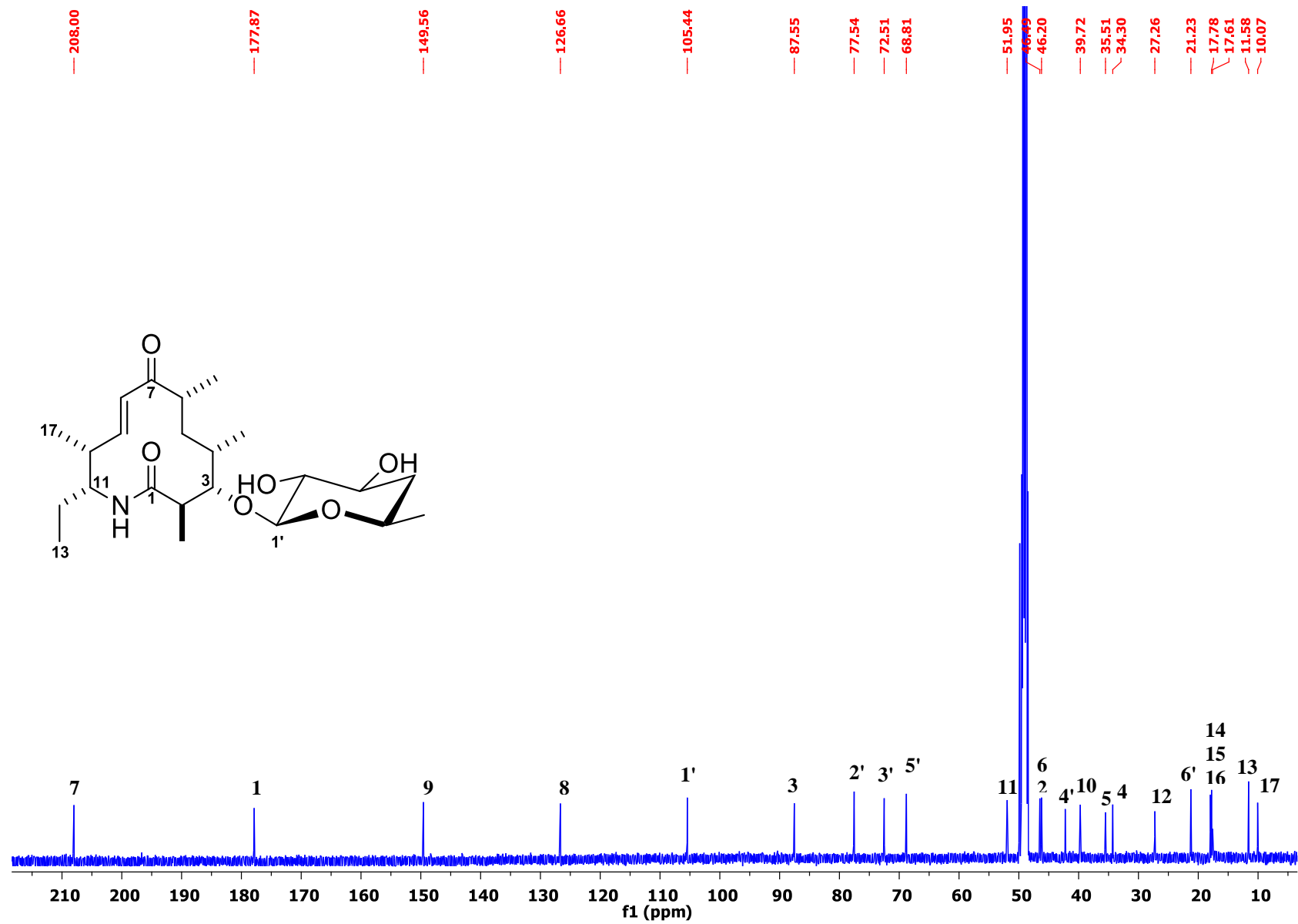


Figure S44. ^{13}C NMR spectrum of **13** in CD_3OD at 500 MHz.

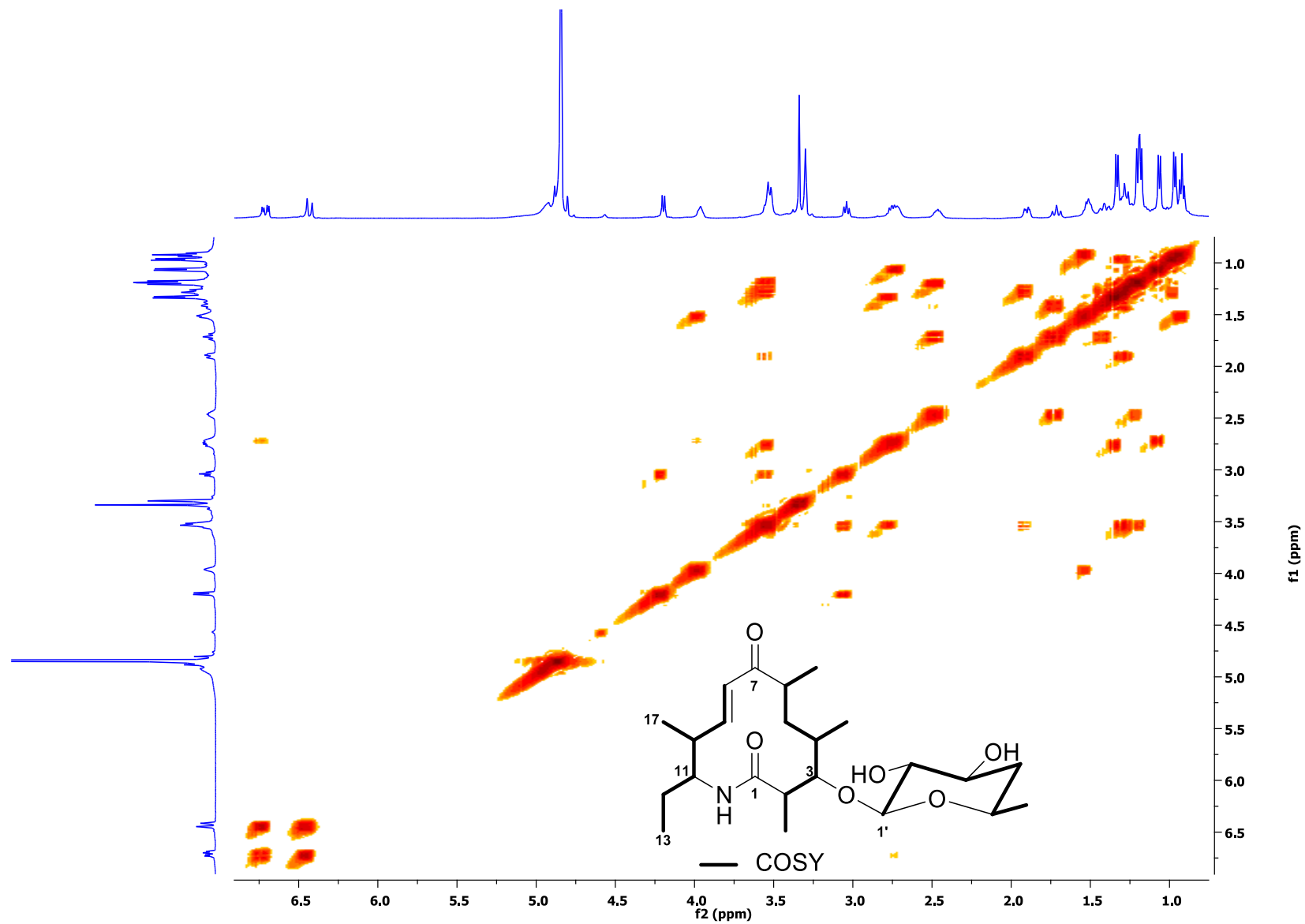


Figure S45. COSY spectrum of **13** in CD₃OD at 500 MHz.

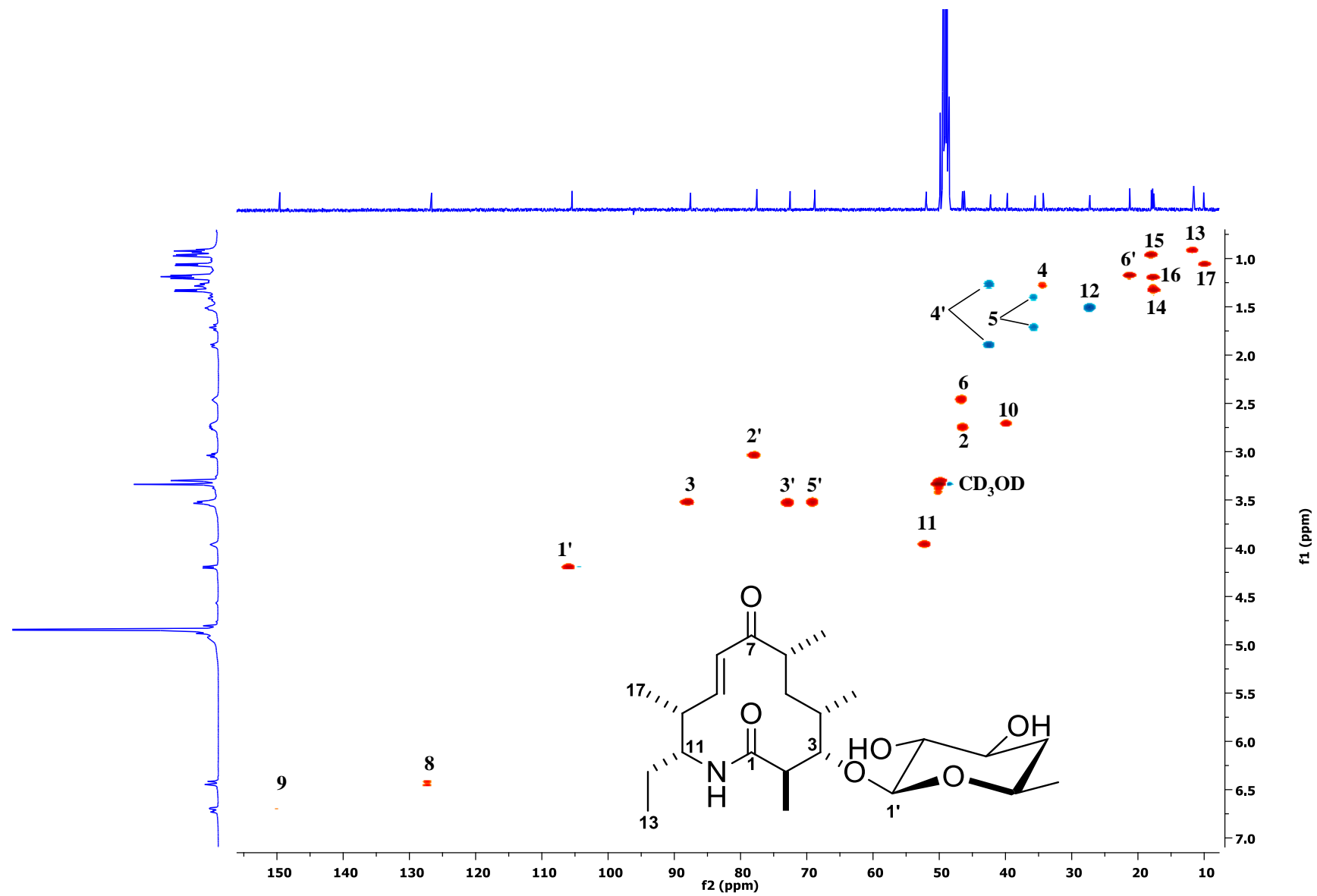


Figure S46. HSQC spectrum of **13** in CD₃OD at 500 MHz.

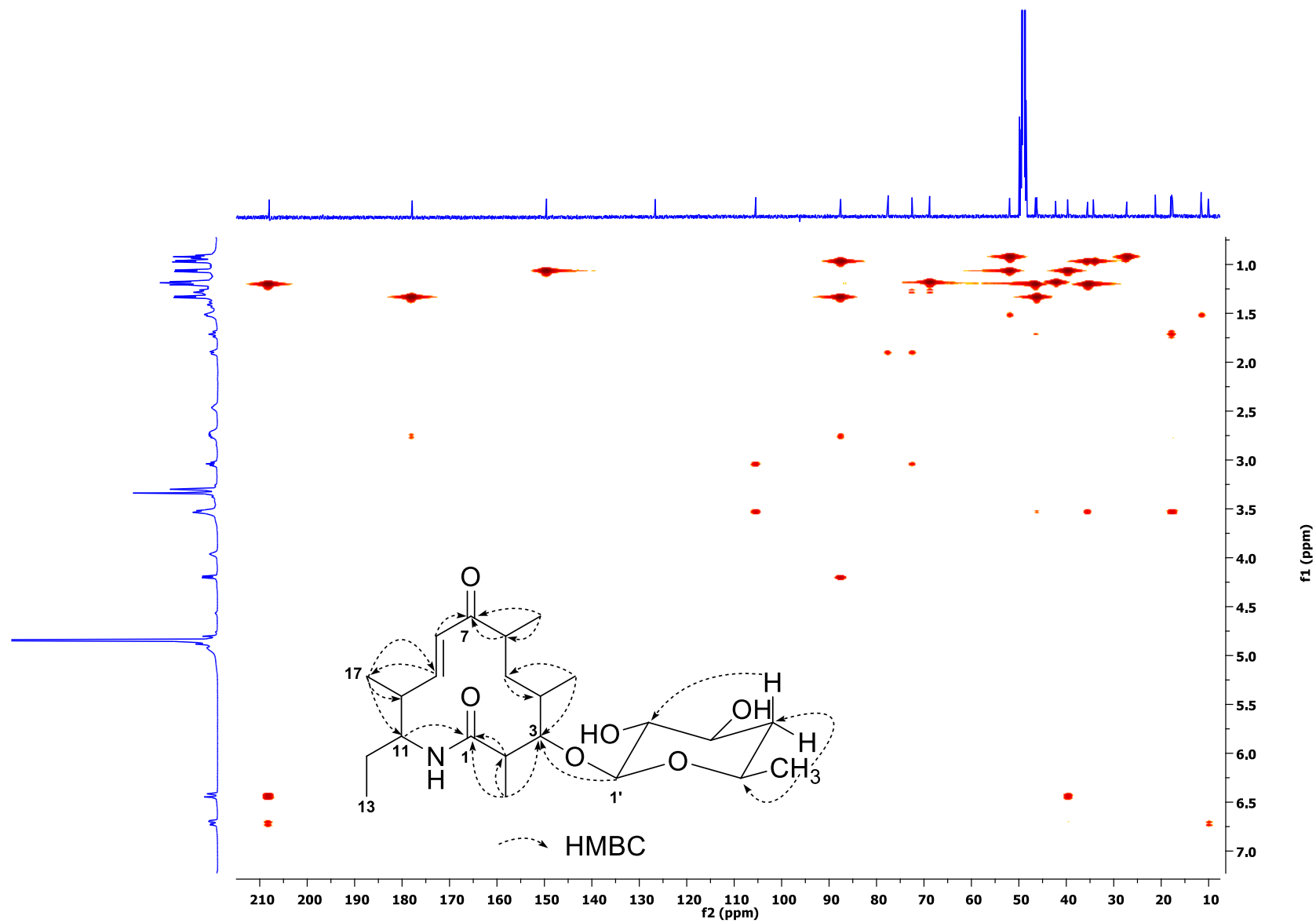


Figure S47. HMBC spectrum of **13** in CD₃OD at 500 MHz.

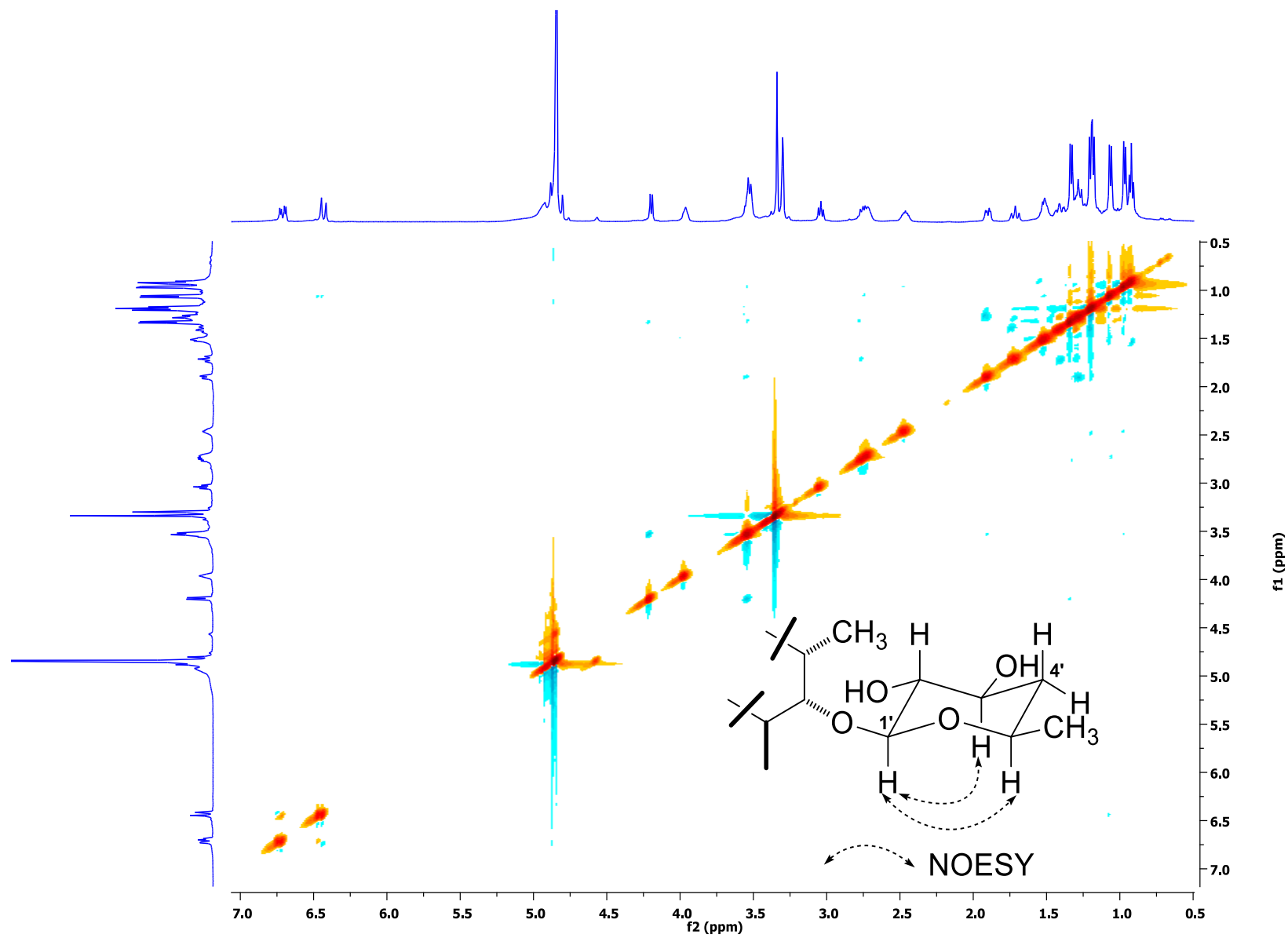


Figure S48. NOESY spectrum of **13** in CD₃OD at 500 MHz.

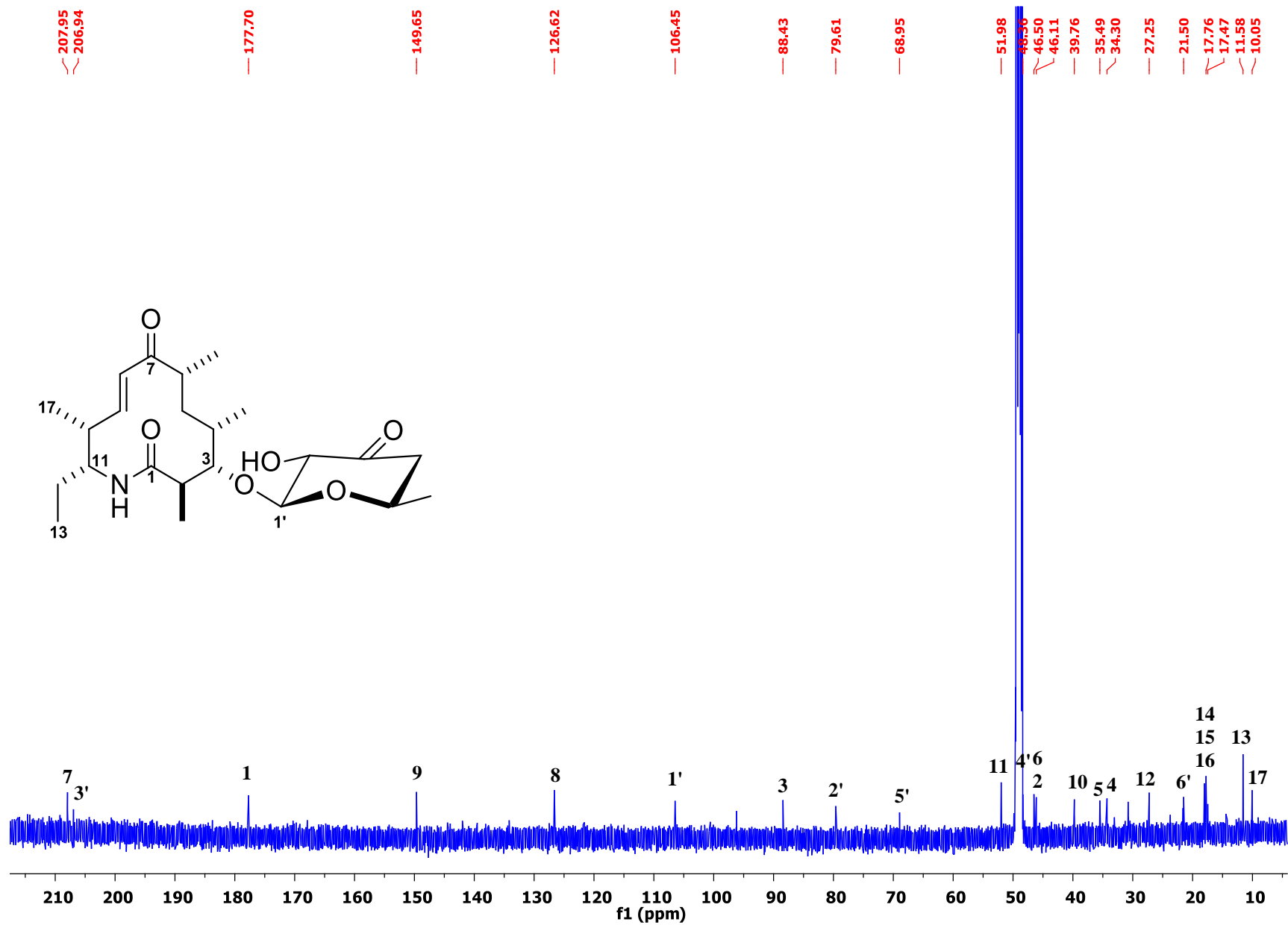


Figure S50. ^{13}C NMR spectrum of **16** in CD_3OD at 125 MHz.

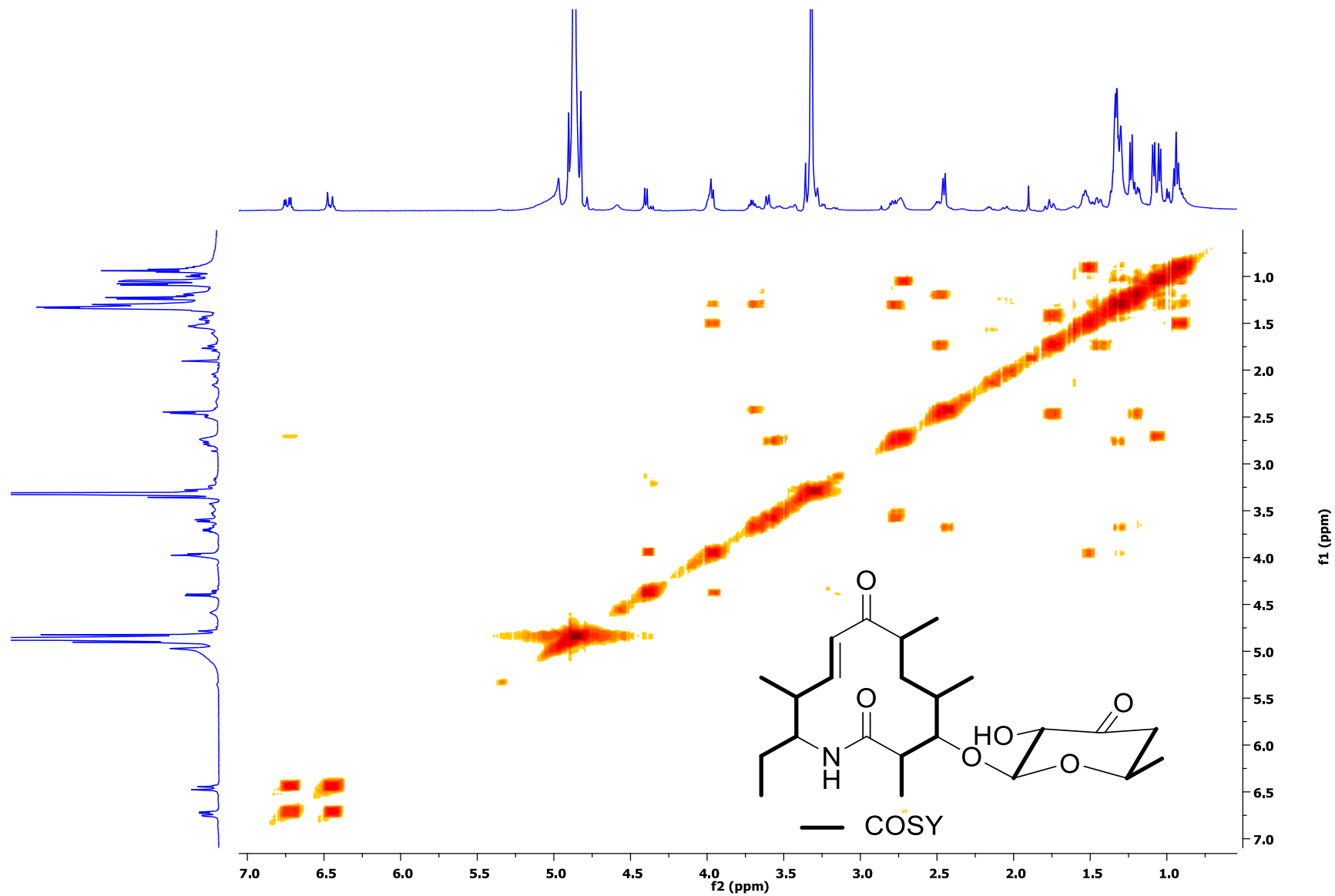


Figure S51. COSY spectrum of **16** in CD₃OD at 500 MHz.

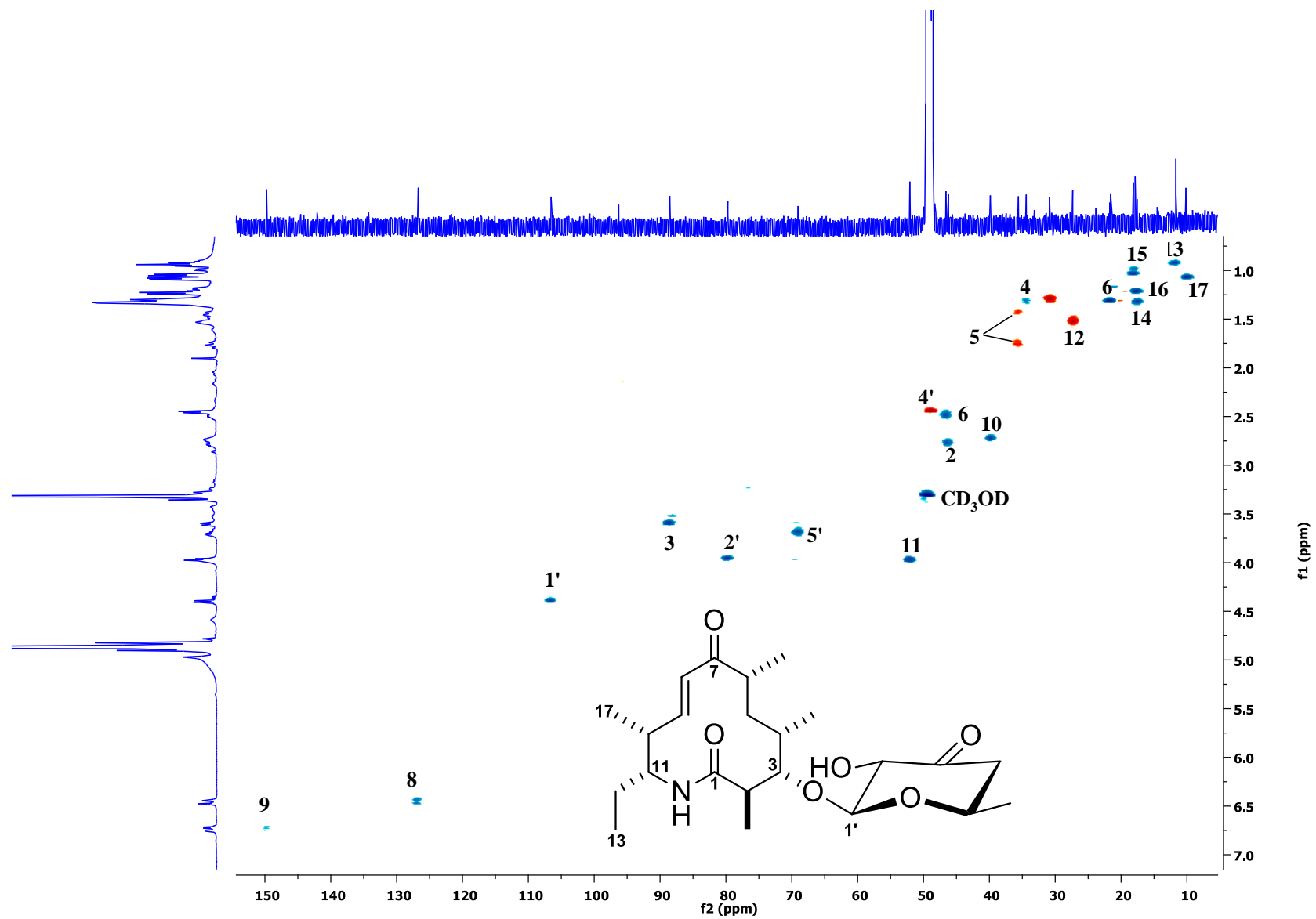


Figure S52. HSQC spectrum of **16** in CD₃OD at 500 MHz.

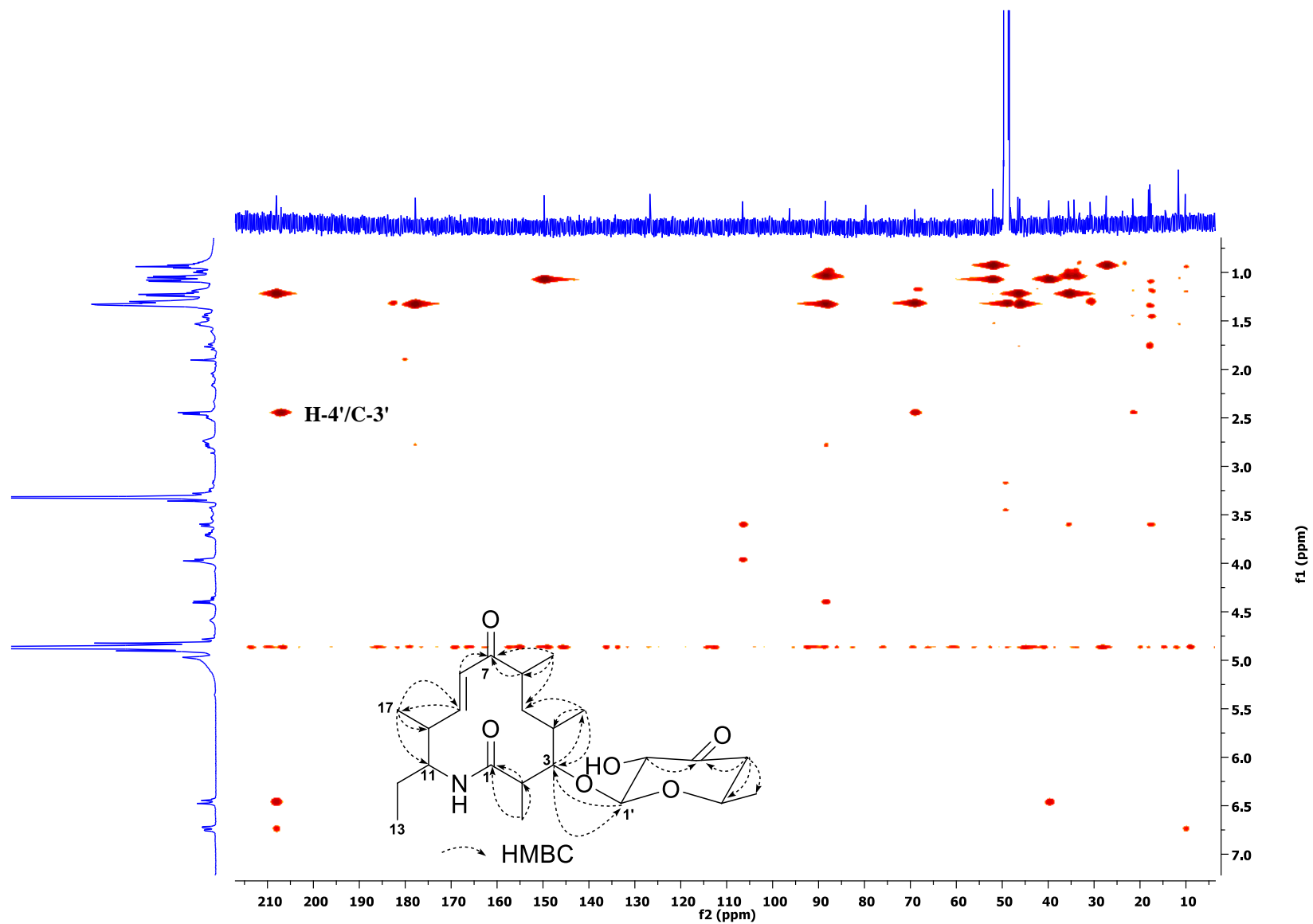


Figure S53. HMBC spectrum of **16** in CD₃OD at 500 MHz.

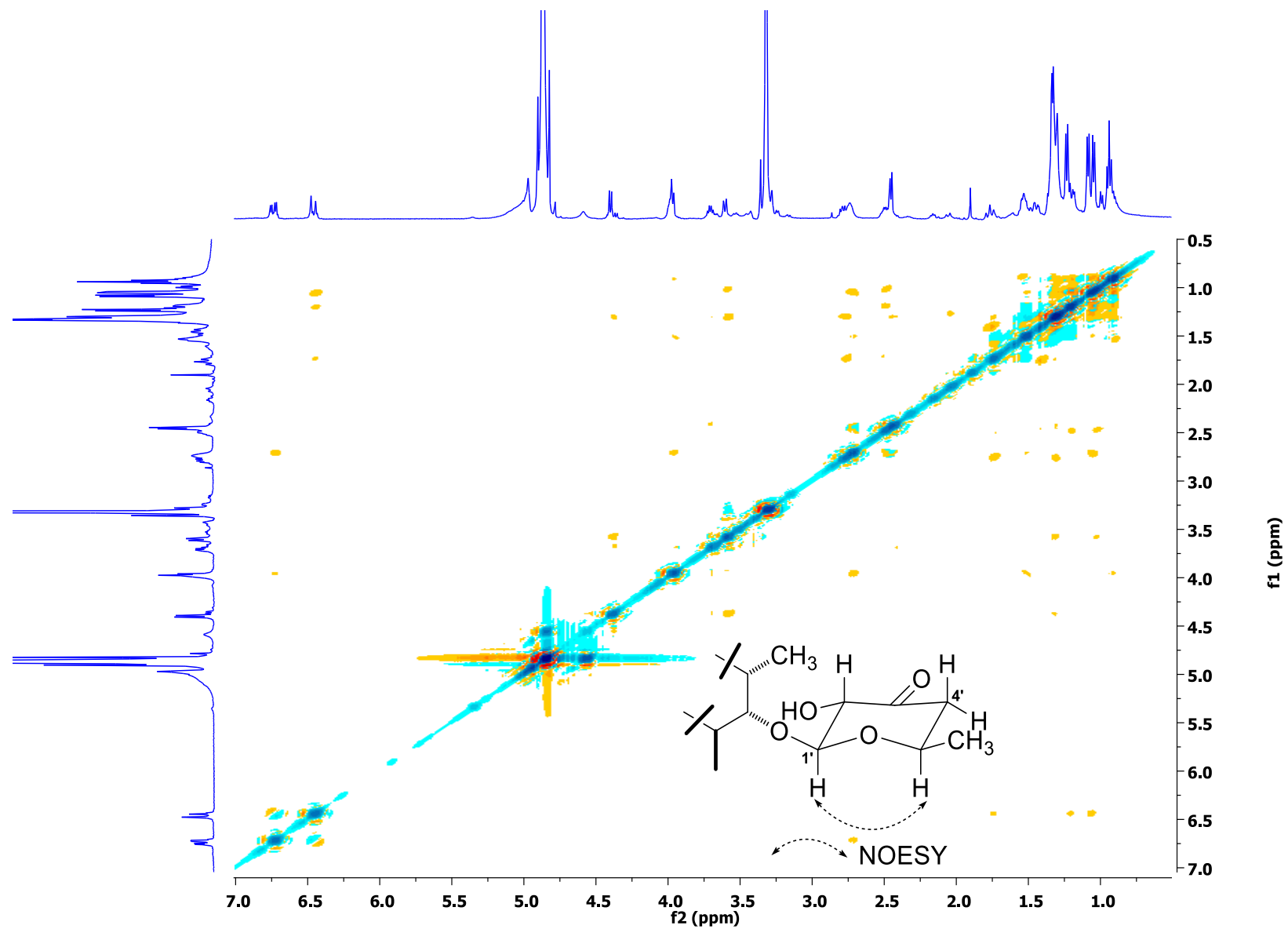


Figure S54. NOESY spectrum of **16** in CD₃OD at 500 MHz.

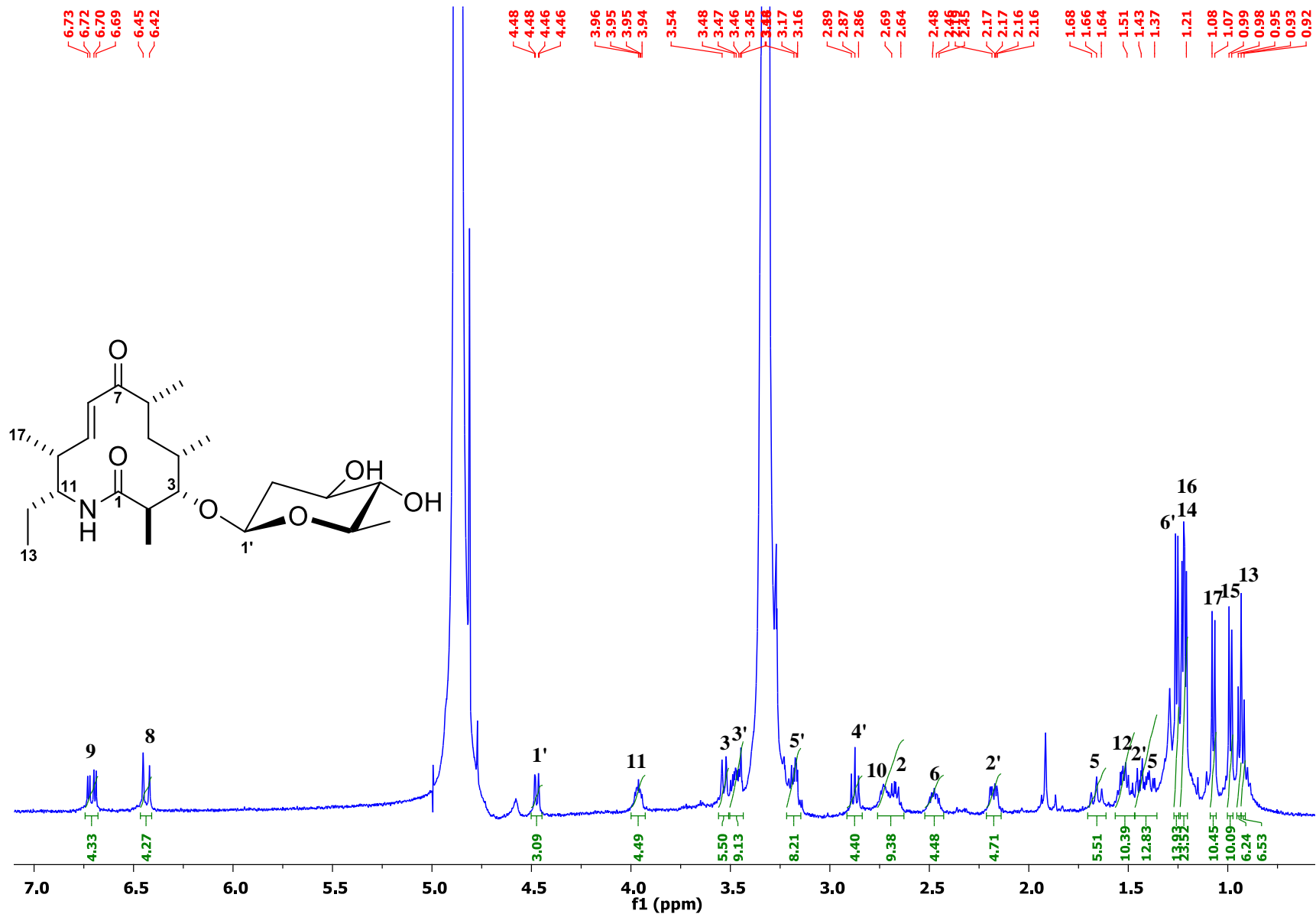


Figure S55. ¹H NMR spectrum of **17** in CD₃OD at 500 MHz.

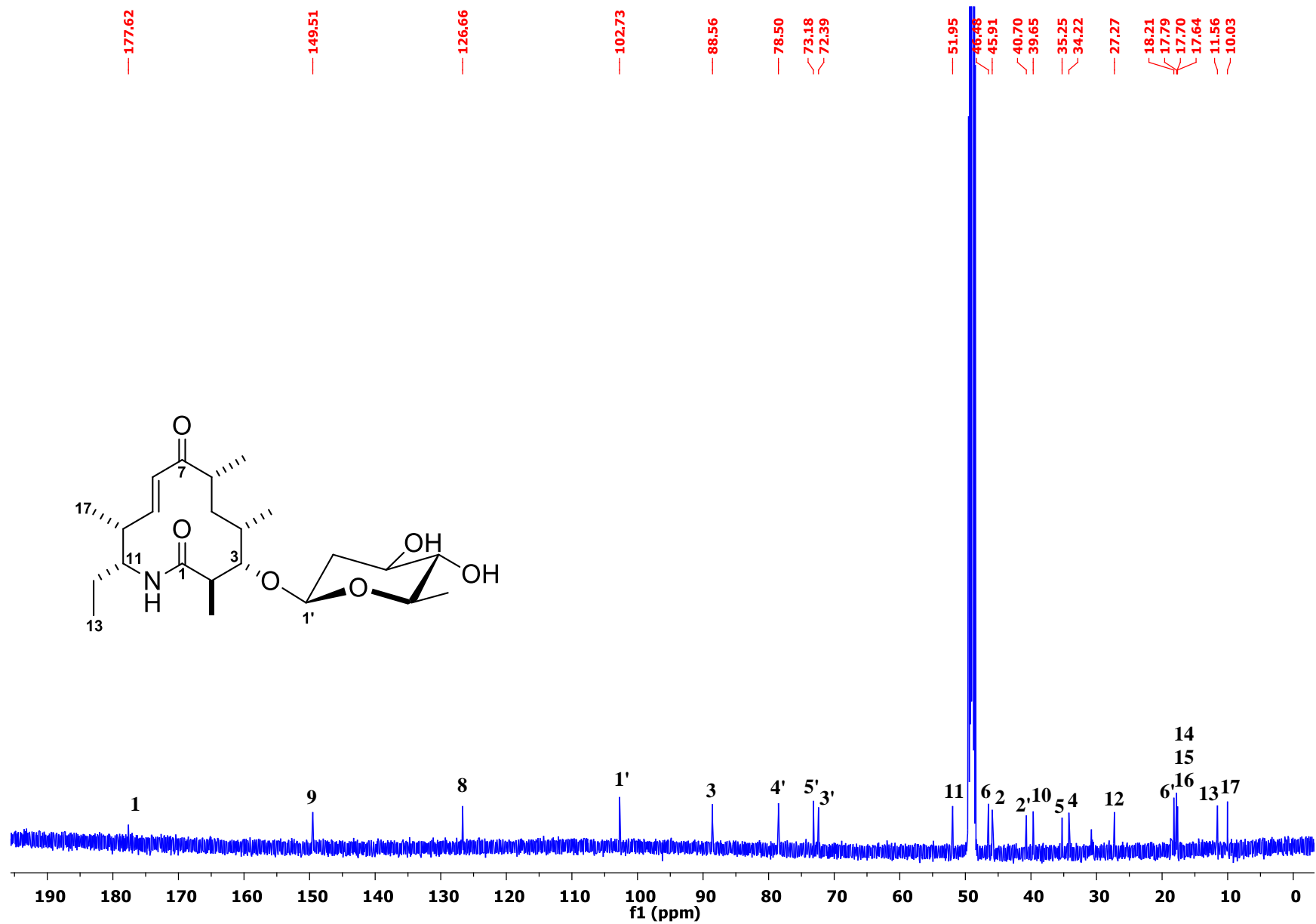


Figure S56. ¹³C NMR spectrum of **17** in CD₃OD at 125 MHz.

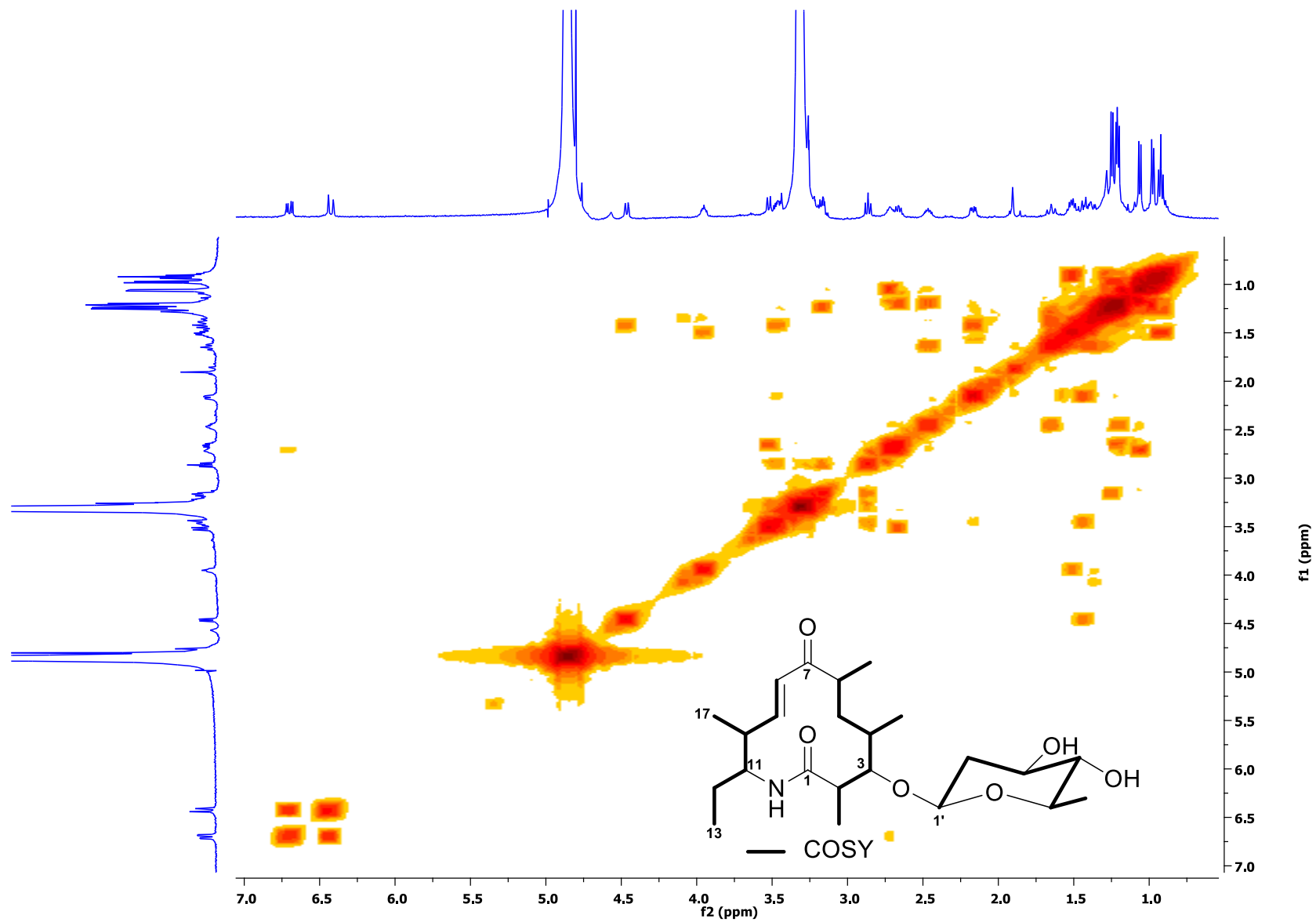


Figure S57. COSY spectrum of **17** in CD₃OD at 500 MHz.

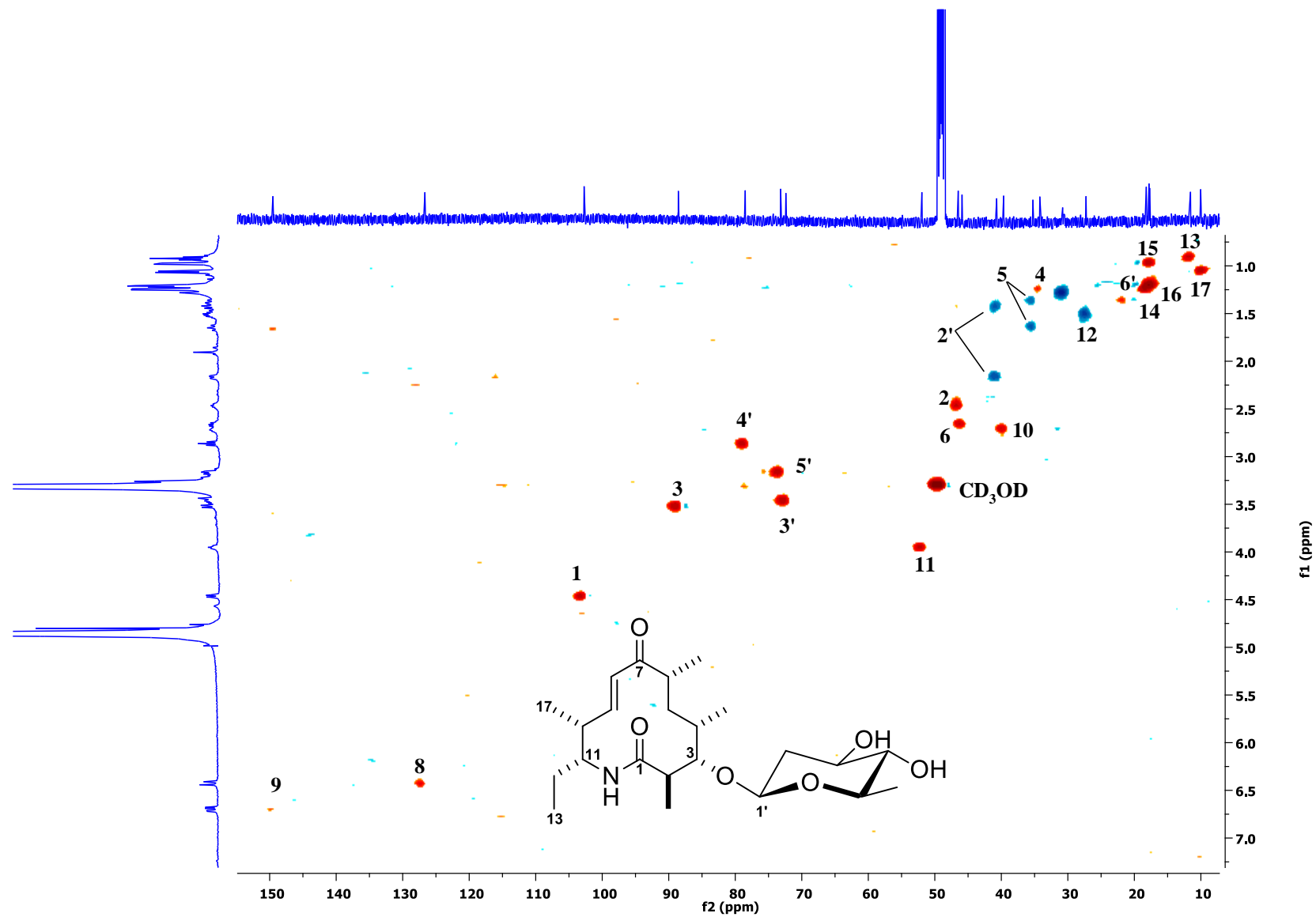


Figure S58. HSQC spectrum of **17** in CD₃OD at 500 MHz.

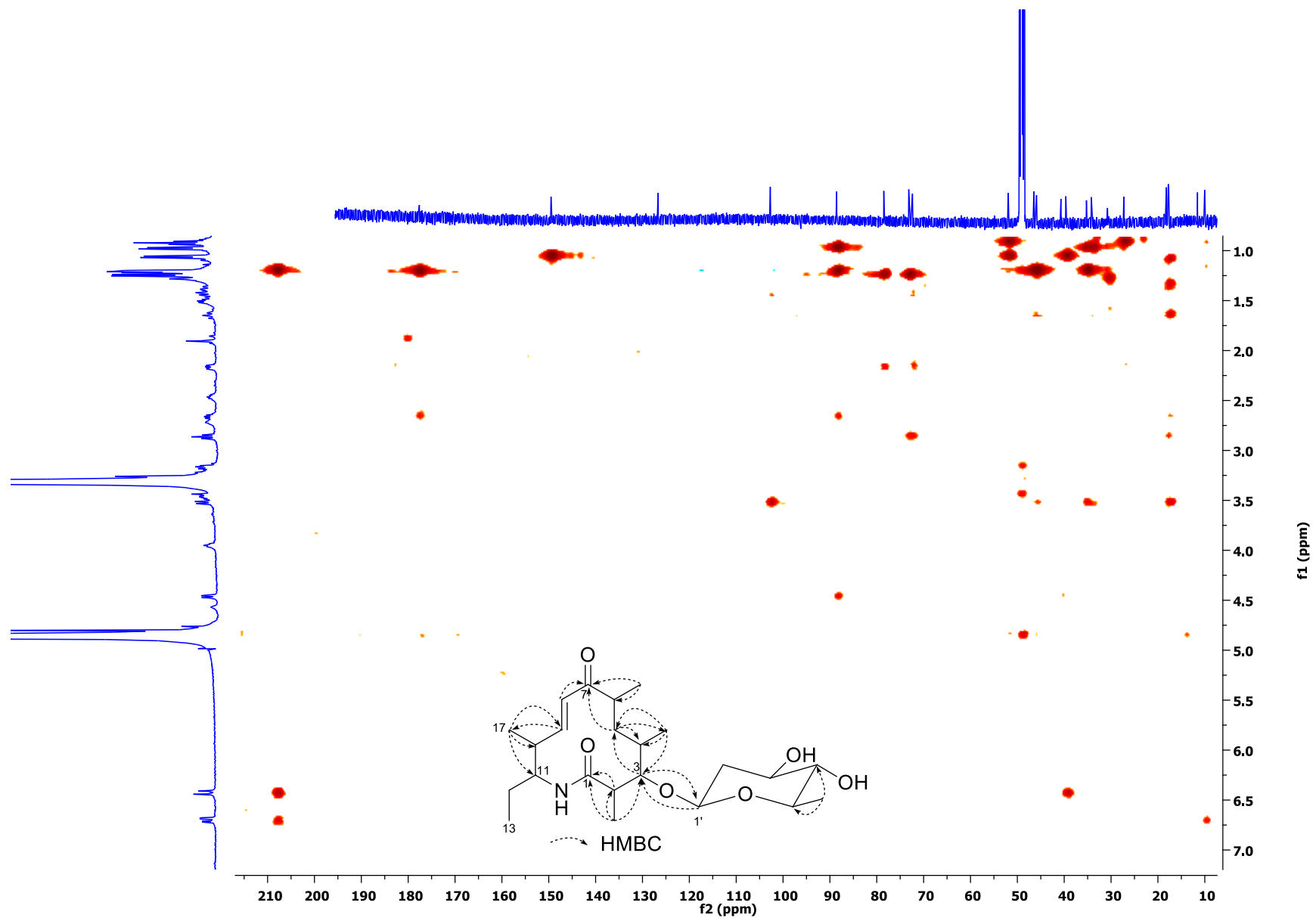


Figure S59. HMBC spectrum of **17** in CD₃OD at 500 MHz.

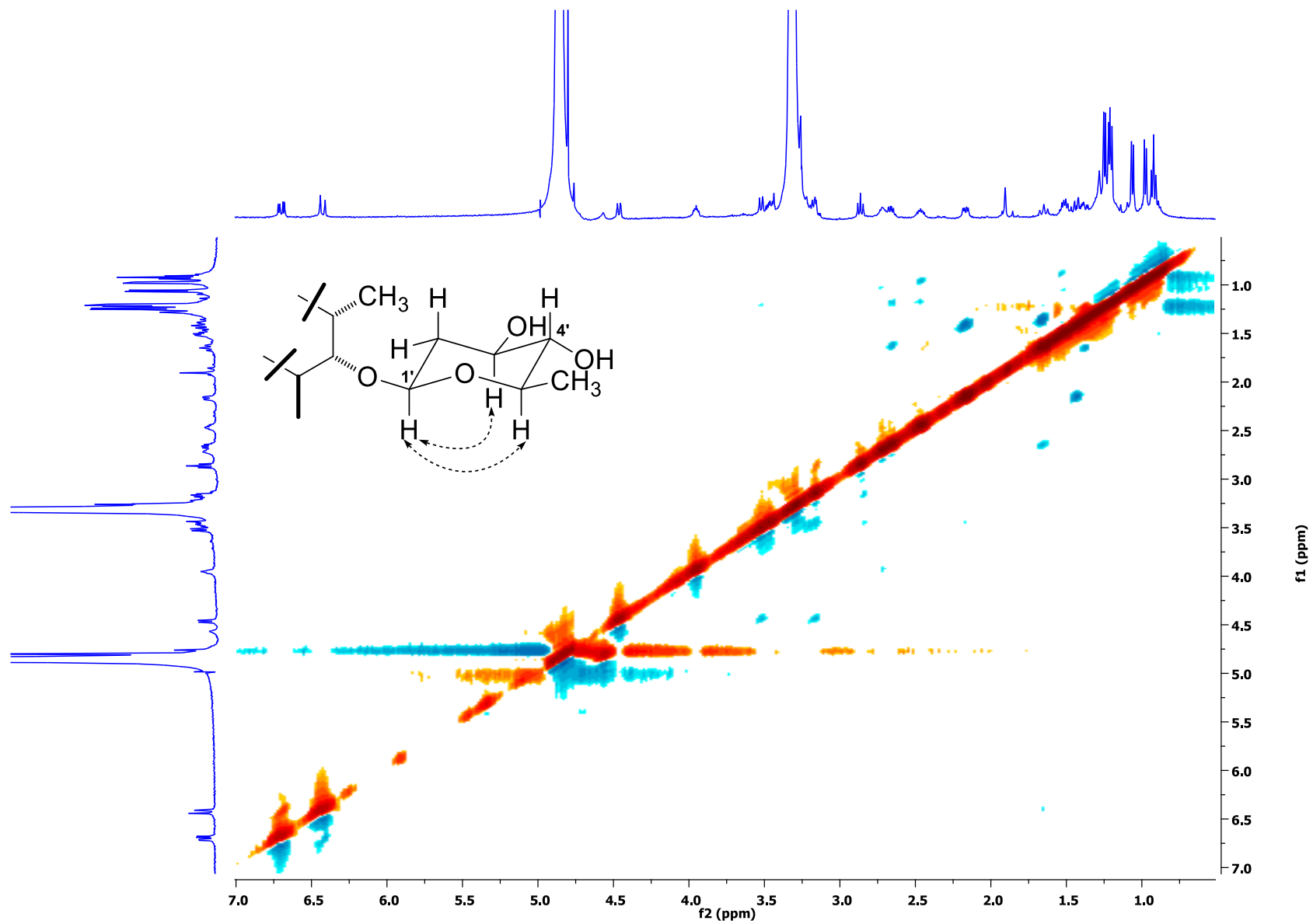


Figure S60. NOESY spectrum of **17** in CD₃OD at 500 MHz.

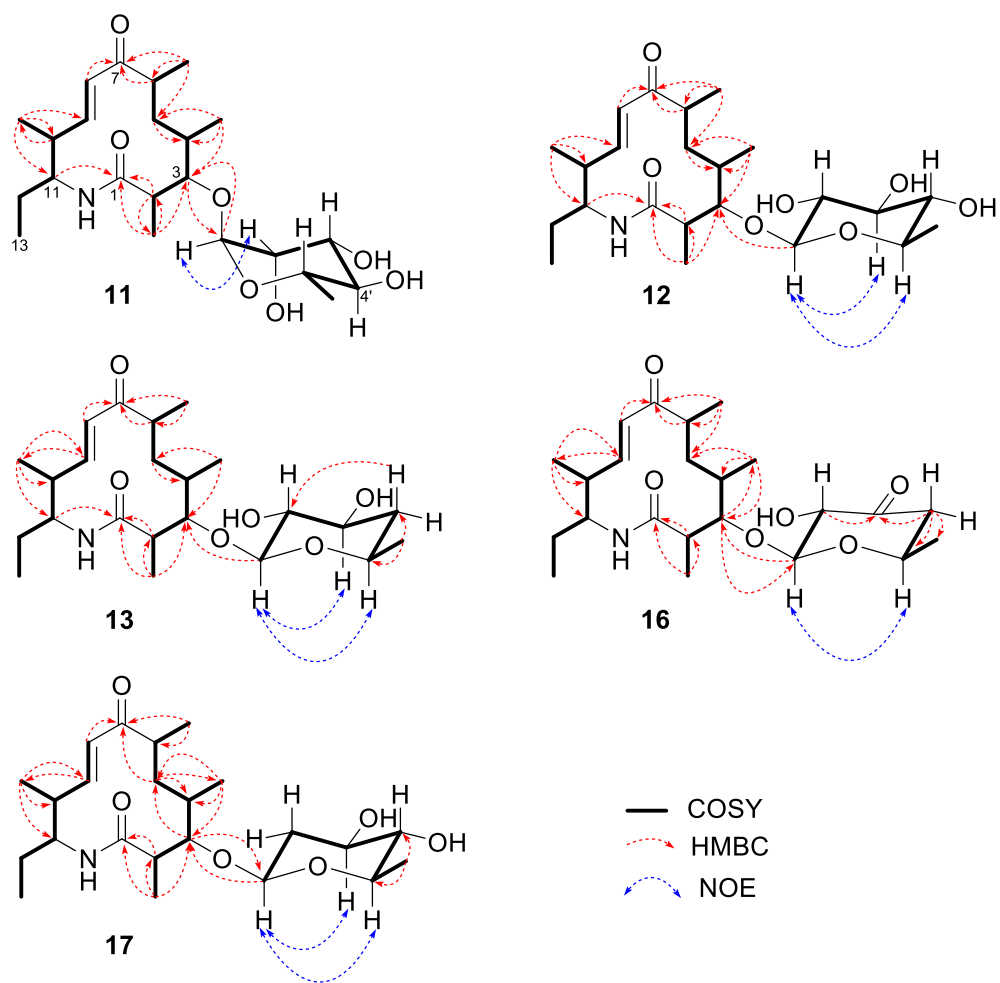


Figure S61. Key COSY, HMBC, and NOESY correlations in AZDM glycosides 11–13, 16, and 17.

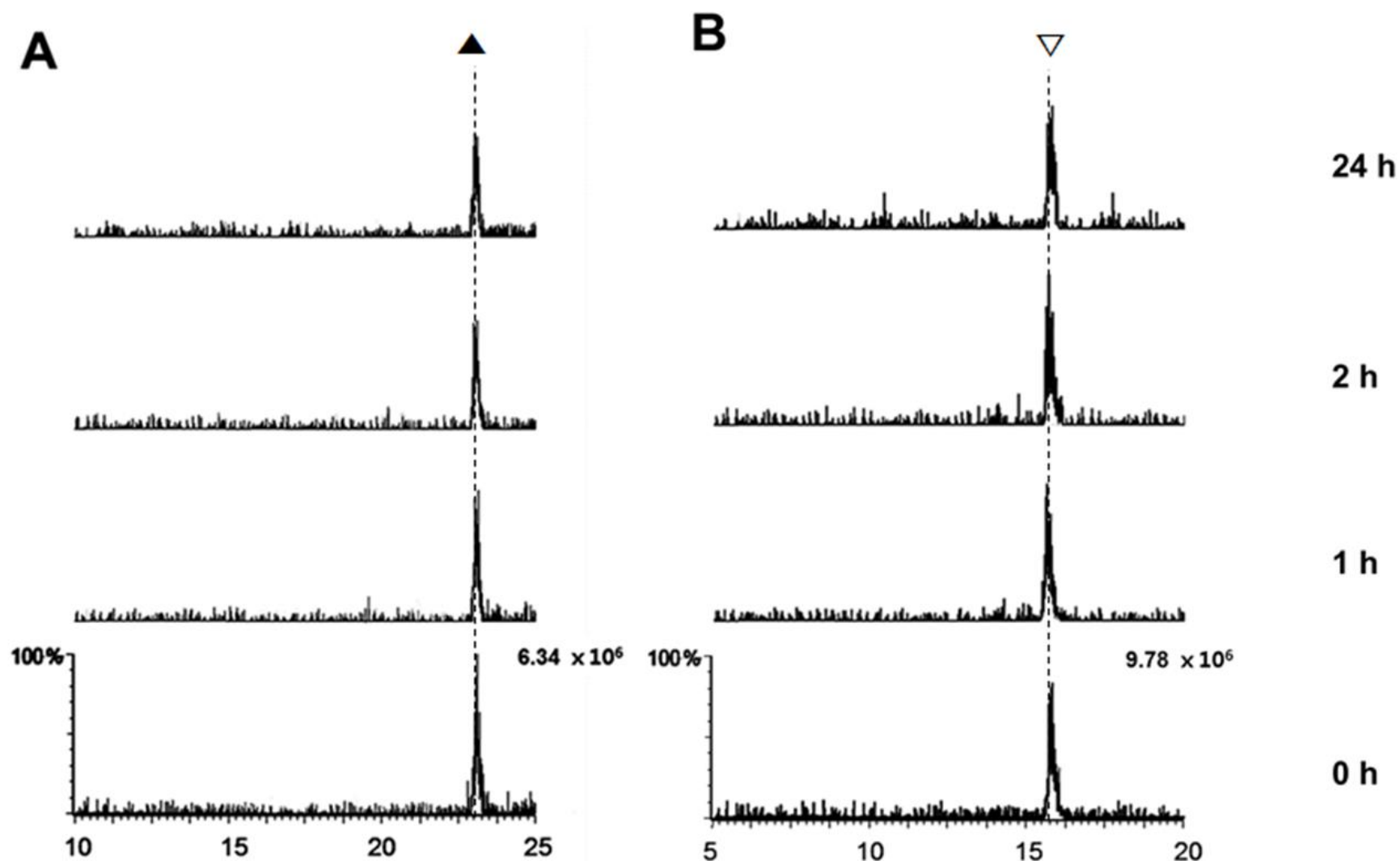


Figure S62. HPLC–ESI-MS chromatogram of erythromycin esterase assay. (A) EIC (m/z 297) for linear form of L-rhamnosyl-10-dml and (B) EIC (m/z 296) for linear form of L-rhamnosyl-AZDM. L-rhamnosyl-10-dml (\blacktriangle), and L-rhamnosyl-AZDM (**11**) (\blacktriangledown). Other possible m/z values for the hydrolysed products were extracted (m/z 443 for linear form of L-rhamnosyl-10-dml, m/z 442 for linear form of L-rhamnosyl-AZDM), but no significant peaks were observed.

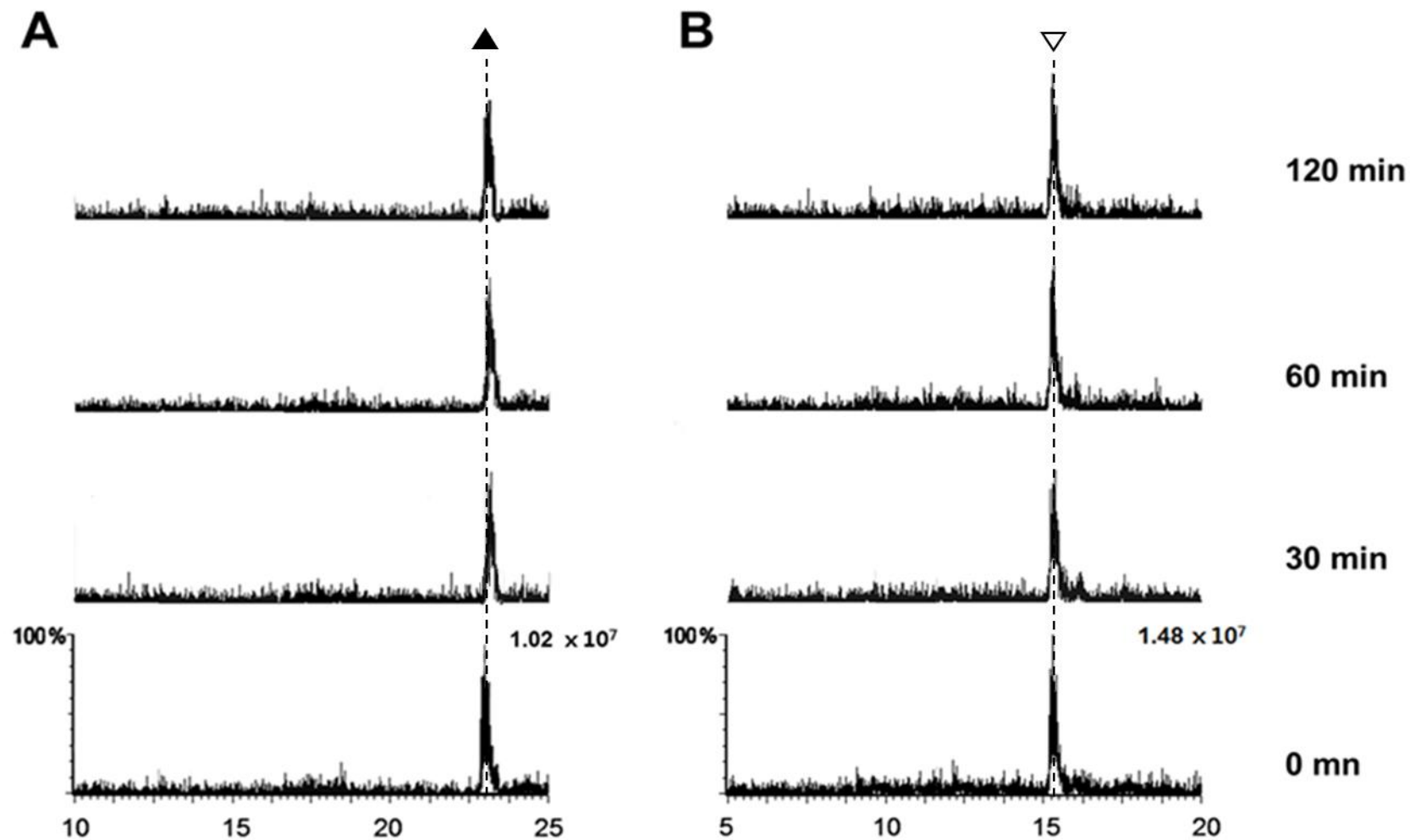


Figure S63. HPLC-ESI-MS chromatogram of simulated gastric fluid (SGF) assay. (A) EIC (m/z 297) for $[M+H]^+$ of 10-dml and (B) EIC (m/z 296) for $[M+H]^+$ of AZDM (**1**). L-rhamnosyl-10-dml (\blacktriangle), and L-rhamnosyl-AZDM (**11**) (∇).

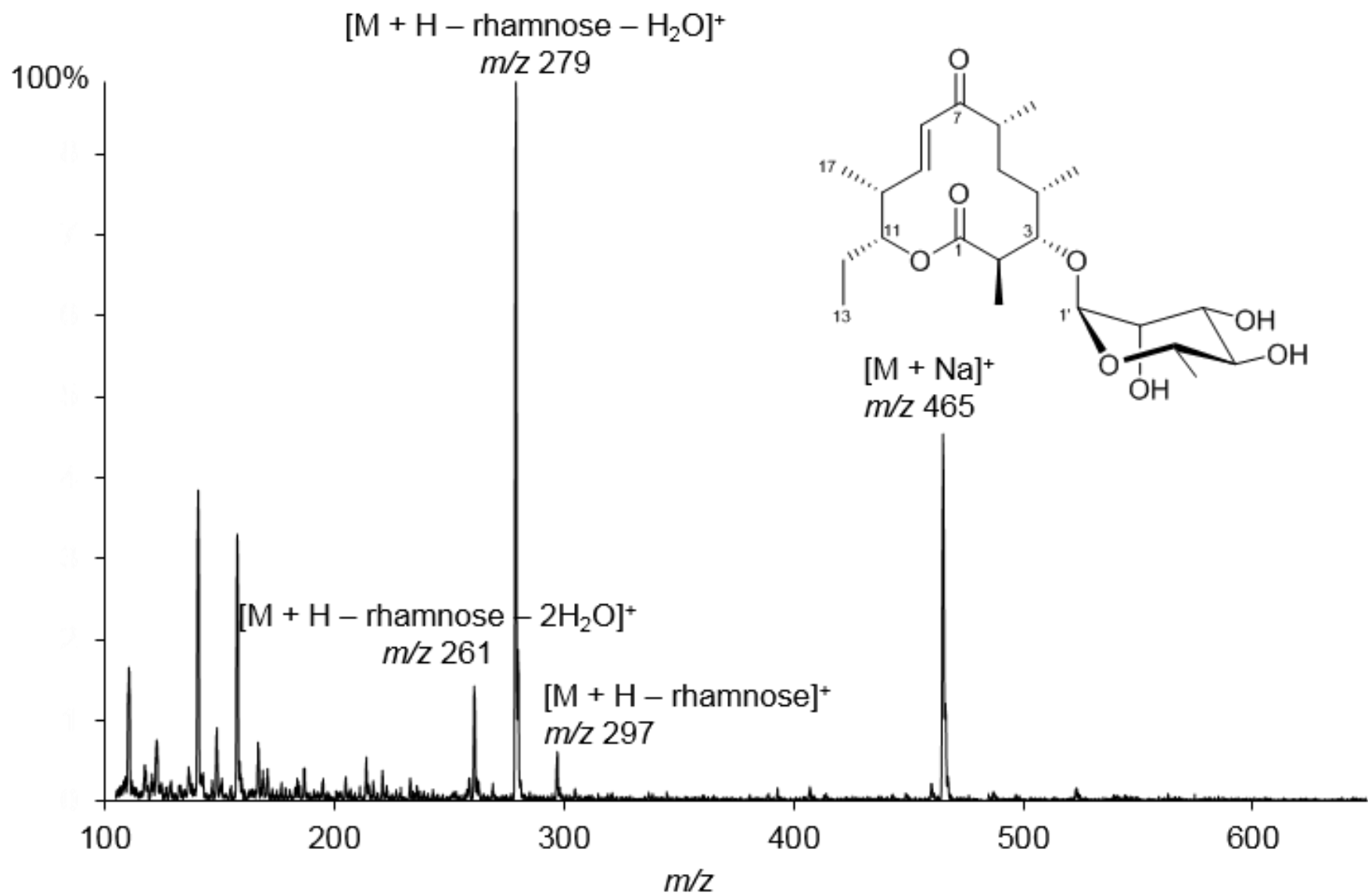


Figure S64. MS spectrum of L-rhamnosyl-10-deoxymethynolide.

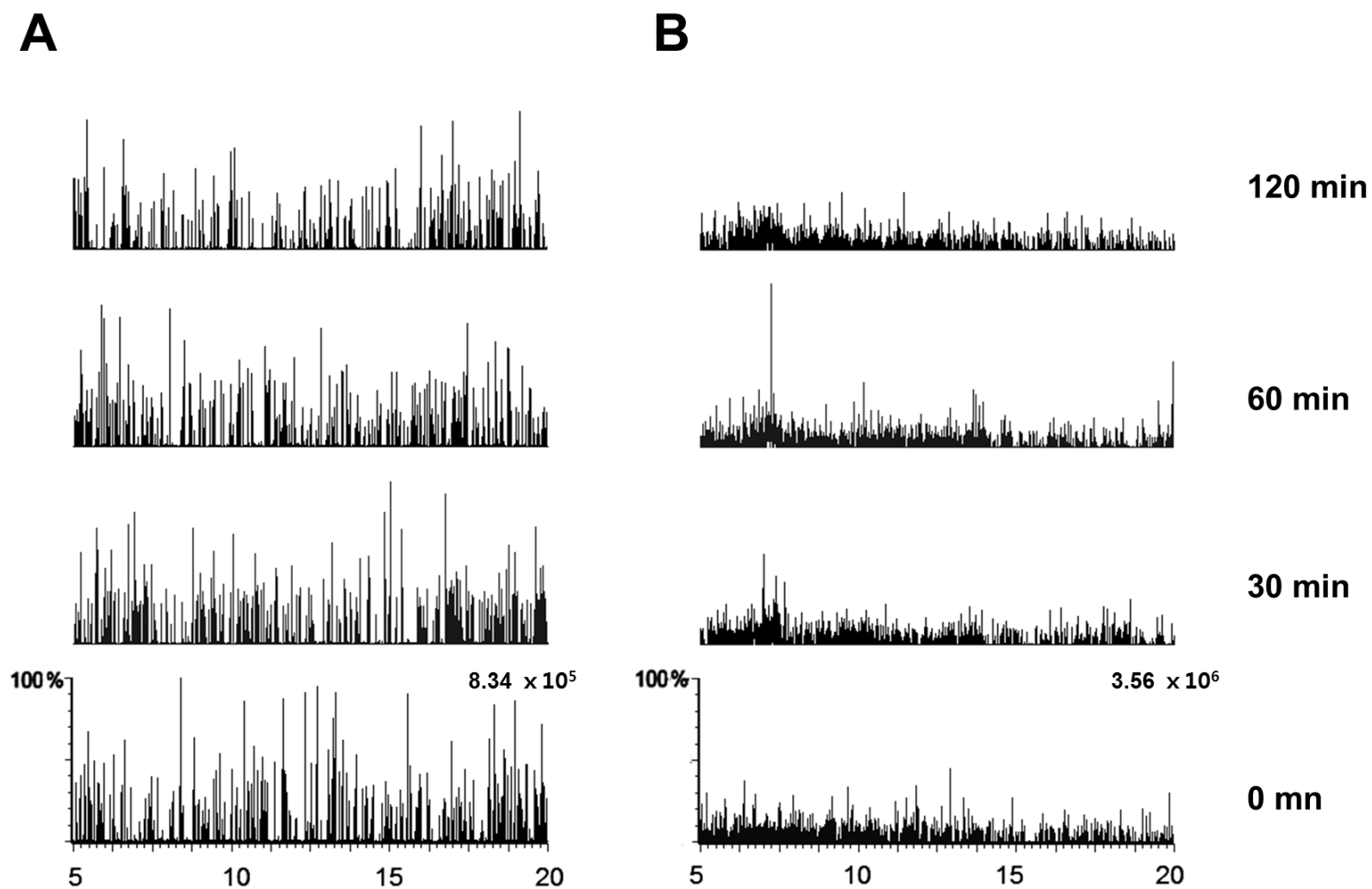


Figure S65. HPLC–ESI-MS chromatogram of liver microsomal assay. (A) EIC (m/z 428) for the desmethylated L-rhamnosyl-AZDM and (B) EIC (m/z 294) for the hydroxylated L-rhamnosyl-AZDM. Other possible m/z values for the desmethylated (m/z 281) and hydroxylated (m/z 480, 275) products were extracted, but no significant peaks were observed.